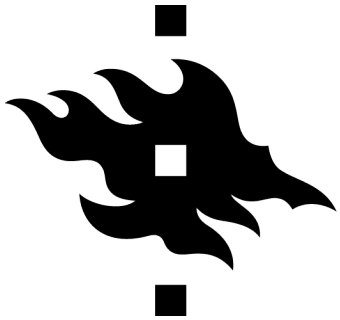

HELSINGIN YLIOPISTO
HELSINGFORS UNIVERSITET
UNIVERSITY OF HELSINKI

Master's thesis

Study of environmental effects on a dispersive transmon qubit

by Antti Vaaranta

Supervisors:
MSc. Marco Cattaneo (University of Helsinki)
PhD. Russell Lake (Bluefors Oy)

Examiners:
Prof. Sabrina Maniscalco (University of Helsinki)
PhD. Russell Lake (Bluefors Oy)

Helsinki, March 18, 2022

University of Helsinki
Faculty of Science
Department of Physics
Master's Programme in Theoretical and Computational Methods

HELSINGIN YLIOPISTO — HELSINGFORS UNIVERSITET — UNIVERSITY OF HELSINKI

Tiedekunta/Osasto — Fakultet/Sektion — Faculty	Laitos — Institution — Department
Faculty of Science	Department of Physics

Tekijä — Författare — Author

Antti Vaaranta

Työn nimi — Arbetets titel — Title

Study of environmental effects on a dispersive transmon qubit

Oppiaine — Läröamne — Subject

Theoretical Physics

Työn laji — Arbetets art — Level	Aika — Datum — Month and year	Sivumäärä — Sidantal — Number of pages
Master's thesis	February 2022	96 pages + 4 appendices

Tiivistelmä — Referat — Abstract

One of the main ways of physically realizing quantum bits for the purposes of quantum technology is to manufacture them as superconducting circuits. These qubits are artificially built two-level systems that act as carriers of quantum information. They come in a variety of types but one of the most common in use is the transmon qubit. The transmon is a more stable, improved version of the earlier types of superconducting qubits with longer coherence times.

The qubit cannot function properly on its own, as it needs other circuit elements around it for control and readout of its state. Thus the qubit is only a small part of a larger superconducting circuit interacting with the qubit. Understanding this interaction, where it comes from and how it can be modified to our liking, allows researchers to design better quantum circuits and to improve the existing ones. Understanding how the noise, travelling through the qubit drive lines to the chip, affects the time evolution of the qubit is especially important. Reducing the amount of noise leads to longer coherence times but it is also possible to engineer the noise to our advantage to uncover novel ways of quantum control.

In this thesis the effects of a variable temperature noise source on the qubit drive line is studied. A theoretical model describing the time evolution of the quantum state is built. The model starts from the basic elements of the quantum circuit and leads to a master equation describing the qubit dynamics. This allows us to understand how the different choices made in the manufacturing process of the quantum circuit affect the time evolution.

As a proof of concept, the model is solved numerically using QuTiP in the specific case of a fixed-frequency, dispersive transmon qubit. The solution shows a decohering qubit with no dissipation. The model is also solved in a temperature range $0\,\mathrm{K} < T \leq 1\,\mathrm{K}$ to show how the decoherence times behave with respect to the temperature of the noise source.

Avainsanat — Nyckelord — Keywords

circuit quantum electrodynamics, open quantum systems, transmon, decoherence

Säilytyspaikka — Förvaringsställe — Where deposited

Kumpula Campus Library

Muita tietoja — Övriga uppgifter — Additional information

This work was conducted as a paid project for Bluefors Oy.

Acknowledgements

First and foremost I wish to thank my supervisors Marco Cattaneo from the University of Helsinki and Russell Lake from Bluefors Oy. Without your support and guidance I would have been very lost in the endless stream of mathematics, theory and technical jargon that is included in the fields of cQED, open quantum systems and quantum technology. You managed to steer me towards the right path time and time again.

I want to also thank Bluefors Oy as a whole, for giving a theoretician such as myself an opportunity to do research and write the thesis on this very interesting topic. I appreciate greatly that a company, whose main purpose after all is to create revenue, values theoretical work this much.

Ilman hyviä ja kannustavia opettajia moni oppilas ja opiskelija ei koskaan löytäisi omia vahvuuksiaan. Omasta aiheestaan innostunut opettaja voi herättää myös opetettavan mielenkiinnon alaa kohtaan. Monista opintopolun varrelle osuneista opettajista minun on kiitettävä erityisesti yläasteen matematiikan ja fysiikan opettajaa Juha Olkkosta. Osa sinun kiinnostuksestasi matematiikkaa ja luonnontieteitä kohtaan tarttui minuun niinä kolmena vuotena, jona yläastetta kävin. Ilman sinun silloista tukea ja kannustusta en todennäköisesti olisi valinnut tätä polkua, jota nyt kuljen.

Opiskelijan elämään mahtuu onneksi paljon muutakin, kuin pelkän tenttikirjan päntäämistä ja laskuharjoitusten tekemistä. Vastapainoa tälle on tuonut erityisesti Karjalainen Osakunta, josta löysin oman akateemisen kotini Helsingissä. Osakunnan viroissa ja tapahtumissa on koettu suurin osa opiskelija-ajan parhaista hetkistä. Kiitos siis koko osakunnalle, sen jäsenille ja muille ystäville, jotka ovat opiskelun riemuja kanssani jakaneet! Onnekseni voin sanoa että teitä on aivan liian monta, jotta voisin tässä tasapuolisesti teidät kaikki nimetä, ketään pois jättämättä.

Lopuksi haluan tietenkin kiittää isää ja äitiä tuesta, kasvatuksesta ja sivistyksen tärkeyden korostamisesta. Ilman rohkaisua en varmasti olisi lähtenyt kauas maailmalle kokeilemaan, mitä fysiikan opiskelu ja tutkimus oikeasti on. Oman osaamisen äärirajoille menemistä ja oman polun seuraamista auttaa tieto siitä, että vaikka kuinka pahasti maailmalla kaatuisin, niin kotiin voisin aina palata, levätä ja sen jälkeen yrittää uudestaan.

Contents

1 Introduction

This is an exciting time to be alive. Especially for a quantum physicist. It is said that the current development of quantum technologies is so groundbreaking that we are currently living the times of a second quantum revolution [1]. The first quantum revolution resulted from the discovery of completely new physics in the beginning of 20th century. The most well-known inventions that arose from the understanding and application of the physical laws of the microscopic realm were lasers and transistors. Although their complete description requires knowledge of the quantum theory, their working principles do not involve precise control on the quantum systems at an individual level. However, the second quantum revolution is just about that: controlling the individual quantum systems such that they behave exactly as we want. We aim to harness the quantum effects to do something for us, rather than just studying the laws of quantum theory and being content with what we find.

At the core of emerging quantum technologies are *qubits*, which are the carriers of quantum information. Qubits allow for building a quantum network for quantum communication purposes [2], they can be used as sensors in quantum metrology [3] and as emulators of more complex quantum systems in quantum simulation [4]. One of the most striking and attention attracting (in the minds of the public and physicists alike) quantum technology is the possibility of building a universal quantum computer. There qubits serve the role of classical bits in normal computers, allowing the user to run algorithms which change the state of qubits such that we are able to perform computation tasks that would not be feasible to be implemented on a classical computer [5].

In all of the examples above we need to be able to control the qubits somehow. After all, what use would a computer, sensor or simulator be if we could not feed in any information and get out results? This requirement of controllability of the quantum state poses a challenge, as we need to be able to have sufficiently strong interaction with the qubit. However, opening up the qubit system for our control allows it also to interact with the environment, which is detrimental to the preparation and longevity of the superposition states used for the computing tasks [6]. Therefore, we need to understand how the qubits are controlled, where the *decoherence* comes from and how it affects the quantum state.

The main building blocks in designing quantum computers are superconducting qubits of

various kinds [7]. They are controlled with microwave signals, which are used to initialize the qubits to desired superposition states and to perform gate operations on them [8]. These microwave signals require the aforementioned openness of the qubit system in order for them to interact with the qubit. Coming from a signal source at room temperature, these microwave signals initially carry a lot of thermal noise that needs to be damped before they reach the superconducting circuit. The damping of the high temperature thermal noise is done by using attenuators at a specific low temperature [8], but these devices themselves add thermal noise corresponding to their temperature.

Although much of the developments in quantum technology have been due to the reduction of noise in the systems, leading to longer coherence times of the quantum states, the effects of carefully engineered noise can be also used to our advantage [9]. Therefore studying the exact nature of the noise and its effects are interesting as it could allow us to uncover novel quantum states of matter and find new approaches in quantum control [10].

Bluefors Oy, a Helsinki based company manufacturing dilution refrigerators for the use of quantum technology, has devised an attenuator installable in the qubit drive line, whose temperature can be changed. This *variable temperature noise source* [11] allows for the study of the effects of noise in quantum states as a funtion of temperature. The main goal of this thesis is to quantify how does this noise source affect the quantum state of a *superconducting transmon qubit*, and to predict how do the choices of the circuit parameters used in the manufacturing process of the qubit affect the state evolution. To reach this goal, we build a theoretical model to characterize the qubit evolution in the presence of this noise source. The beginnings of the model are the very basic elements of the superconducting circuit of the qubit. Using *circuit quantum electrodynamics* and the *theory of open quantum systems*, we end up with a master equation that describes the time evolution of the qubit. Solving this master equation shows how the quantum state of the qubit behaves in time, in the presence of noise coming from the variable temperature noise source.

This thesis is organized as follows: the first two chapters concentrate on giving the necessary theoretical background on the topics we need in order to analyze the qubit and its superconducting circuit. The next two chapters then concentrate on first deriving the theoretical model in a specific case of a dispersive transmon qubit and then on solving it and presenting the results.

In chapter 2 we give an introduction to circuit quantum electrodynamics, an architecture for building and analyzing superconducting quantum circuits. After discussing the quantization process of a simple electrical circuit we move on to consider how to treat dissipative elements quantum mechanically. After a brief discussion about qubits both as mathematical and physical entities, we move to chapter 3, where we discuss the theory of open quantum systems. There, a brief reminder of quantum mechanics is in order before moving to discuss the actual open quantum system dynamics and to derive the *Lindblad master equation* in a general case.

In chapter 4 we begin to formulate and derive the theoretical model for solving the qubit dynamics. We begin with the quantization of the circuit under study by first drawing its circuit diagram and then quantizing the resulting Hamiltonian. Using the obtained

Hamiltonian, we derive a master equation that describes the qubit dynamics when it interacts with its circuitry and the variable temperature noise source, which is modelled as a $50\,\Omega$ resistor. After this, we move on to chapter 5, which is dedicated to solving the master equation. In this chapter, we discuss selected analytical solutions to the master equation and present results from the numerical simulations of the master equation. The last chapter of this thesis is 6, where we conclude our work and discuss the obtained results.

2 Circuit Quantum Electrodynamics

Quantum physics is generally regarded as the study of the microscopic world, where the deterministic rules of classical physics break down and become intrinsically probabilistic. Usually the length-scale associated with objects, such as electrons, photons and other particles, which are noticeably influenced by the quantum effects, are atomic or sub-atomic. Thus direct observation of these particles is difficult and can alter the fragile quantum state.

In the past the role of a quantum physicist has been to study the already existing properties of these quantum particles and to discover new quantum phenomena from nature. The idea of engineering man-made atoms to be used in future applications, for example in quantum simulation and computation was, for a long time, inconceivable. However, in recent years it has become possible for researchers and engineers to manufacture so-called *artificial atoms* with carefully specified behaviour [12]. This is thanks to the emergence of a relatively new field in physics called *circuit quantum electrodynamics* [13] or cQED for short.

The authors of a recent cQED review paper [7] define the field as follows: *"Circuit quantum electrodynamics is the study of the interaction of nonlinear superconducting circuits, acting as artificial atoms or as qubits for quantum information processing, with quantized electromagnetic fields in the microwave frequency domain"*. This definition states that we are talking about quantum effects of electrical circuits, that happen to be superconducting. From the electrical circuits we are able to construct qubits and artificial atoms by using inductors, capacitors and other circuit elements [10] and we study their interaction with the electromagnetic field [7, 14]. It is notable that, by being able to construct electric circuits that exhibit quantum effects, we bring the quantum phenomena out of the microscopic world. Indeed, these *mesoscopic circuits* have microscopic properties albeit being macroscopic in a sense that they contain a large number of particles [15].

The idea of observing quantum effects in macroscopic scale was not new or special in the time when the core ideas of cQED were proposed for the first time by Blais et al. [13]. For example the phenomena of superfluidity and superconductivity are usually regarded as prime examples of macroscopic quantum effects [16]. However, Anthony Leggett argued in his 1980 paper that these phenomena are not prime examples of actual macroscopical quantum states [17]. Then the question arose whether or not we can observe effects

like quantum tunneling, entanglement or energy level quantization at all in macroscopic systems [7, 17].

While raising the question about the existence of macroscopical quantum effects, Leggett also argued that superconducting systems (and especially *superconducting quantum interference devices* or SQUIDs) would be an ideal testing ground when trying to observe these phenomena [17]. This fuelled the interest to study superconducting circuits which culminated to the realization of a superposition state in a macroscopic device in 1999 when Nakamura et al. published their milestone discovery [18]. They managed to superpose two charge states of the device and control the quantum state evolution. Thus the first *superconducting qubit* was born.

The appearance of an artificially produced qubit opened up new prospects of research. Soon a system of two qubits was built, which showed the existence of entanglement in macroscopic systems [19]. It was indeed possible to observe truly macroscopic quantum effects. Eventually the urge to realize better systems with more qubits and with enhanced lifetime led to the formulation of cQED in 2004 by Blais et al.[13].

The advantage of cQED is that in designing a qubit or an artificial atom we can obtain the quantum features, such as energy spectra and coupling strengths, directly from the used macroscopic circuit parameters [20]. The parameters we are able to design are thus not fundamental and can be tailored to our liking, depending on what the systems is designed for [15]. Indeed, the power of the cQED architecture has not gone unnoticed as it is the most widely used design architecture in quantum computation [7].

In this chapter we aim to gain sufficient knowledge and understanding about the cQED architecture to be able to apply it to a actual qubit circuit later in chapter 4. To accomplish this, we begin with a simple model of a harmonic oscillator constructed as a superconducting parallel LC-circuit. Understanding the connection between the classical circuit model of an LC-oscillator and the emerging quantum description of the circuit as a single bosonic mode allows for more complicated treatment of the circuit diagrams encountered later. Then we extend the treatment from a single LC-oscillator to an infinite collection of them, when we discuss the dissipation in superconducting circuits due to the presence of resistors and obtain a quantum description thereof. Finally, we discuss about qubits themselves, starting from their theoretical description and finishing with the current state-of-the-art physical realization called *transmon qubit*, that is based on the same principles as Nakamura's qubit from 1999 [18] but with vastly improved properties.

2.1 QUANTIZATION OF AN LC-CIRCUIT

We begin our journey through the realm of circuit quantum electrodynamics by studying one of the simplest but also one of the most useful cases possible, that is the harmonic oscillator. In electronics the dynamics corresponding to harmonic motion are obtained

by constructing a lumped element circuit[1] with a capacitor in parallel with an inductor, and one node of the circuit connected to ground. This circuit, whose schematic is shown in figure 2.1, is characterized by the inductance L and capacitance C of its elements or equivalently by its angular frequency $\omega_r = 1/\sqrt{LC}$ and characteristic impedance $Z_r = \sqrt{L/C}$.

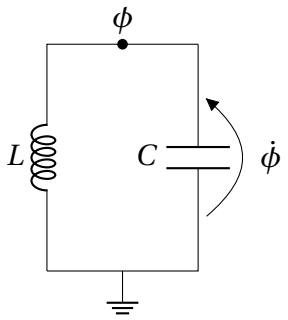

Figure 2.1: A parallel LC-circuit with node flux ϕ and voltage $V = \dot{\phi}$ between the top node and ground.

To compute the dynamics of the circuit, we identify its kinetic and potential energies in order to use the Lagrangian formalism. It's a well known result of classical electrodynamics [21] that the energy of an inductor is proportional to the current flowing through it

$$E_L = \frac{1}{2} L I^2 , \tag{2.1}$$

and the energy of the capacitor is proportional to the voltage difference between its plates

$$E_C = \frac{1}{2} C V^2 . \tag{2.2}$$

Following the method in [15], we introduce a position-like variable[2] called *generalized flux*, or branch flux, as the integral over time of the voltage variations across certain element b of the circuit

$$\phi_b(t) = \int_{-\infty}^{t} V_b(t') \mathrm{d}t' , \tag{2.3}$$

where we assume the lower limit of integration to be sufficiently far in the past, such that the circuit had been at rest with no voltages or currents present. Note that (2.3) is the integrated version of the Faraday's law $V_b = \dot{\phi}_b$, an equality which will often be used in this work. Using this identity between the voltage and time derivative of the flux together with the relation $\phi = LI$ between flux and current, allows us to write the capacitive energy as a kinetic term in the Lagrangian, while the inductive energy becomes the potential term.[3] Remarkably, we are able to reduce the complex dynamics of an enormous number of electrons in the circuit to one single degree of freedom ϕ in the Lagrangian formalism [14]

$$\mathscr{L}_{LC} = E_{kin} - E_{pot} = \frac{1}{2} C \dot{\phi}^2 - \frac{1}{2L} \phi^2 , \tag{2.4}$$

where the roles of "mass" and "spring constant" of the harmonic oscillator are played by the capacitance C and the inverse inductance $1/L$ respectively.

[1] Meaning an approximation of a spacially distributed circuit where its elements are thought of as being discrete.

[2] In the Lagrangian sense, where the position-like variable will be associated with the potential term and the velocity-like variable with the kinetic term.

[3] It should be noted that the choice of ϕ being the coordinate in our description is (in this case) arbitrary, since we would get the same result by using Q as the coordinate and ϕ as the momentum. However, later on, when encountering non-linear inductors (see section 2.3), it will turn out that the choice of ϕ as the coordinate is more convenient [14].

The standard procedure of defining a momentum conjugate of the generalized position coordinate[4] as $Q = \partial \mathscr{L}_{\mathrm{LC}}/\partial \dot{\phi}$, which satisfies the Poisson bracket $\{\phi, Q\} = 1$ of classical Hamiltonian mechanics[5], allows us to move to the Hamiltonian description via the Legendre transformation of the Lagrangian (2.4)

$$H_{\mathrm{LC}} = \dot{\phi}\frac{\partial \mathscr{L}_{\mathrm{LC}}}{\partial \dot{\phi}} - \mathscr{L}_{\mathrm{LC}} = \frac{Q^2}{2C} + \frac{\phi^2}{2L}. \tag{2.5}$$

So far, we have analysed the LC-oscillator in figure 2.1 in a purely classical fashion. However, since we are ultimately interested in the quantum properties of a circuit that comprises of these oscillators, we need to quantize the circuit Hamiltonian (2.5). Here two slightly different ways of quantization are presented. These two approaches are quite similar, but the reader might be more familiar with the first one and after going through it should feel more confident in reading through the second. The latter is a bit more general and allows for an easier treatment of *Josephson junctions*, which we will encounter in the later sections of this chapter.

Approach 1

Using the angular frequency of the LC-circuit $\omega_{\mathrm{r}} = 1/\sqrt{LC}$, we can write the Hamiltonian (2.5) in a suggestive form [7]:

$$H_{\mathrm{LC}} = \frac{Q^2}{2C} + \frac{1}{2}C\omega_{\mathrm{r}}^2\phi^2, \tag{2.6}$$

which closely resembles the Hamiltonian of a mechanical harmonic oscillator with momentum Q, mass C and position ϕ.

As shown in [7], the quantization is done by promoting the variables for the generalised flux ϕ and charge Q to corresponding operators $\hat{\phi}$ and $\hat{Q}$. The Poisson bracket between the dynamical variables is replaced by the commutator between the operators, obeying the canonical commutation relation

$$\{\phi, Q\} = 1 \quad \Rightarrow \quad [\hat{\phi}, \hat{Q}] = \mathrm{i}\hbar. \tag{2.7}$$

Following the standard treatment of the quantum harmonic oscillator (QHO) [22], we can identify how to write the flux and charge operators using the annihilation operator $\hat{a}$ and the creation operator $\hat{a}^\dagger$. This procedure is outlined in the box below and used extensively in other parts of the thesis.

QHO:

The Hamiltonian for a particle of mass m and oscillation frequency ω reads

$$\hat{H}_{\mathrm{QHO}} = \frac{\hat{p}^2}{2m} + \frac{1}{2}m\omega^2\hat{x}^2. \tag{2.8}$$

The position operator $\hat{x}$ and the momentum operator $\hat{p}$ are written in terms of the

[4] In this case generalized charge is the conjugate variable of generalized flux.

[5] $\{\phi, Q\} = \frac{\partial\phi}{\partial\phi}\frac{\partial Q}{\partial Q} - \frac{\partial\phi}{\partial Q}\frac{\partial Q}{\partial\phi} = 1 - 0 = 1$.

ladder operators as [22]

$$\hat{x} = \sqrt{\frac{\hbar}{2m\omega}}(\hat{a}^\dagger + \hat{a}), \qquad \hat{p} = \mathrm{i}\sqrt{\frac{\hbar m\omega}{2}}(\hat{a}^\dagger - \hat{a}). \tag{2.9}$$

LC-circuit:
The Hamiltonian for the quantized LC-circuit reads

$$\hat{H}_{\mathrm{LC}} = \frac{\hat{Q}^2}{2C} + \frac{1}{2}C\omega_{\mathrm{r}}^2\hat{\phi}^2. \tag{2.10}$$

We identify that the capacitance C corresponds to mass m of QHO and $\omega_{\mathrm{r}} = 1/\sqrt{LC}$ is the oscillation frequency. Thus it's easy to identify how the flux and charge operators $\hat{\phi}$ and $\hat{Q}$ are written in terms of the ladder operators:

$$\hat{\phi} = \sqrt{\frac{\hbar}{2C\omega_{\mathrm{r}}}}(\hat{a}^\dagger + \hat{a}), \qquad \hat{Q} = \mathrm{i}\sqrt{\frac{\hbar C\omega_{\mathrm{r}}}{2}}(\hat{a}^\dagger - \hat{a}). \tag{2.11}$$

Using the expressions in equation (2.11) in the quantized LC-oscillator Hamiltonian equation (2.10) allows us to present it in the well known form

$$\hat{H}_{\mathrm{LC}} = \hbar\omega_{\mathrm{r}}(\hat{a}^\dagger\hat{a} + 1/2), \tag{2.12}$$

which is diagonal in the number basis $|n\rangle$, with $\hat{a}^\dagger\hat{a}|n\rangle = n|n\rangle$ for $n \in \mathbb{N}$, where n is the number of quanta in the LC-circuit. These quanta of angular frequency ω_{r} are created by the creation operator $\hat{a}^\dagger$ and destroyed by the the annihilation operator $\hat{a}$.

Approach 2
The circuit in figure 2.1 is superconducting so it could be good idea to normalize the flux ϕ and charge Q in terms of parameters which appear in the superconductivity theory. Following Ref. [8] we define the reduced flux $\Phi = 2\pi\phi/\phi_0$ and reduced charge $n = Q/(2e)$. Here $\phi_0 = h/(2e)$ is the superconducting magnetic flux quantum and $2e$ comes from the charge of a Cooper pair. Applying this change of variables to equation (2.5), we obtain

$$H_{\mathrm{LC}} = 4\frac{e^2}{2C}n^2 + \frac{1}{2}\frac{\phi_0^2}{(2\pi)^2 L}\Phi^2 = 4E_{\mathrm{C}}n^2 + \frac{1}{2}E_{\mathrm{L}}\Phi^2. \tag{2.13}$$

We defined the capacitive and inductive energies as $E_{\mathrm{C}} = e^2/(2C)$ and $E_{\mathrm{L}} = (\phi_0/(2\pi))^2/L$. It should be noted that the new variables Φ and n are still conjugate variables but with a Poisson bracket $\{\phi, n\} = 1/\hbar$.[6] Therefore, when we promote Φ and n to corresponding operators $\hat{\Phi}$ and $\hat{n}$ their commutation relation becomes

$$\{\Phi, n\} = \frac{1}{\hbar} \quad \Rightarrow \quad [\hat{\Phi}, \hat{n}] = \mathrm{i}. \tag{2.14}$$

The Hamiltonian in equation (2.13) still describes harmonic motion. Similarly to Approach 1 we can write the operators $\hat{\Phi}$ and $\hat{n}$ in terms of the creation and annihillation operators

[6] $\{\phi, n\} = \frac{\partial\Phi}{\partial\phi}\frac{\partial n}{\partial Q} - \frac{\partial\Phi}{\partial Q}\frac{\partial n}{\partial\phi} = \frac{\pi}{\phi_0 e} = \frac{2\pi}{h} = \frac{1}{\hbar}$

as [8]

$$\hat{\Phi} = \left(\frac{2E_C}{E_L}\right)^{\frac{1}{4}} (\hat{a}^\dagger + \hat{a}), \qquad \hat{n} = \mathrm{i}\left(\frac{E_L}{32E_C}\right)^{\frac{1}{4}} (\hat{a}^\dagger - \hat{a}). \tag{2.15}$$

Using the above equations we may write the Hamiltonian of the harmonic oscillator in an identical form to equation (2.12) but with $\omega_r = \sqrt{8E_L E_C}/\hbar$.

The path from a classical LC-oscillator circuit diagram from figure 2.1 to its quantum equivalent Hamiltonian equation (2.12) sheds light on the fact that we can treat the LC-oscillator as a container of bosons, each of which has fixed angular frequency ω_r which is determined by the circuit parameters L and C. This allows us to engineer the properties of the "bosons" to our liking.

It is noteworthy that the above method of circuit quantization by finding the kinetic and potential energies and the corresponding Hamiltonian is not limited to the simple case of an LC-oscillator, but can be applied to more complex cases, as can be seen in later sections. However, we are restricted to dealing with circuits composed only of linear[7] capacitive and linear or non-linear inductive elements [15]. The third and last category of passive circuit elements, the resistors, is not considered in this formalism because modelling the dissipated energy at some time t would lead to cumbersome expressions [10]. However, we are able to construct a Hamiltonian formalism of dissipation, as can be seen in the next section where we apply the Caldeira-Leggett model [23] to resistors.

2.2 TREATMENT OF DISSIPATIVE ELEMENTS

In quantum mechanics the time-independent Hamiltonians are invariant with respect to time translation, which leads to energy conservation according to Noether's theorem. This can be seen for example by considering the Heisenberg equation of motion (see section 3.1.1)

$$\frac{\mathrm{d}}{\mathrm{d}t}\hat{A}_H(t) = \frac{\mathrm{i}}{\hbar}\left[\hat{H}_H, \hat{A}_H(t)\right] + \left(\frac{\partial \hat{A}_S}{\partial t}\right)_H, \tag{2.16}$$

which tells how an operator $\hat{A}$ evolves in time in the Heisenberg picture. If we considered the case where the operator in question is the Hamiltonian itself, $\hat{A}_H = \hat{H}_H$, we would see that the Hamiltonian is a constant of motion[8] that is not changing in time, and thus the energy of our system would be conserved. The dynamics of such a system is said to be *reversible*.

The difficulty in dealing with dissipative elements, such as resistors, in this way is that their behaviour is *irreversible*. By adding resistors to our circuits, we can no longer treat them as isolated systems where energy is conserved, because the resistors dissipate energy out of the system. The Hamiltonian treatment in section 2.1 is reversible, conserving the system

[7] A capacitor is an element whose voltage depends directly only on charge via some function: $v(t) = f(Q(t))$ with capacitance $C(Q) = \left(\frac{\mathrm{d}f}{\mathrm{d}Q}\right)^{-1}$. A capacitor is linear if its capacitance is independent of the charge and thus a constant $C(Q) = C$. Similarly a linear inductor has a constant inductance, which doesn't depend on the flux: $L(\phi) = L$ [15].

[8] This is because we would get $\frac{\mathrm{d}}{\mathrm{d}t}\hat{H}_H(t) = \frac{\mathrm{i}}{\hbar}[\hat{H}_H, \hat{H}_H(t)] = 0$ since the Hamiltonian commutes with itself and we assume that the Hamiltonian doesn't depend on time.

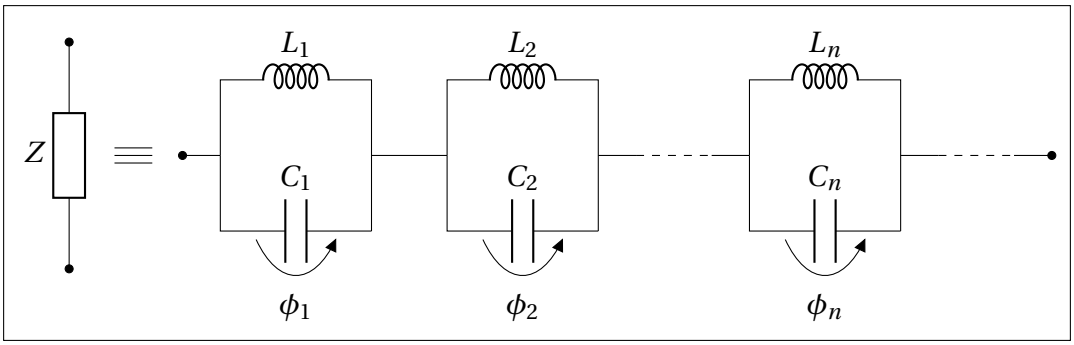

Figure 2.2: We can represent the impedance Z of a resistor as an infinite series of LC-oscillators using the extended Foster's first form. The node fluxes ϕ_n are defined such that their time derivative $\dot{\phi}_n$ represent the voltage drop over the corresponding LC oscillator in our decomposition. Figure adapted from [10].

energy and thus not immediately usable for the treatment of resistors. Fortunately, we can overcome this problem by extending the formalism via the usage of Caldeira-Leggett model [23], which applies to systems with linear dissipation [15].

2.2.1 A HAMILTONIAN FORMALISM FOR A RESISTOR

In order to treat a dissipative element, such as a resistor, in the Hamiltonian formalism, we need to overcome the problem of inherent reversibility of the Hamiltonian equations, which was discussed in the intro to this section. This is accomplished by using the Caldeira-Leggett model [23] in the context of cQED alongside with network synthesis methods developed by Ronald Foster in 1924 [24].

In 1924 Ronald Foster proved that any passive, lossless circuit impedance can be presented using either a series of parallel LC-oscillators (called Foster's first form) or parallel series LC-oscillators (called Foster's second form) [24]. Usually, in network synthesis, these series are finite, thus yielding a purely imaginary impedance. Keeping in mind that our current goal is to get a model for quantum dissipation that describes the lossy nature of a resistor, we extend (following the example of [15] and [10]) the series of parallel LC-oscillators encountered in Foster's first form to be infinitely long (see figure 2.2). As can be seen later, this ultimately leads to the appearance of an impedance with a real and imaginary part, and we argue that the real part of the impedance is the resistance of the resistor in our model.

When we choose to represent the resistor as an infinite series of LC-oscillators, we transform our model into one that has an infinite number of degrees of freedom. Previously the whole resistor was described only by its resistance R, but now it is described by the separate node fluxes between each parallel LC-oscillator of the infinite series, as shown in figure 2.2. As argued by Vool and Devoret in [15], the change from a finite number of degrees of freedom to an infinite one allows for the emergence of irreversible dynamics of the system on physical timescales. The timescale during which the system evolves and measurements are made is much smaller than the corresponding *Poincaré recurrence time* [25, 26] needed for the actual reversibility of the system dynamics. Thus the system is seemingly irreversible.

We begin building the model for quantum dissipation in resistors, the Caldeira-Leggett model in cQED, by analysing the impedances in figure 2.2. We know from basic electrodynamics [21] that the impedances of capacitors and inductors are frequency dependent and are given by

$$Z_{\mathrm{C}}(\omega) = \frac{1}{-\mathrm{i}\omega C}, \qquad Z_{\mathrm{L}}(\omega) = -\mathrm{i}\omega L, \tag{2.17}$$

where C and L are respectively the corresponding capacitance and inductance of the elements and ω is the angular frequency of the AC signal which is used to drive the circuit. Using the impedances from equation (2.17), we can find the impedance of a single parallel LC-circuit, like the one in figure 2.1, as

$$Z_{\mathrm{LC}_{||}} = \left(-\mathrm{i}\omega C + \frac{\mathrm{i}}{\omega L} \right)^{-1}. \tag{2.18}$$

Here we used the well known fact that impedances in parallel sum as their reciprocals. We can write the above expression in terms of the resonance frequency $\omega_{\mathrm{r}} = 1/\sqrt{LC}$ of the oscillator as

$$Z_{\mathrm{LC}_{||}} = \frac{\mathrm{i}}{2C}\left(\frac{1}{\omega + \omega_{\mathrm{r}}} + \frac{1}{\omega - \omega_{\mathrm{r}}} \right). \tag{2.19}$$

Using equation (2.19) we can write the total impedance $Z_\infty(\omega)$ of the network in figure 2.2 as a sum of the individual LC-oscillator impedances, each of which has a different capacitance C_j and resonance frequency ω_j:

$$Z_\infty(\omega) = \sum_{j=1}^{\infty} \frac{\mathrm{i}}{2C_j}\left(\frac{1}{\omega + \omega_j} + \frac{1}{\omega - \omega_j} \right). \tag{2.20}$$

Following the procedure in [10], we choose the different capacitances C_j and resonance frequencies ω_j such that they are described by some very small frequency difference $\Delta\omega$, which is the difference in the resonance frequencies between two neighbouring oscillators in the decomposition:

$$C_j = \frac{\pi}{2\Delta\omega \mathrm{Re}[Z(j\Delta\omega)]}, \qquad \omega_j = j\Delta\omega, \tag{2.21}$$

where $Z(\omega)$ is the impedance whose action we want to mimic through the decomposition. This will later be set to (approximately, in a certain range) the impedance of the resistor (that is the resistance R). Using the equation (2.21) above and the formula for the resonance frequency, we can compute the corresponding inductance L_j of each oscillator in figure 2.2. We get

$$L_j = \frac{2\Delta\omega \mathrm{Re}[Z(j\Delta\omega)]}{\pi\omega_j^2}. \tag{2.22}$$

We can now plug the chosen capacitance values from equation (2.21) to equation (2.20) describing the total impedance Z_∞ of the oscillator network. This yields

$$Z_\infty(\omega) = \sum_{j=1}^{\infty} \frac{\mathrm{i}}{\pi}\Delta\omega \mathrm{Re}[Z(\omega_j)]\left(\frac{1}{\omega + \omega_j} + \frac{1}{\omega - \omega_j} \right). \tag{2.23}$$

The summation over j essentially goes over the whole frequency space in steps of $\Delta\omega$ because of the definition from equation (2.21): $\omega_j = j\Delta\omega$. Thus if we let $\Delta\omega$ to become infinitesimal, we can replace the sum by an integral over ω_j

$$\begin{aligned} Z_\infty(\omega) &= \frac{\mathrm{i}}{\pi}\int_0^\infty \mathrm{d}\omega_j \mathrm{Re}[Z(\omega_j)]\left(\frac{1}{\omega+\omega_j}+\frac{1}{\omega-\omega_j}\right) \\ &= \frac{\mathrm{i}}{\pi}\int_0^\infty \mathrm{d}\omega_j \frac{\mathrm{Re}[Z(\omega_j)]}{\omega+\omega_j} + \frac{\mathrm{i}}{\pi}\int_0^\infty \mathrm{d}\omega_j \frac{\mathrm{Re}[Z(\omega_j)]}{\omega-\omega_j}. \end{aligned} \tag{2.24}$$

In the above equation we have faced a small problem. The first term on the right-hand side of equation (2.24) does not converge for $\omega < 0$ and the second term does not converge for $\omega > 0$. To face this issue, we introduce a small term $\mathrm{i}\epsilon$ in the denominators, which pulls our integrand to the complex plane. This allows us to use the results of complex analysis to our advantage, more specifically the Sokhotski-Plemelj theorem for the real line, which states that

$$\lim_{\epsilon\to 0^+}\int_a^b \mathrm{d}x \frac{f(x)}{x\pm\mathrm{i}\epsilon} = \mp\mathrm{i}\pi f(0) + \mathrm{P.V.}\int_a^b \mathrm{d}x\frac{f(x)}{x}, \tag{2.25}$$

where $a < 0 < b$, f is defined and continuous on the integration interval and P.V. denotes the Cauchy principal value. Assigning the small imaginary term to the denominators of integrals in equation (2.24) gives us the following form, where the Sokhotski-Plemelj theorem (2.25) can be used:

$$Z_\infty(\omega) = \lim_{\epsilon\to 0^+}\frac{\mathrm{i}}{\pi}\int_0^\infty \mathrm{d}\omega_j \frac{\mathrm{Re}[Z(\omega_j)]}{\omega+\omega_j+\mathrm{i}\epsilon} + \frac{\mathrm{i}}{\pi}\int_0^\infty \mathrm{d}\omega_j \frac{\mathrm{Re}[Z(\omega_j)]}{\omega-\omega_j+\mathrm{i}\epsilon}. \tag{2.26}$$

Now we need to analyse the integrals in the above equation in the two regimes, where the angular frequency ω is either positive or negative.

$\underline{\omega < 0}$:
The second integral in (2.26) doesn't diverge since $\omega < 0$ so we can take the limit $\epsilon \to 0$ there to get

$$Z_\infty(\omega) = \lim_{\epsilon\to 0^+}\frac{\mathrm{i}}{\pi}\int_0^\infty \mathrm{d}\omega_j \frac{\mathrm{Re}[Z(\omega_j)]}{\omega+\omega_j+\mathrm{i}\epsilon} + \frac{\mathrm{i}}{\pi}\int_0^\infty \mathrm{d}\omega_j \frac{\mathrm{Re}[Z(\omega_j)]}{\omega-\omega_j}. \tag{2.27}$$

To the first integral we employ a change of variables $x = \omega + \omega_j$ to get the integral into the proper form for Sokhotski-Plemelj theorem (2.25):

$$Z_\infty(\omega) = \lim_{\epsilon\to 0^+}\frac{\mathrm{i}}{\pi}\int_\omega^\infty \mathrm{d}x \frac{\mathrm{Re}[Z(x-\omega)]}{x+\mathrm{i}\epsilon} + \frac{\mathrm{i}}{\pi}\int_0^\infty \mathrm{d}\omega_j \frac{\mathrm{Re}[Z(\omega_j)]}{\omega-\omega_j}. \tag{2.28}$$

Applying (2.25) to the first integral gives

$$Z_\infty(\omega) = \mathrm{Re}[Z(\omega)] + \frac{\mathrm{i}}{\pi}\left[\int_0^\infty \mathrm{d}\omega_j \frac{\mathrm{Re}[Z(\omega_j)]}{\omega-\omega_j} + \mathrm{P.V.}\int_0^\infty \mathrm{d}\omega_j \frac{\mathrm{Re}[Z(\omega_j)]}{\omega+\omega_j}\right], \tag{2.29}$$

where we also changed back to the original integration variable.

$\underline{\omega > 0}$:
Now the first integral in (2.26) doesn't diverge since $\omega > 0$ so we can take the limit $\epsilon \to 0$ there to get

$$Z_\infty(\omega) = \frac{\mathrm{i}}{\pi}\int_0^\infty \mathrm{d}\omega_j \frac{\mathrm{Re}[Z(\omega_j)]}{\omega+\omega_j} + \lim_{\epsilon\to 0^+}\frac{\mathrm{i}}{\pi}\int_0^\infty \mathrm{d}\omega_j \frac{\mathrm{Re}[Z(\omega_j)]}{\omega-\omega_j+\mathrm{i}\epsilon}. \tag{2.30}$$

Now employing a change of variables $x = \omega - \omega_j$ to the second integral to get it to the same form as in (2.25):

$$Z_\infty(\omega) = \frac{\mathrm{i}}{\pi}\int_0^\infty \mathrm{d}\omega_j \frac{\mathrm{Re}[Z(\omega_j)]}{\omega+\omega_j} + \lim_{\epsilon\to 0^+}\frac{\mathrm{i}}{\pi}\int_{-\infty}^\omega \mathrm{d}x \frac{\mathrm{Re}[Z(\omega-x)]}{x+\mathrm{i}\epsilon}. \tag{2.31}$$

Again we can apply Sokhotski-Plemelj (2.25) to the second integral to get

$$Z_\infty(\omega) = \mathrm{Re}[Z(\omega)] + \frac{\mathrm{i}}{\pi}\left[\int_0^\infty \mathrm{d}\omega_j \frac{\mathrm{Re}[Z(\omega_j)]}{\omega+\omega_j} + \mathrm{P.V.}\int_0^\infty \mathrm{d}\omega_j \frac{\mathrm{Re}[Z(\omega_j)]}{\omega-\omega_j}\right], \tag{2.32}$$

where we again moved back to the original integration variable.

Comparing the impedances $Z_\infty(\omega)$ from equations (2.29) and (2.32), we can see that they look very similar. We can combine the two results together into one equation[9]

$$Z_\infty(\omega) = \mathrm{Re}[Z(\omega)] + \frac{\mathrm{i}}{\pi}\left[\mathrm{P.V.}\int_0^\infty \mathrm{d}\omega_j \frac{\mathrm{Re}[Z(\omega_j)]}{\omega+\omega_j} + \mathrm{P.V.}\int_0^\infty \mathrm{d}\omega_j \frac{\mathrm{Re}[Z(\omega_j)]}{\omega-\omega_j}\right], \tag{2.33}$$

and notice that

$$\mathrm{Re}[Z_\infty(\omega)] = \mathrm{Re}[Z(\omega)], \tag{2.34}$$

$$\mathrm{Im}[Z_\infty(\omega)] = \frac{1}{\pi}\left[\mathrm{P.V.}\int_0^\infty \mathrm{d}\omega_j \frac{\mathrm{Re}[Z(\omega_j)]}{\omega+\omega_j} + \mathrm{P.V.}\int_0^\infty \mathrm{d}\omega_j \frac{\mathrm{Re}[Z(\omega_j)]}{\omega-\omega_j}\right]. \tag{2.35}$$

We can see from the above equations that we have managed to obtain a real part for the impedance $Z_\infty(\omega)$. This is quite remarkable because remembering that the impedance of a single LC-oscillator given in equation (2.19) is purely imaginary, we were able to produce something real from an infinite series of imaginary impedances. Mathematically this was possible due to one of the key assumptions in the Caldeira-Leggett model for the resistor, namely assuming of having the resonance frequencies for the individual oscillators infinitesimally close to each other. This allowed for integration over the whole frequency space and, by using the tools of complex analysis, gave rise to a real impedance that happens to match the real part of the impedance of which we are interested in. A physical argument is provided in Ref. [10]. Dealing with an infinite series of LC-circuits corresponds to sending a signal down the infinitely long chain of LC-circuits and since the signal will never reach the end of the chain it will never reflect from the end returning to the start of the chain.

[9] We obtained equation (2.33) by considering cases $\omega < 0$ and $\omega > 0$. The case $\omega = 0$, corresponding to DC current, is trivial with vanishing impedance as can be seen from equation (2.20). If we deal with AC signals we need not bother about this.

Therefore we will not observe any recurrence time for the signals, since they are travelling through the LC-chain forever. This is seen as dissipation at the input.

We can now choose the impedance of interest $Z(\omega)$ in equations (2.34) and (2.35) such that it stays approximately constants with respect to frequency, mimicking the behaviour of a real resistor. This behaviour is obtained, for example, by choosing [10]

$$Z_{\mathrm{R}}(\omega) = R\frac{\omega_C^2}{\omega_C^2+\omega^2} + \mathrm{i}R\frac{\omega\omega_C}{\omega_C^2+\omega^2}, \tag{2.36}$$

where R is the resistance of the resistor and ω_C is some large cutoff frequency such that the above equation is valid in the range $\omega \ll \omega_C$[10]. In this range we get the simple result for the impedance $Z_\infty(\omega)$ of the infinite LC-oscillator network as $Z_\infty(\omega) \approx R$, because the imaginary part is vanishingly small.

So far we have been able to produce a network consisting of parallel LC-oscillators shown in figure 2.2 and to show that this infinite network manages to produce an impedance that is equivalent to a usual resistor in a certain frequency range. Thus we can indeed think of the resistor as an infinite collection of LC-oscillators. This makes the final step in the derivation of the quantum dissipation, that is the Caldeira-Leggett model, for cQED straightforward. The last step is to express the resistor in the Hamiltonian formalism, that is to quantize it.

Knowing that the resistor can be modelled as a collection of LC-oscillators, we can quantize it by considering the quantization of the separate LC-oscillators that constitute the network. We choose to parametrize the problem as shown in figure 2.2, where each of the fluxes ϕ_j is associated with the voltage difference over the jth LC-circuit [10]. In this way the LC-circuits are not coupled and can be treated as independent harmonic oscillators with angular frequency ω_j. Applying the quantization procedure described in section 2.1 to each LC-oscillator, we get the Hamiltonian of the resistor as

$$H_{\mathrm{R}} = \sum_{j=1}^{\infty} \hbar\omega_j(\hat{a}_j^\dagger\hat{a}_j + 1/2) = \sum_{j=1}^{\infty} \hbar\omega_j\hat{a}_j^\dagger\hat{a}_j + \sum_{j=1}^{\infty}\hbar\omega_j/2\,. \tag{2.37}$$

The last term is just a constant, arising from the summation over the resonance frequencies of the LC-oscillator or, physically, over the modes of the electromagnetic field. Fortunately this term can be discarded because of two reasons. The first one is that Hamiltonian dynamics are not affected by the addition or removal of constants. The second reason rephrases the first one in a more experimentally oriented way. The argument provided by Peskin and Schroeder in the Introduction to Quantum Field Theory textbook [27] is that the infinite constant, the sum over all modes of the zero-point energies, cannot be actually measured because the experimentalists detect only energy differences from the ground state of the Hamiltonian. In the context of quantum optics, the same problem is discussed more in depth in [28] before getting to the same conclusion that the infinite energy term can be thrown away. Thus we ignore the last term in equation (2.37) here and in all of the calculations that follow.

[10] Note that the choice of the real part of impedance $Z_{\mathrm{R}}(\omega)$ gives rise to the imaginary part, as can be seen from equation (2.35). In Appendix A it is shown that equation (2.36) does indeed fulfil equations (2.34) and (2.35).

Finally, we have obtained a simple form for the resistor Hamiltonian

$$H_{\mathrm{R}} = \sum_{j=1}^{\infty} \hbar\omega_j \hat{a}_j^{\dagger}\hat{a}_j \,. \tag{2.38}$$

We can interpret this equation as meaning that the resistor acts as a bosonic bath with an infinite number of modes. Coupling a system to this bath will result in dissipation of the system's energy into the resistor and its infinite degrees of freedom.

In conclusion, we have managed to obtain a Hamiltonian description for a resistor, that captures its inherently dissipative and non-reversible behaviour by describing it as an infinite collection of non-dissipative components. Starting from an extended Foster's first form in figure 2.2 and quantizing it we end up to equation (2.38), which shows that the Caldeira-Leggett model essentially deals with the description of quantum dissipation arising from the infinite bosonic bath.

When we couple the bath to another quantum system and let them interact, we can observe decoherence effects on the smaller system of interest. Usually this smaller system is a qubit or a qubit and its readout circuitry. In the next section we will focus on the theoretical description of qubits in the cQED formalism.

2.3 ABOUT QUANTUM BITS

The modern world is built on digital technology. And digital technology, at its most fundamental level, is built on *bits*. Streams of zeros and ones are part of our everyday life without us noticing them or paying too much attention to them. The flow of bits grants us an abundance of information on almost anything we can imagine, sometimes even if we are not in need of it. Indeed, the bit is a fundamental concept in classical information theory describing a basic unit of classical information. Analogously, in the quantum world, the *quantum bit*, or qubit for short, is a basic unit of quantum information. The fields of quantum information and quantum computation are built solely upon the study of qubits [5] but they are useful also in other areas of novel quantum technologies such as quantum communication, metrology and sensing to name a few [29].

Qubits can be discussed in two distinctly different ways. On one hand they are some abstract mathematical objects with certain properties that make them useful for computation and carriers of information. This way of thinking about them is purely theoretical but allows us to understand how they behave generally, without worrying about the exact physical implementation of them [5]. But, on the other hand, experimental physicists and engineers must be able to somehow realize the qubits as real-life, physical objects. Somehow the mathematical properties of the qubits need to be brought into this realization that can be used in experiments. This section aims to explain how the connection between the abstract mathematical point of view and real-life implementation of a qubit is made.

2.3.1 THEORETICAL DESCRIPTION OF A QUBIT

A classical bit can be only in one of the two states 0 or 1, whereas as a qubit can be in its ground state $|0\rangle$, in its excited state $|1\rangle$ or in any superposition of these two states[11]

$$|\psi\rangle = \alpha|0\rangle + \beta|1\rangle\,, \tag{2.39}$$

with $\alpha, \beta \in \mathbb{C}$ and $|\alpha|^2 + |\beta|^2 = 1$. Therefore, in principle, the number of possible states for a qubit is infinite, whereas for a classical bit the number of possible states is two. The ground and excited states $|0\rangle$ and $|1\rangle$ are also called the *computational basis states* and they form and orthonormal basis of the two dimensional Hilbert space of the qubit [5].

Even though the quantum state of the qubit $|\psi\rangle$ is a superposition of the basis states (and with infinitely many possible combinations), we must stress that once the qubit undergoes a measurement the state *collapses* to one of the two possible basis states. Thus we can only observe either the qubit giving an answer 0 or 1 but with probabilities given by $|\alpha|^2$ and $|\beta|^2$ respectively. This collapse of the wave function is a fundamental property of quantum mechanics and its meaning and origin have been debated since the beginning of quantum theory [30]. But rather than focusing on the discussion on the interpretation of the fundamental principles of quantum theory (such as superposition, entanglement and tunneling), we take them as mathematical consequences of the theory and focus on constructing a useful picture of the quantum state of the qubit. This picture will help us to understand how different environmental effects such as dissipation and dephasing affect the qubit's quantum state.

A useful picture to think about the quantum state of the qubit is the geometrical representation called the *Bloch sphere* [5]. This allows us to visualize the quantum state geometrically as a point within a sphere.

We start by noting that the complex coefficients α and β in Eq. (2.39) can be written as $\alpha = r_\alpha e^{ia}$ and $\beta = r_\beta e^{ib}$ for some real numbers r_α and r_β describing the magnitude, and a and b describing the phase of α and β respectively. Thus the *pure state* $|\psi\rangle$ can be written as

$$|\psi\rangle = r_\alpha e^{ia}|0\rangle + r_\beta e^{ib}|1\rangle\,. \tag{2.40}$$

Equation (2.39) can be multiplied by a phase factor e^{-ia} without changing the measurement outcomes because the probabilities given by the coefficients $\alpha' = e^{-ia}\alpha$ and $\beta' = e^{-ia}\beta$ are invariant:

$$|\alpha'|^2 = \alpha e^{-ia}\alpha^* e^{ia} = \alpha\alpha^* = |\alpha|^2$$

and similarly for $|\beta'|^2$. We can say that the *global phase* of the quantum state can be neglected. Thus we can write the qubit state as

$$|\psi'\rangle = e^{-ia}|\psi\rangle = r_\alpha|0\rangle + r_\beta e^{i(b-a)}|1\rangle = r_\alpha|0\rangle + r_\beta e^{i\phi}|1\rangle\,, \tag{2.41}$$

[11] It should be noted that here we describe the qubit as a perfect two-level system but qubits with more than two levels can also be treated theoretically. These are called *qutrits* for three distinct levels or *qudits* for $n > 3$ distinct excitation levels [5, 20].

where we defined $\phi = b - a$. We have now reduced the number of necessary parameters to describe the quantum state from four to three. Next we change the coefficient of basis state $|1\rangle$ from polar coordinates to cartesian coordinates, giving simply

$$|\psi'\rangle = r_\alpha |0\rangle + (x + \mathrm{i}y)|1\rangle . \tag{2.42}$$

To this form we apply the normalization condition $\langle\psi'|\psi'\rangle = 1$ giving us

$$r_\alpha^2 + |x + \mathrm{i}y|^2 = r_\alpha^2 + x^2 + y^2 = 1 .$$

This is an equation for a unit sphere in cartesian coordinates. Now we can transform from the cartesian coordinates to spherical coordinates. The factor r_α represents now the z coordinate. The coordinate transformation is given by $x = r\sin\theta\cos\phi$, $y = r\sin\theta\sin\phi$, $z = r\cos\theta$, with $\theta \in [0,\pi]$ and $\phi \in [0,2\pi]$. Now with radius $r = 1$ we get from Eq. 2.42

$$|\psi'\rangle = \cos\theta|0\rangle + \sin\theta(\cos\phi + \mathrm{i}\sin\phi)|1\rangle = \cos\theta|0\rangle + \mathrm{e}^{\mathrm{i}\phi}\sin\theta|1\rangle , \tag{2.43}$$

with only two real parameters θ and ϕ defining the pure quantum state. However, there is some redundancy in the above expression because some points are counted twice. Let's consider two quantum states $|\psi\rangle$ and $|\psi\rangle_o$, which are exactly opposite to each other. The state $|\psi\rangle$ corresponds to a point $(1,\theta,\phi)$ on the surface of a sphere and its basis representation is

$$|\psi\rangle = \cos\theta|0\rangle + \mathrm{e}^{\mathrm{i}\phi}\sin\theta|1\rangle .$$

The state $|\psi\rangle_o$ corresponds to a point $(1,\pi-\theta,\pi+\phi)$. Its basis representation is then

$$\begin{aligned} |\psi\rangle_o &= \cos(\pi-\theta)|0\rangle + \mathrm{e}^{\mathrm{i}(\pi+\phi)}\sin(\pi-\theta)|1\rangle \\ &= -\cos\theta - \mathrm{e}^{\mathrm{i}\phi}\sin\theta|1\rangle \\ &= -|\psi\rangle . \end{aligned}$$

We see from the above that when a quantum state $|\psi\rangle$ moves to a point on the surface of the sphere which is opposite to its original place it picks up a minus sign. This is a global phase factor and we know that it can be neglected since it doesn't affect the measurement results. Thus in the Bloch sphere representation we restrict the angle θ to only half values ($\theta \in [0,\pi/2]$) to get rid of the redundancy. This is obtained by using half angles in the qubit state equation

$$|\psi\rangle = \cos\frac{\theta}{2}|0\rangle + \mathrm{e}^{\mathrm{i}\phi}\sin\frac{\theta}{2}|1\rangle . \tag{2.44}$$

The pictorial representation of an arbitrary state $|\psi\rangle$ on the Bloch sphere is shown in figure 2.3. The $\hat{z}$ axis of the Bloch sphere is the qubit quantization axis and is named the *longitudinal axis* and the $\hat{y}$ and $\hat{x}$ axes are both called *transverse axis* [8].

In the derivation of equation (2.44) we assumed initially that the qubit is in a pure state as in equation (2.39). This gave us a Bloch sphere representation for the pure states being the points on the surface of the sphere. Next we aim to extend this picture to *mixed states*, which are represented by density matrices.

A qubit density matrix is a 2×2 positive semi-definite Hermitian matrix with unit trace [31]. The Pauli matrices together with the identity matrix constitute a basis on the vector

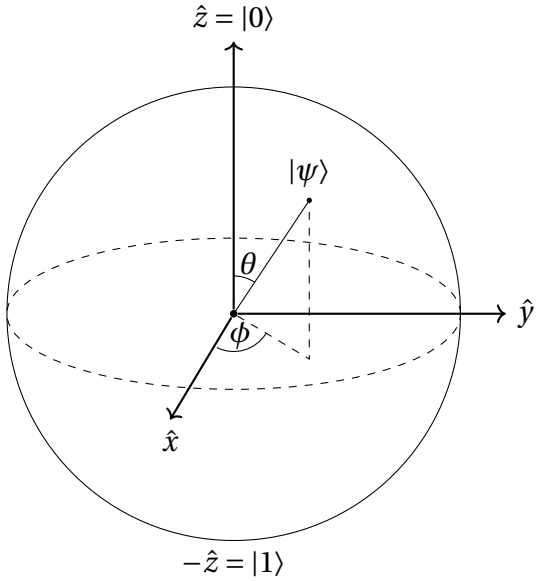

Figure 2.3: A Bloch sphere representation of a single, arbitrary qubit state $|\psi\rangle$.

space of complex 2×2 matrices. Thus we can write the qubit density matrix in this basis decomposition as

$$\rho = r_1 \mathbb{1} + r'_x \sigma_x + r'_y \sigma_y + r'_z \sigma_z = \begin{bmatrix} r_1 + r'_z & r'_x - \mathrm{i} r'_y \\ r'_x + \mathrm{i} r'_y & r_1 - r'_z \end{bmatrix},$$

with some real coefficients r_1, r'_x, r'_y, r'_z. The restriction of unit trace sets $\mathrm{Tr}(\rho) = 1 \Rightarrow r_1 = \frac{1}{2}$. Therefore we can write the mixed state density matrix as

$$\rho = \frac{1}{2} \begin{bmatrix} 1 + r_z & r_x - \mathrm{i} r_y \\ r_x + \mathrm{i} r_y & 1 - r_z \end{bmatrix} = \frac{\mathbb{1} + \mathbf{r} \cdot \sigma}{2}, \tag{2.45}$$

where we defined the *Bloch vector* $\mathbf{r}$ as $\mathbf{r} = (r_x, r_y, r_z) = (2r'_x, 2r'_y, 2r'_z)$ and $\sigma = (\sigma_x, \sigma_y, \sigma_z)$. Positive semi-definiteness of the density matrix restricts all of the eigenvalues of ρ to being positive, thus forcing the determinant to be positive.[12] This gives us the following condition:

$$\det(\rho) = \frac{1}{2}(1 - r_x^2 - r_y^2 - r_z^2) \geq 0. \tag{2.46}$$

From here notice that the case in which $r_x^2 + r_y^2 + r_z^2 = 1$ corresponds to the surface of the sphere and is the case of a pure state that we derived earlier. However equation (2.46) does not restrict us to the surface of the sphere. The points within the sphere are also available. The restriction we get for equation (2.45) from Eq. (2.46) is that $|\mathbf{r}|^2 \leq 1$. If $|\mathbf{r}|^2 = 1$ we have a pure state and if $|\mathbf{r}|^2 < 1$ we have a mixed state. An interesting point to note is the origin of the Bloch sphere, which corresponds to $|\mathbf{r}|^2 = 0$. In that case we have $\rho = \mathbb{1}/2$, which is the *maximally mixed state*.

[12] This is because the determinant of a matrix is equal to the product of its eigenvalues. Thus if all eigenvalues are positive, then so is the determinant [32].

We have now gone through the derivation of the Bloch sphere representation for a single qubit. It gives a concise geometrical interpretation of a qubit's quantum state, whether it be pure or mixed. However, we need to note that the intuition we gain from this description is limited because there does not exist a known, simple generalization of the Bloch sphere for multiple qubits [5]. Nevertheless, for single qubit states we can use it to better understand the effects of certain operations and phenomena by seeing how these effects change the state on the Bloch sphere. We return to these processes in chapter 5, when we consider the effect of environmental coupling to quantum states. Next we turn our attention to a physical implementation of the qubit and see that while the theoretical treatment of the qubit as a perfect two level system is beautifully concise, the reality is a bit more complicated.

2.3.2 PHYSICAL IMPLEMENTATION: A TRANSMON QUBIT

As discussed before, qubits are two level systems. Thus any physical realization of a qubit must have two distinct quantum states that can be distinguished from the other possible states of the system [33]. This is trivial if the physical set-up is naturally two level, such as an electron with spin $\frac{1}{2}$ or a photon with horizontal and vertical polarization. While manufacturing qubits using electrons [34] or photons [35] is possible, the main way of realizing qubits nowadays are the superconducting qubits using the cQED architecture [13, 7] we have been discussing in this chapter. These systems have inherently more than two possible energy levels, so care must be taken when manufacturing them to make sure a qubit-like behaviour can be obtained. Now we shall discuss a *transmission-line shunted plasma oscillation qubit* or a transmon developed by Koch et al. in 2007 [36], which is the most popular way of realizing a superconducting qubit at this time [7]. We shall see how it is built from actual circuit elements using cQED architecture and what design choices enable it to function as a qubit.

A transmon is a specific type of qubit developed from a so-called *Cooper pair box*, in which the basis states represent the presence or absence of superconducting charge carriers, *Cooper pairs*, in the superconducting chip [18]. In the most simple terms we can analyze the transmon as a quantum LC-oscillator (like in figure 2.1), where the linear inductor is replaced by a *Josephson junction* with a non-linear inductance [20, 8]. This is depicted in figure 2.4. Let's take a closer look at how this works and enables us to construct a working qubit.

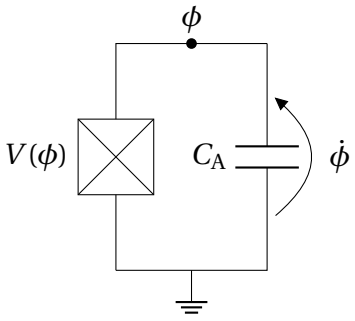

Figure 2.4: A transmon qubit built from a Josephson junction (box with a cross) and a shunt capacitor.

A Josephson junction is a superconducting circuit element, which has two superconducting islands separated by a non-superconducting insulator. The Cooper pairs in the superconducting regions can tunnel through the insulator in a phenomenon called the *Josephson effect* [37]. The Josephson junction is depicted in figure 2.5. The Josephson effect creates an observable current through and voltage across

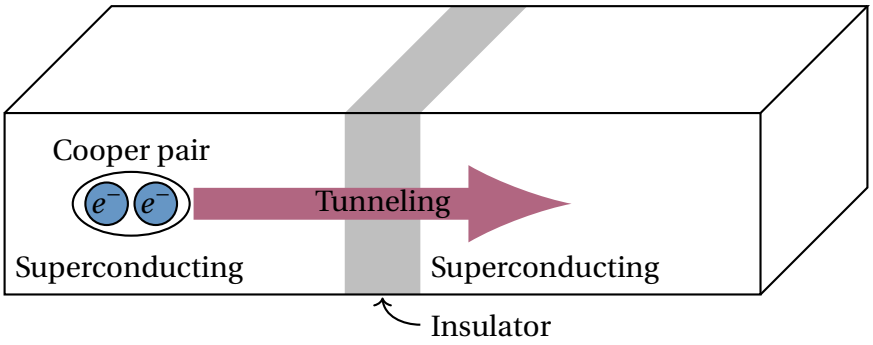

Figure 2.5: Schematic of a Josephson junction. A non-superconducting insulator separates two superconducting regions. The Cooper pairs can tunnel back and forth between the superconducting materials through the insulating barrier. Figure adapted from [20].

the junction, whose values are given by the equations [20]

$$I(t) = I_c \sin(\chi(t)), \tag{2.47}$$

$$V(t) = \frac{\hbar}{2e}\dot{\chi}(t), \tag{2.48}$$

where χ is a superconducting phase difference between the two islands and I_c is the critical current of the junction, depending on its exact geometry. Integrating equation (2.48) with respect to time gives us a relation between the superconducting phase difference χ and the generalized flux ϕ through the junction as $\phi = \hbar\chi/(2e)$. Using this expression in equation (2.47) gives the following relation between the current and generalized flux:

$$I(t) = \dot{Q}(t) = I_c \sin\left(\frac{2e\phi(t)}{\hbar}\right) = I_c \sin\left(2\pi\frac{\phi(t)}{\phi_0}\right), \tag{2.49}$$

where we used the definition of superconducting magnetic flux quantum $\phi_0 = h/(2e)$ from section 2.1. As we have an equation for the current in terms of generalized flux, we can compute the inductance this produces as [15, 20]

$$L(\phi) = \left(\frac{\partial I}{\partial \phi}\right)^{-1} = \frac{\phi_0}{2\pi I_c}\frac{1}{\cos\left(2\pi\frac{\phi}{\phi_0}\right)} = \frac{L_J}{\cos\left(2\pi\frac{\phi}{\phi_0}\right)}, \tag{2.50}$$

where we defined the *Josephson inductance* $L_J = \phi_0/(2\pi I_c)$. We can immediately notice that the inductance of the Josephson junction is non-linear and dependent on the flux ϕ. This behaviour is crucial in the construction of a superconducting qubit as we will see later.

We would like now to find the Lagrangian of the transmon circuit in figure 2.4 in a similar manner as we did in section 2.1. This requires finding the corresponding energies for the circuit elements. The shunt capacitor has not changed so its energy is the same as in equation (2.2) but the inductive energy of the Josephson junction needs to be calculated.

To obtain the inductive energy of the Josephson junction we can think about how much power has gone through the element from the beginning of dynamics to some arbitrary

time t. The power of the junction is of course given by

$$P(t) = V(t)I(t) = \dot{\phi}(t)I_\mathrm{c}\sin\left(2\pi\frac{\phi(t)}{\phi_0}\right). \tag{2.51}$$

Integrating this from $t' = -\infty$ to $t' = t$ gives the stored energy in the inductor. The time $t' = -\infty$ means a time sufficiently far in the past when the circuit was at rest with no currents or voltages affecting it. The energy of the Josephson junction becomes

$$E(\phi) = \int_{-\infty}^{t} P(t')\mathrm{d}t' = \left(\frac{\phi_0}{2\pi}\right)^2\frac{1}{L_\mathrm{J}}\left[1-\cos\left(2\pi\frac{\phi(t)}{\phi_0}\right)\right] = E_\mathrm{J}\left[1-\cos\left(2\pi\frac{\phi(t)}{\phi_0}\right)\right], \tag{2.52}$$

where $E_\mathrm{J} = \phi_0^2/((2\pi)^2 L_\mathrm{J})$ is the *Josephson energy*. We can see that the energy is also non-linear. Now we are ready to build the Lagrangian of the transmon circuit:

$$\mathscr{L} = \frac{1}{2}C_\Sigma\dot{\phi}^2 - E_\mathrm{J}\left[1-\cos\left(2\pi\frac{\phi(t)}{\phi_0}\right)\right] = \frac{1}{2}C_\Sigma\dot{\phi}^2 + E_\mathrm{J}\cos\left(2\pi\frac{\phi(t)}{\phi_0}\right), \tag{2.53}$$

where the constant term was dropped out since the Lagrangian and Hamiltonian equations are invariant with respect to the addition of a constant. The parameter $C_\Sigma = C_\mathrm{A} + C_\mathrm{J}$ is now the sum of the shunt capacitance C_A and the self-capacitance of the junction C_J [8]. From the transmon Lagrangian (2.53) we get the Hamiltonian via the Legendre transformation:

$$H = \frac{Q}{2C_\Sigma} - E_\mathrm{J}\cos\left(2\pi\frac{\phi(t)}{\phi_0}\right). \tag{2.54}$$

Now we are almost ready to quantize the equation. Before that, we perform the same change of variables used in section 2.1 in approach 2 to the LC-circuit quantization. Now we see why it was useful to think about reduced charge and flux back then. Noticing that the argument of the cosine function is exactly the reduced flux $\Phi = 2\pi\phi/\phi_0$ and that the reduced charge becomes again $n = Q/(2e)$, we get [8]

$$H = 4E_\mathrm{C}n^2 - E_\mathrm{J}\cos(\Phi) \quad \Rightarrow \quad \hat{H} = 4E_\mathrm{C}\hat{n}^2 - E_\mathrm{J}\cos(\hat{\Phi}). \tag{2.55}$$

The Hamiltonian was quantized by promoting the variables n and Φ to corresponding operators with the commutation relation $\left[\hat{\Phi},\hat{n}\right] = \mathrm{i}$ (see equation (2.14)). The appearance of the cosine term in the Hamiltonian arises from the non-linear inductive potential of the Josephson junction. This makes the qubit with Hamiltonian (2.55) an anharmonic oscillator. Its energy levels are not evenly spaced like in the case of a quantum harmonic oscillator. They are much more complex and given in terms of Mathieu functions. The exact energy levels for Hamiltonian (2.55) can be found in Koch et al. [36].

The unevenness of the energy levels spacing allows us to separate the two lowest energy levels as a computational subspace for qubit operations.[13] If the spacing were even with $\omega_{n,n+1} = \hbar\omega_\mathrm{r}$ for all n, we could not distinguish between the different excitation states. Sending a pulse with energy $\hbar\omega_\mathrm{r}$ could lead to excitation $|1\rangle \rightarrow |2\rangle$ (or any other jump to the next energy level), which is not what we want. The anharmonicity of the inductive potential

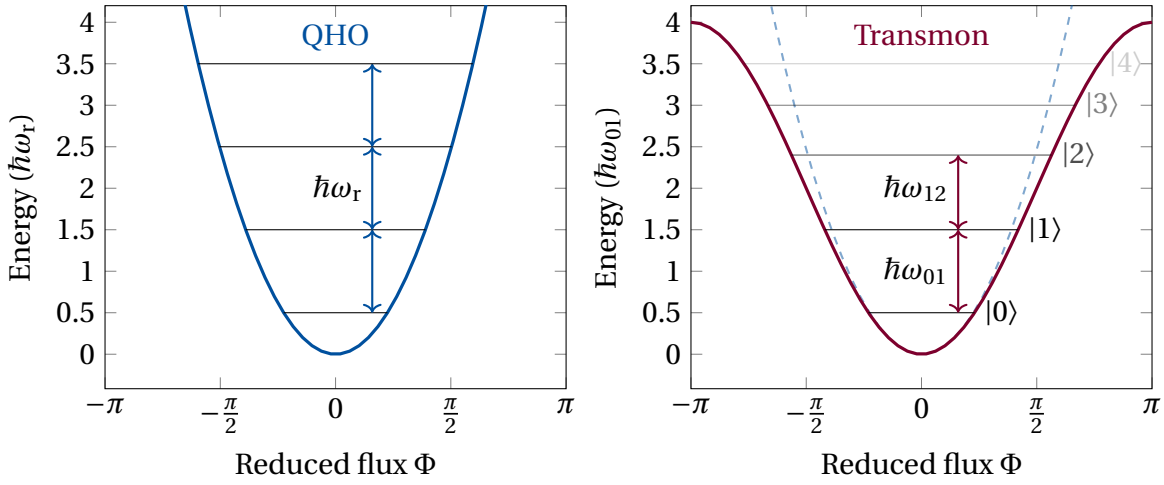

Figure 2.6: The quadratic potential of the harmonic oscillator yields equidistantly spaced energy levels (in blue). The transmon potential is sinusoidal and thus non-linear (in red). It yields nonequidistant energy levels[14], thus allowing to isolate levels $|0\rangle$ and $|1\rangle$ as a computational subspace. Figure adapted from [8].

leads to $\omega_{01} \neq \omega_{12}$ so that we cannot accidentally excite the qubit to unwanted energy levels. The difference between the harmonic and anharmonic potentials is shown in figure 2.6.

To be precise, the Hamiltonian in equation (2.55) holds for both Cooper pair boxes and transmons alike. Now we make a distinction why do we talk about transmons in this thesis. We can see from the Hamiltonian that the coefficients E_C and E_J determine if the Hamiltonian has more capacitive or inductive energy. It turns out that the setup with $E_J \leq E_C$ is highly sensitive to charge noise (variations in $\hat{n}$), and this has been proven challenging to mitigate [8]. The so called *transmon regime* is reached when $E_J \gg E_C$, mitigating the charge noise and allowing for better performance of the qubit [8, 15, 36].[15] The ratio $E_J/E_C \geq 50$ is sufficiently high for the charge noise reduction [36].

◆ ◆ ◆

In this chapter we have introduced the necessary tools and methods of cQED to treat actual circuits, composed of real circut elements, quantum mechanically. We started by considering the treatement of the simple but useful case of an LC-oscillator and its

[13] When neglecting the higher excited states, the anharmonicity is paired with very low temperatures of the qubit chip, which makes the higher excited states unlikely to be populated. In this way we can choose the two-level system to be the ground and first excited state of our artificial atom, which we then call a qubit.

[14] The energy level values shown for the transmon are just for illustrative purposes. They are not exact. The exact transmon energy levels can be obtained by solving the qubit Hamiltonian (2.55) and the solution is given in [36]. Even though the energy values are not exact the figure points out the clear anharmonicity between the energy levels, which is an important factor in constructing a qubit.

[15] Increasing the E_J/E_C ratio does have a drawback; it decreases the anharmonicity of the energy levels. However, it turns out that by increasing E_J/E_C the noise decreses exponentially while the anharmonicity decreases as a weak power law. Thus we can find a regime of negligible noise but still sufficient anharmonicity for qubit operations [36].

quantization. Then we moved to discuss a more complex case of a resistive, dissipative element and its quantization. Albeit quantum mechanics describes inherently reversible processes, we were able to construct a quantum description of a resistor using the extended Foster's first form for the resistor as an infinite series of parallel LC-oscillators. Quantization of this yielded the Caldeira-Leggett model for the resistor, leading us to think about it as a bath of infinite harmonic oscillators. In the last section we discussed the theory of quantum bits and looked at a specific type of qubit physical implementation, namely the transmon qubit. We traced the steps needed to understand how this differs from other superconducting qubits and how it is treated in the cQED architecture.

All of the above was done with a specific goal in mind: to describe an actual circuit and find its Hamiltonian. But before delving into that, we need to introduce another important theoretical model to describe the qubit and its dynamics. Indeed, the qubit will interact with its environment (if not, then we would not be able to read it). Therefore the qubit is not a closed system but an open quantum system.

3 Theory of Open Quantum Systems

When students studying theoretical physics encounter quantum mechanics for the first time, they meet an idealized version of the theory. In basic quantum mechanics the isolated quantum system lives alone in its Hilbert space, with nothing to interact with. The dynamics of such a system is given by the Schrödinger equation, which the students can solve exactly in some carefully selected cases. However, as is the case in most areas of physics (if not in all of them), this is just an idealization.

In Nature there is no such a thing as an isolated system [38]. On the contrary, in reality every quantum system is open, interacting with an external environment [39]. The quantum states are not alone after all. But the standard treatment of quantum mechanics, where time evolution is unitary, is not sufficient to describe the coupling to environment, which is in itself a large quantum system. We need to expand the theory to the *theory of open quantum systems*, which considers also non-unitary time evolution of states.

As stated, in reality every quantum system is open. Therefore it is easy to imagine that the theory of open quantum systems is found in several subfields of modern physics that somehow deal with quantum phenomena. It is used in atomic and nuclear physics [40], photonics [41], biological physics [42] and in mesoscopic physics [43] to name a few. As this thesis studies the behaviour of a superconducting qubit in a resistive environment, we are applying open quantum systems theory to mesoscopic physics. Also, in the development of quantum technology using superconducting qubits the theory of open quantum systems is used extensively for example in quantum metrology [44, 45], quantum computation [46] or in the study of quantum thermodynamics [47].

A pictorial representation of the prevailing problem with open quantum systems is depicted in figure 3.1. In the most general case a system of interest is actually a subsystem of a much larger system, which also includes the environment. The environment can be for example a radiation field or a thermal bath. It usually consists of many degrees of freedom (much more than in the subsystem) and is often modelled as an infinite collection of harmonic oscillators [31]. Our interest lies in describing the dynamics of the subsystem and inferring the equations of motion for this subsystem from the equations of motion of the total system [38]. We also hope that the dynamics of the subsystem is easier to compute than the dynamics of the total system, environment included.

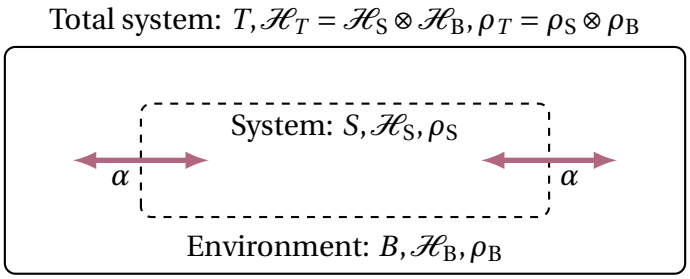

Figure 3.1: A pictorial depiction of an open quantum system. The open system S interacts with the environment B via the coupling α. The total system $T = S + B$ is closed and is the tensor product of the system and environment. Figure adapted from [31].

In this chapter we aim to gain sufficient knowledge of the theory of open quantum systems in order to be able to apply it later to a Hamiltonian describing an actual superconducting qubit and its circuit. We start by recalling standard quantum mechanics and its different pictures, because we first need to understand how closed and isolated quantum systems work before we start loosening the restrictions and start to consider open quantum systems. After the brief review of quantum mechanics, we move to discuss open quantum system dynamics. There we provide a way of deriving the *master equation*, which is the equation of motion for stochastic processes such as quantum state evolution. The derivation presented here is physically motivated but several other ways also exist (see Refs. [31, 39]). Lastly, we meet a formulation which is useful in bringing the derived master equation into a form which is more easily solvable using computer programs.

3.1 BRIEF REMINDER OF QUANTUM MECHANICS

We need to be familiar with the basics of quantum mechanics in order to grasp the nature of the open quantum systems theory. Therefore we briefly recall how the usual quantum mechanics, encountered in the introductory courses, works. The structure of this discussion follows mainly the steps in Breuer and Petruccione [31], starting from the *Schrödinger picture* quantum mechanics after which we consider the Heisenberg and interaction pictures. We don't go through all the mathematical details needed to construct a rigorous quantum theory but only the bits that are most crucial and needed for further discussion about open quantum systems. A reader interested in a more thorough treatment of quantum mechanics can look for the introductory textbooks in quantum mechanics for example from Griffiths [22] or Sakurai [48].

We begin by considering a pure state $|\psi(t)\rangle$ that describes the quantum state of some arbitrary system. According to quantum mechanics, the time-evolution of the state vector $|\psi(t)\rangle$ is given by the Schrödinger equation

$$\mathrm{i}\hbar \frac{\mathrm{d}}{\mathrm{d}t} |\psi(t)\rangle = \hat{H}(t) |\psi(t)\rangle \,. \tag{3.1}$$

The Hamiltonian operator $\hat{H}(t)$ describes the total energy of the system which, in general,

can depend on time. The Schrödinger equation can be solved by postulating[1] the existence of a time-evolution operator $\hat{U}(t, t_0)$ such that it transforms the state vector from an earlier time t_0 to a later time t:

$$|\psi(t)\rangle = \hat{U}(t, t_0)\,|\psi(t_0)\rangle\,. \tag{3.2}$$

For simplicity let's set $t_0 = 0$ for here on out. Clearly the time-evolution operator has an initial condition $\hat{U}(t, t) = \mathbb{1}$ for any time t, since if the time is not evolving the state $|\psi(t)\rangle$ must stay the same. Let's now plug equation (3.2) into (3.1) to get a differential equation for $\hat{U}(t,0)$

$$\mathrm{i}\hbar\frac{\mathrm{d}}{\mathrm{d}t}\hat{U}(t,0) = \hat{H}(t)\hat{U}(t,0)\,. \tag{3.3}$$

Taking the adjoint of the above equation gives

$$-\mathrm{i}\hbar\frac{\mathrm{d}}{\mathrm{d}t}\hat{U}^\dagger(t,0) = \hat{U}^\dagger(t,0)\hat{H}(t)\,, \tag{3.4}$$

where we used the fact that the Hamiltonian is Hermitian and $(AB)^\dagger = B^\dagger A^\dagger$.

Let's now consider the time derivative of a product $\hat{U}^\dagger(t,0)\hat{U}(t,0)$.

$$\begin{aligned}\frac{\mathrm{d}}{\mathrm{d}t}\big(\hat{U}^\dagger(t,0)\hat{U}(t,0)\big) &= \frac{\mathrm{d}\hat{U}^\dagger(t,0)}{\mathrm{d}t}\hat{U}(t,0) + \hat{U}^\dagger(t,0)\frac{\mathrm{d}\hat{U}(t,0)}{\mathrm{d}t}\\ &= \frac{\mathrm{i}}{\hbar}\hat{U}^\dagger(t,0)\hat{H}(t)\hat{U}(t,0) - \frac{\mathrm{i}}{\hbar}\hat{U}^\dagger(t,0)\hat{H}(t)\hat{U}(t,0)\\ &= 0\,.\end{aligned} \tag{3.5}$$

Because of equation (3.5), $\hat{U}^\dagger\hat{U}$ must be a constant. And due to the initial condition $\hat{U}(0,0) = \mathbb{1}$ we must have

$$\hat{U}^\dagger\hat{U} = \hat{U}\hat{U}^\dagger = \mathbb{1}. \tag{3.6}$$

An operator, which satisfies equation (3.6) is called *unitary*.

Now we make a distinction between time dependent and time independent Hamiltonians. If the Hamiltonian is time independent we call the system *isolated*. Then the energy of the system is bound to be constant. If the system Hamiltonian is time dependent and its dynamics can still be described in unitary fashion, we have a *closed* system [31].

Considering now an isolated system with time independent Hamiltonians, we can solve equation (3.3) easily by integrating both sides with respect to time and get

$$\hat{U}(t,0) = \mathrm{e}^{-\mathrm{i}\hat{H}t/\hbar}\,. \tag{3.7}$$

For time dependent Hamiltonians we would (in general) need to employ time-ordering in a so called Dyson series [48].

As discussed, the Schrödinger equation gives the time evolution for a pure state $|\psi(t)\rangle$. Let's then consider a system which is in a statistical ensemble of pure states, that is it's in a mixed

[1] Actually the Schrödinger equation and the existence of the time-evolution operator $\hat{U}$ are both the same postulate, just formulated differently [38].

state. We can describe the mixed states as density matrices. Let's say that at time $t = 0$ the system's state is characterized by a density matrix

$$\hat{\rho}(0) = \sum_i p_i \left|\psi_i(0)\right\rangle \left\langle\psi_i(0)\right| , \tag{3.8}$$

where the coefficients p_i are probabilities which sum to unity.

The representation for the state at time t is easy to get by using equation (3.2) and its adjoint:

$$\begin{aligned}\hat{\rho}(t) &= \sum_i p_i \hat{U}(t,0) \left|\psi_i(0)\right\rangle \left\langle\psi_i(0)\right| \hat{U}^\dagger(t,0) \\ &= \hat{U}\hat{\rho}(0)\hat{U}^\dagger .\end{aligned} \tag{3.9}$$

When we differentiate (3.9) with respect to time we recover an equation of motion for the density matrix.

$$\begin{aligned}\frac{\mathrm{d}}{\mathrm{d}t}\hat{\rho}(t) &= \frac{\mathrm{d}}{\mathrm{d}t}\left[\hat{U}\hat{\rho}(0)\hat{U}^\dagger\right] \\ &= \frac{\mathrm{d}\hat{U}}{\mathrm{d}t}\hat{\rho}(0)\hat{U}^\dagger + \hat{U}\hat{\rho}(0)\frac{\mathrm{d}\hat{U}^\dagger}{\mathrm{d}t} \\ &= -\frac{\mathrm{i}}{\hbar}\hat{H}(t)\hat{U}\hat{\rho}(0)\hat{U}^\dagger + \frac{\mathrm{i}}{\hbar}\hat{U}\hat{\rho}(0)\hat{U}^\dagger\hat{H}(t) \\ &= -\frac{\mathrm{i}}{\hbar}\left[\hat{H}(t), \hat{\rho}(t)\right] ,\end{aligned} \tag{3.10}$$

where we used equations (3.3), (3.4) and (3.9) as an aid. The derived equation is called the *Liouville-von Neumann* equation. It is the Schrödinger equation equivalent for mixed states. Equation (3.10) is the usual form for the Liouville-von Neumann equation encountered in quantum mechanics. However, we write it in a slightly different form

$$\frac{\mathrm{d}}{\mathrm{d}t}\hat{\rho}(t) = \mathscr{L}(t)\hat{\rho}(t) , \tag{3.11}$$

where $\mathscr{L}(t)$ is the *Liouvillian superoperator* or just the Liouvillian. It is a superoperator, which means that it acts on operators, just like an operator acts on vectors. The Liouvillian $\mathscr{L}$ is defined in equation (3.11) as

$$\mathscr{L}(t) = -\frac{\mathrm{i}}{\hbar}\left[\hat{H}(t), \cdot\right] , \tag{3.12}$$

where the dot is replaced by the operator to which the Liouvillian acts on. In the case of time independent Hamiltonian, equation (3.11) has the well known solution

$$\hat{\rho}(t) = \mathrm{e}^{\mathscr{L}t}\hat{\rho}(0) . \tag{3.13}$$

If the Hamiltonian depended on time we would again need time ordering for the general solution [31].

3.1.1 THE HEISENBERG PICTURE

In the previous part we assumed that the quantum states, whether they were pure states $|\psi(t)\rangle$ or mixed states $\hat{\rho}(t)$, carried all time dependence. This picture of quantum mechanics is called the Schrödinger picture. An equivalent formulation is obtained by letting the operators acting on the Hilbert space $\mathscr{H}$ carry all time dependence, which leaves states time independent. This formulation is called the *Heisenberg picture*. To make sure that these two pictures actually coincide and describe the same quantum mechanics we require that the observable quantities, that is the expectation values of operators, remain unchanged between the two pictures. This requirement gives

$$\langle \hat{A} \rangle = \langle \psi(t) | \hat{A} | \psi(t) \rangle = \left\langle \psi(0) \middle| \hat{U}^\dagger \hat{A} \hat{U} \middle| \psi(0) \right\rangle = \langle \hat{A}_\mathrm{H} \rangle \tag{3.14}$$

for pure states and

$$\langle \hat{A} \rangle = \mathrm{Tr}\left[\hat{A}\hat{\rho}(t)\right] = \mathrm{Tr}\left[\hat{A}\hat{U}\hat{\rho}(0)\hat{U}^\dagger\right] = \mathrm{Tr}\left[\hat{U}^\dagger \hat{A}\hat{U}\hat{\rho}(0)\right] = \mathrm{Tr}\left[\hat{A}_\mathrm{H}\hat{\rho}(0)\right] = \langle \hat{A}_\mathrm{H} \rangle \tag{3.15}$$

for density matrices. Above we denoted the Heisenberg picture operator by the subscript $_\mathrm{H}$. Here we can spot how the Schrödinger picture operators are transformed to the Heisenberg picture via the canonical transformation

$$\hat{A}_\mathrm{H}(t) = \hat{U}^\dagger(t,0)\hat{A}\hat{U}(t,0)\,. \tag{3.16}$$

Note that the transformation between the pictures arises from the requirement of coinciding expectation values for the observables.

Taking the time derivative of (3.16) gives us an equation of motion for the operators [48]

$$\begin{aligned}
\frac{\mathrm{d}}{\mathrm{d}t}\hat{A}_\mathrm{H}(t) &= \frac{\mathrm{d}}{\mathrm{d}t}\left(\hat{U}^\dagger \hat{A}\hat{U}\right) \\
&= \frac{\mathrm{d}\hat{U}^\dagger}{\mathrm{d}t}\hat{A}\hat{U} + \hat{U}^\dagger\frac{\partial \hat{A}}{\partial t}\hat{U} + \hat{U}^\dagger\hat{A}\frac{\mathrm{d}\hat{U}}{\mathrm{d}t} \\
&= \frac{\mathrm{i}}{\hbar}\hat{U}^\dagger\hat{H}\hat{U}\hat{U}^\dagger\hat{A}\hat{U} - \frac{\mathrm{i}}{\hbar}\hat{U}^\dagger\hat{A}\hat{U}\hat{U}^\dagger\hat{H}\hat{U} + \left(\frac{\partial \hat{A}}{\partial t}\right)_\mathrm{H} \\
&= \frac{\mathrm{i}}{\hbar}\left[\hat{H}_\mathrm{H}, \hat{A}_\mathrm{H}(t)\right] + \left(\frac{\partial \hat{A}}{\partial t}\right)_\mathrm{H}.
\end{aligned} \tag{3.17}$$

This is called the *Heisenberg equation of motion*. If the Schrödinger picture operator $\hat{A}$ is time independent and we consider an isolated system, we can write the above equation simply as

$$\frac{\mathrm{d}\hat{A}_\mathrm{H}}{\mathrm{d}t} = \frac{\mathrm{i}}{\hbar}\left[\hat{H}, \hat{A}_\mathrm{H}\right], \tag{3.18}$$

because then the Heisenberg picture Hamiltonian $H_\mathrm{H} = \hat{U}^\dagger\hat{H}\hat{U}$ reduces to the Schrödinger picture one.

3.1.2 THE INTERACTION PICTURE

Having considered the Schrödinger and Heisenberg pictures of quantum mechanics, we consider the third picture that we use extensively when considering the open quantum system dynamics. This is called the *interaction picture* and it's most useful, as the name suggests, when considering some free Hamiltonians interacting with each other . We start to characterize the interaction picture by considering a Hamiltonian that can be written as a sum of two parts [31]

$$\hat{H}(t) = \hat{H}_0 + \hat{H}_\mathrm{I}(t)\,, \tag{3.19}$$

where $\hat{H}_0$ represents the sum of energies of the systems in study without an interaction and is taken to be time independent. The term $\hat{H}_\mathrm{I}(t)$ describes the interaction between the systems and can, in general, depend on time.

Now we say that the time-evolution operator corresponding to Hamiltonian (3.19) can be written as a product the two parts [31]

$$\hat{U}(t,0) = \hat{U}_0(t,0)\hat{U}_\mathrm{I}(t,0)\,, \tag{3.20}$$

where $\hat{U}_0$ corresponds to the time evolution of the free part and $\hat{U}_\mathrm{I}$ corresponds to the time evolution of the interaction part. Therefore the expectation value of some (Schrödinger picture) observable $\hat{A}$ is given by

$$\langle\hat{A}\rangle = \mathrm{Tr}\left[\hat{A}\hat{U}\hat{\rho}(0)\hat{U}^\dagger\right] = \mathrm{Tr}\left[\hat{A}\hat{U}_0\hat{U}_\mathrm{I}\hat{\rho}(0)\hat{U}_\mathrm{I}^\dagger\hat{U}_0^\dagger\right] = \mathrm{Tr}\left[\hat{U}_0^\dagger\hat{A}\hat{U}_0\hat{U}_\mathrm{I}\hat{\rho}(0)\hat{U}_\mathrm{I}^\dagger\right] = \mathrm{Tr}\left[\tilde{A}(t)\tilde{\rho}(t)\right]. \tag{3.21}$$

Above we introduced the interaction picture operator

$$\tilde{A}(t) = \hat{U}_0^\dagger\hat{A}\hat{U}_0 \tag{3.22}$$

and the interaction picture density matrix

$$\tilde{\rho}(t) = \hat{U}_\mathrm{I}\hat{\rho}(0)\hat{U}_\mathrm{I}^\dagger. \tag{3.23}$$

The tilde on top of an operator $\tilde{O}$ denotes interaction picture. It can be seen from the definitions (3.22) and (3.23) that the time evolution of the operators is generated by the free part $\hat{H}_0$ and the time evolution of the states by the interaction part $\hat{H}_\mathrm{I}$. Therefore the interaction picture can be thought of as an intermediate formulation between the Schrödinger and Heisenberg picures. This can be seen more clearly by setting $\hat{H}_0 = 0$ in the Hamiltonian (3.19). This would yield $\hat{U}_0 = \mathbb{1}$ and $\hat{U}_\mathrm{I} = \hat{U}$, corresponding to the Schrödinger picture. Similarly, by setting $\hat{H}_\mathrm{I} = 0$ in (3.19) we would recover the Heisenberg picture with $\hat{U}_0 = \hat{U}$ and $\hat{U}_\mathrm{I} = \mathbb{1}$ [31].

The time evolution operator of the interaction part $\hat{U}_\mathrm{I}$ satisfies the differential equation (3.3) with the interaction Hamiltonian [31]

$$\mathrm{i}\hbar\frac{\mathrm{d}}{\mathrm{d}t}\hat{U}_\mathrm{I}(t,0) = \tilde{H}_\mathrm{I}(t)\hat{U}_\mathrm{I}(t,0)\,, \tag{3.24}$$

where $\tilde{H}_\mathrm{I}(t) = \hat{U}_0^\dagger\hat{H}_\mathrm{I}\hat{U}_0$ is the interaction part of the Hamiltonian $\hat{H}(t)$ in the interaction picture. We can then differentiate (3.23) with respect to time, use equation (3.24), and

following similar lines of reasoning as in deriving equation (3.10) we end up with

$$\frac{\mathrm{d}}{\mathrm{d}t}\tilde{\rho}(t) = -\frac{\mathrm{i}}{\hbar}\left[\tilde{H}_{\mathrm{I}}(t), \tilde{\rho}(t)\right]. \tag{3.25}$$

This is the Liouville-von Neumann equation in the interaction picture and the starting point of our discussion about open quantum systems.

The emergence of the interaction picture can also be found out to be a special case of a general unitary transformation of the Hamiltonian. Let's here derive a useful result for how an arbitrary unitary transformation changes the Hamiltonian. Let $\hat{U}$ be the transformation in question. It maps quantum states $|\psi(t)\rangle$ to other states $|\psi(t)\rangle'$ as

$$|\psi(t)\rangle' = \hat{U}|\psi(t)\rangle\,. \tag{3.26}$$

The new states must also evolve according to the Schrödinger equation (3.1) with the transformed Hamiltonian $\hat{H}'$. This gives

$$\begin{aligned}
\mathrm{i}\hbar\frac{\mathrm{d}}{\mathrm{d}t}|\psi(t)\rangle' &= \hat{H}'|\psi(t)\rangle' \\
\Rightarrow \mathrm{i}\hbar\frac{\mathrm{d}\hat{U}}{\mathrm{d}t}|\psi(t)\rangle + \mathrm{i}\hbar\hat{U}\frac{\mathrm{d}}{\mathrm{d}t}|\psi(t)\rangle &= \hat{H}'\hat{U}|\psi(t)\rangle \\
\Rightarrow \mathrm{i}\hbar\hat{U}\frac{\mathrm{d}}{\mathrm{d}t}|\psi(t)\rangle &= \hat{H}'\hat{U}|\psi(t)\rangle - \mathrm{i}\hbar\frac{\mathrm{d}\hat{U}}{\mathrm{d}t}|\psi(t)\rangle \\
\Rightarrow \mathrm{i}\hbar\frac{\mathrm{d}}{\mathrm{d}t}|\psi(t)\rangle &= \underbrace{\left[\hat{U}^\dagger\hat{H}'\hat{U} - \mathrm{i}\hbar\hat{U}^\dagger\frac{\mathrm{d}\hat{U}}{\mathrm{d}t}\right]}_{\hat{H}}|\psi(t)\rangle\,.
\end{aligned}$$

The original Hamiltonian is given in terms of the transformed Hamiltonian in the brackets. We can solve for $\hat{H}'$ to get

$$\hat{H}' = \hat{U}\hat{H}\hat{U}^\dagger + \mathrm{i}\hbar\frac{\mathrm{d}\hat{U}}{\mathrm{d}t}\hat{U}^\dagger\,. \tag{3.27}$$

This gives the general unitary transformation of the Hamiltonian. A special case of this is now the interaction picture, because setting $\hat{U} = \mathrm{e}^{-\mathrm{i}\hat{H}_0 t/\hbar}$ recovers the interaction picture for the original Hamiltonian of the form (3.19).

3.2 OPEN QUANTUM SYSTEM DYNAMICS

The dynamics of the closed quantum systems discussed in the last section were all described by the unitary time evolution operator[2] $U(t,0)$ and the Liouville-von Neumann equation of motion. The unitarity (and thus reversibility) of the dynamics was an underlying assumption in the preceding discussion. Now we relax that requirement by considering open quantum systems.

[2]Here and in what follows we drop the hat describing the operator for simplicity. It should be clear from context when operators are considered.

As Breuer and Petruccione [31] put it, *"an open system is a quantum system S which is coupled to another quantum system B called the environment."* Thus we are considering two distinct systems, S and B, of which S is our main system of interest (the one whose dynamics we want to compute) while B is its environment that affects the dynamics in a non-trivial manner. S is the open quantum system interacting with environment B. It represents a subsystem of the complete system $S+B$, which we take to be a closed system [31]. See again figure 3.1 for a pictorial description.

Let's denote the Hilbert space of the "universe"[3] Hamiltonian H_T as $\mathscr{H}_\mathrm{T}$. Next we decompose the total Hamiltonian and its Hilbert space into Hamiltonian of the system H_S with Hilbert space $\mathscr{H}_\mathrm{S}$ and Hamiltonian of the environment H_B with Hilbert space $\mathscr{H}_\mathrm{B}$. The Hilbert space of the universe can be written as the *tensor product* between the system and environment Hilbert spaces $\mathscr{H}_\mathrm{T} = \mathscr{H}_\mathrm{S} \otimes \mathscr{H}_\mathrm{B}$ [31]. The total Hamiltonian becomes

$$H_\mathrm{T} = H_\mathrm{S} \otimes \mathbb{1}_\mathrm{B} + \mathbb{1}_\mathrm{S} \otimes H_\mathrm{B} + \alpha H_\mathrm{I}\,, \tag{3.28}$$

where we show explicitly the tensor product structure of the free part of the total Hamiltonian. H_I describes the interaction between the system and its environment and α is a dimensionless quantity, which measures the strength of the interaction [38].

Let's now begin the analysis for the open system dynamics, following references [31, 38, 39] and [49]. We consider the system dynamics in the interaction picture, since our ultimate interest lies in the effects of the environmental interaction on the system. Since we assume the complete system with Hamiltonian H_T to be closed, we can use the Liouville-von Neumann equation (3.25) to describe its dynamics

$$\frac{\mathrm{d}}{\mathrm{d}t}\tilde{\rho}_\mathrm{T}(t) = -\frac{\mathrm{i}\alpha}{\hbar}\big[\tilde{H}_\mathrm{I}(t), \tilde{\rho}_\mathrm{T}(t)\big]\,. \tag{3.29}$$

Here we were able to move the quantity α to the front since it's just some number. The tilde denotes again interaction picture operators. Integrating this with respect to time gives us

$$\tilde{\rho}_\mathrm{T}(t) = \tilde{\rho}_\mathrm{T}(0) - \frac{\mathrm{i}\alpha}{\hbar}\int_0^t \big[\tilde{H}_\mathrm{I}(t'), \tilde{\rho}_\mathrm{T}(t')\big]\mathrm{d}t'\,. \tag{3.30}$$

Let's substitute (3.30) into the right hand side of (3.29) to get

$$\frac{\mathrm{d}}{\mathrm{d}t}\tilde{\rho}_\mathrm{T}(t) = -\frac{\mathrm{i}\alpha}{\hbar}\big[\tilde{H}_\mathrm{I}(t), \tilde{\rho}_\mathrm{T}(0)\big] - \frac{\alpha^2}{\hbar^2}\int_0^t \big[\tilde{H}_\mathrm{I}(t), \big[\tilde{H}_\mathrm{I}(t'), \tilde{\rho}_\mathrm{T}(t')\big]\big]\mathrm{d}t' \tag{3.31}$$

At this point we are dealing with the complete state density matrix ρ_T. Since we are ultimately interested in the dynamics of the system only, we trace over the environment in an operation called the *partial trace* (see Refs. [31, 39] for its mathematical formulation). This operation allows us to obtain only the system dynamics, while the environment effect is described by some numerical coefficients. More concretely, we get for the complete system density matrix[4]

$$\mathrm{Tr}_\mathrm{B}[\rho_\mathrm{T}] = \mathrm{Tr}_\mathrm{B}[\rho_\mathrm{S} \otimes \rho_\mathrm{B}] = \rho_\mathrm{S}\,\mathrm{Tr}[\rho_\mathrm{B}] = \rho_\mathrm{S}\,, \tag{3.32}$$

[3] This refers to the system of everything, which is the smaller system of interest plus the bath.

[4] Here we assume that the total system's state is separable as a tensor product. More on this soon, when the Born approximation is discussed.

because the density matrix has unit trace by definition. Taking the partial trace of equation (3.31) gives

$$\frac{\mathrm{d}}{\mathrm{d}t}\tilde{\rho}_{\mathrm{S}}(t) = -\frac{\mathrm{i}\alpha}{\hbar}\mathrm{Tr}_{\mathrm{B}}\left\{\left[\tilde{H}_{\mathrm{I}}(t),\tilde{\rho}_{\mathrm{T}}(0)\right]\right\} - \frac{\alpha^2}{\hbar^2}\int_0^t \mathrm{Tr}_{\mathrm{B}}\left\{\left[\tilde{H}_{\mathrm{I}}(t),\left[\tilde{H}_{\mathrm{I}}(t'),\tilde{\rho}_{\mathrm{T}}(t')\right]\right]\right\}\mathrm{d}t'. \tag{3.33}$$

To continue from here we need to perform our first approximation.

3.2.1 BORN APPROXIMATION

The *Born approximation* or the *weak coupling approximation* states that the coupling strength between the system and its environment is weak. In our case this means that $\alpha/\hbar \ll 1$.[5] Let's assume that in the beginning there exists no correlations between the system and its environment such that the total density matrix separates as $\rho_{\mathrm{T}}(0) = \rho_{\mathrm{S}}(0)\otimes\rho_{\mathrm{B}}$. This means that the system and environment are not entangled with each other.

Now taking the environment to be huge compared to the system, the non-trivial time evolution of the system should not have a noticeable effect on the environment's state [39]. Thus we can assume that the total density matrix separates for all time evolution as [31]

$$\rho_{\mathrm{T}}(t) \approx \rho_{\mathrm{S}}(t)\otimes\rho_{\mathrm{B}}\,. \tag{3.34}$$

We take the state of the environment ρ_B to be in a time independent, stationary state.[6] More precisely the environment is in a *thermal state*, which is at thermal equilibrium at some temperature T. The thermal state density matrix is given by (see Appendix B for derivation)

$$\rho_{\mathrm{Th}}(\omega) = \frac{1}{1+\bar{n}(\omega)}\sum_{n=0}^{\infty}\left(\frac{\bar{n}(\omega)}{1+\bar{n}(\omega)}\right)^n |n\rangle\langle n|\,, \tag{3.35}$$

where $\bar{n}(\omega)$ is the expected number of quanta given by the Bose-Einstein distribution for some angular frequency ω.

Using the Born approximation (3.34) in equation (3.33) yields:

$$\frac{\mathrm{d}}{\mathrm{d}t}\tilde{\rho}_{\mathrm{S}}(t) = -\frac{\mathrm{i}\alpha}{\hbar}\mathrm{Tr}_{\mathrm{B}}\left\{\left[\tilde{H}_{\mathrm{I}}(t),\rho_{\mathrm{S}}(0)\otimes\rho_{\mathrm{B}}\right]\right\} - \frac{\alpha^2}{\hbar^2}\int_0^t \mathrm{Tr}_{\mathrm{B}}\left\{\left[\tilde{H}_{\mathrm{I}}(t),\left[\tilde{H}_{\mathrm{I}}(t'),\tilde{\rho}_{\mathrm{S}}(t')\otimes\rho_{\mathrm{B}}\right]\right]\right\}\mathrm{d}t'. \tag{3.36}$$

This looks a bit complicated but will keep simplifying as we move on.

Let's consider the form of the interaction Hamiltonian H_{I}. As it determines the interactions between the system and bath, it must be composed of some kind of a product between the corresponding operators. If not, the terms would just be added to the free Hamiltonians. Therefore we can conclude that the interaction Hamiltonian is in its most general form

$$H_{\mathrm{I}} = \sum_{\beta} A_\beta \otimes B_\beta\,, \tag{3.37}$$

[5] The Born approximation makes our derivation perturbative in nature. We could insert the integral form of the complete state (3.30) into the Liouville-von Neumann equation (3.29) more than once. This would yield a power series in coupling strength $\alpha/\hbar$ but since we assume $\alpha/\hbar \ll 1$ we can neglect the terms of order $\mathcal{O}(\alpha^3)$ [38].

[6] This means that $[H_B, \rho_B] = 0$.

where A_β are operators acting on the system Hilbert space $\mathscr{H}_\mathrm{S}$ and B_β are environment operators acting on $\mathscr{H}_\mathrm{B}$. The index β runs over all the terms that exist in H_I.

Now we take a closer look at the first term in equation (3.36). Since the interaction Hamiltonian can be decomposed as in equation (3.37), we write the trace in the first term as

$$\begin{aligned}
\mathrm{Tr}_\mathrm{B}\left\{\left[\tilde{H}_\mathrm{I}(t),\rho_\mathrm{S}(0)\otimes\rho_\mathrm{B}\right]\right\} &= \sum_\beta \mathrm{Tr}_\mathrm{B}\left\{\left[\tilde{A}_\beta(t)\otimes\tilde{B}_\beta(t),\rho_\mathrm{S}(0)\otimes\rho_\mathrm{B}\right]\right\} \\
&= \sum_\beta \mathrm{Tr}_\mathrm{B}\left\{\left(\tilde{A}_\beta(t)\otimes\tilde{B}_\beta(t)\right)\left(\rho_\mathrm{S}(0)\otimes\rho_\mathrm{B}\right)-\left(\rho_\mathrm{S}(0)\otimes\rho_\mathrm{B}\right)\left(\tilde{A}_\beta(t)\otimes\tilde{B}_\beta(t)\right)\right\} \\
&= \sum_\beta \mathrm{Tr}_\mathrm{B}\left\{\left(\tilde{A}_\beta\rho_\mathrm{S}\right)\otimes\left(\tilde{B}_\beta\rho_\mathrm{B}\right)-\left(\rho_\mathrm{S}\tilde{A}_\beta\right)\otimes\left(\rho_\mathrm{B}\tilde{B}_\beta\right)\right\} \\
&= \sum_\beta\left(\tilde{A}_\beta\rho_\mathrm{S}\right)\mathrm{Tr}\left\{\tilde{B}_\beta\rho_\mathrm{B}\right\}-\sum_\beta\left(\rho_\mathrm{S}\tilde{A}_\beta\right)\mathrm{Tr}\left\{\rho_\mathrm{B}\tilde{B}_\beta\right\}.
\end{aligned}$$

Here we used the mixed product property of the Kronecker product $(A\otimes B)(C\otimes D)=(AC)\otimes(BD)$ [50]. The remaining traces are over the environment Hilbert space. Since we assume the environment to be in a thermal state given by the equation (3.35) the traces become zero. This is because we can assume without any loss of generality that the expectation values for the bath operators $\mathrm{Tr}\left[\rho_\mathrm{B}\tilde{B}_\beta\right]=\langle\tilde{B}_\beta\rangle=0$ for all β, or if this is not the case we can transform the Hamiltonian into a form where it's true by just introducing an energy shift [38]. Therefore we have

$$\mathrm{Tr}_\mathrm{B}\left\{\left[\tilde{H}_\mathrm{I}(t),\rho_\mathrm{S}(0)\otimes\rho_\mathrm{B}\right]\right\}=0. \tag{3.38}$$

This simplifies equation (3.36). Let's now use the interaction Hamiltonian decomposition (3.37) there to get

$$\frac{\mathrm{d}}{\mathrm{d}t}\tilde{\rho}_\mathrm{S}(t)=-\frac{\alpha^2}{\hbar^2}\sum_{\beta,\beta'}\int_0^t \mathrm{Tr}_\mathrm{B}\left\{\left[\underbrace{\tilde{A}_\beta^\dagger(t)\otimes\tilde{B}_\beta^\dagger(t)}_{\tilde{H}_\mathrm{I}=\tilde{H}_\mathrm{I}^\dagger},\left[\tilde{A}_{\beta'}(t')\otimes\tilde{B}_{\beta'}(t'),\tilde{\rho}_\mathrm{S}(t')\otimes\rho_\mathrm{B}\right]\right]\right\}\mathrm{d}t'. \tag{3.39}$$

Now we need to open up the double commutator in the integrand. Using the fact that the transpose distributes in tensor products ($(A\otimes B)^\top=A^\top\otimes B^\top$) but not for normal matrix products ($(AB)^\top=B^\top A^\top$) we get after some algebra

$$\begin{aligned}
\frac{\mathrm{d}}{\mathrm{d}t}\tilde{\rho}_\mathrm{S}(t)=-\frac{\alpha^2}{\hbar^2}\sum_{\beta,\beta'}\int_0^t \mathrm{d}t'\,\mathrm{Tr}_\mathrm{B}\Big\{&\left(\tilde{A}_\beta^\dagger(t)\otimes\tilde{B}_\beta^\dagger(t)\right)\left(\tilde{A}_{\beta'}(t')\otimes\tilde{B}_{\beta'}(t')\right)\left(\tilde{\rho}_\mathrm{S}(t')\otimes\rho_\mathrm{B}\right) \\
&-\left(\tilde{A}_{\beta'}(t')\otimes\tilde{B}_{\beta'}(t')\right)\left(\tilde{\rho}_\mathrm{S}(t')\otimes\rho_\mathrm{B}\right)\left(\tilde{A}_\beta^\dagger(t)\otimes\tilde{B}_\beta^\dagger(t)\right)\Big\}+\mathrm{h.c.},
\end{aligned} \tag{3.40}$$

where h.c. denotes the Hermitian conjugate. Usage of the mixed product property for Kronecker products allows us to separate the system and environment operators to their own blocks:

$$\begin{aligned}
\frac{\mathrm{d}}{\mathrm{d}t}\tilde{\rho}_\mathrm{S}(t)=-\frac{\alpha^2}{\hbar^2}\sum_{\beta,\beta'}\int_0^t \mathrm{d}t'\,\mathrm{Tr}_\mathrm{B}\Big\{&\left(\tilde{A}_\beta^\dagger(t)\tilde{A}_{\beta'}(t')\tilde{\rho}_\mathrm{S}(t')\right)\otimes\left(\tilde{B}_\beta^\dagger(t)\tilde{B}_{\beta'}(t')\rho_\mathrm{B}\right) \\
&-\left(\tilde{A}_{\beta'}(t')\tilde{\rho}_\mathrm{S}(t')\tilde{A}_\beta^\dagger(t)\right)\otimes\left(\tilde{B}_{\beta'}(t')\rho_\mathrm{B}\tilde{B}_\beta^\dagger(t)\right)\Big\}+\mathrm{h.c.}.
\end{aligned} \tag{3.41}$$

The partial trace ignores the contribution of the system operators and only acts on states living in the environment Hilbert space $\mathscr{H}_\mathrm{B}$. Therefore we have after some algebra

$$\frac{\mathrm{d}}{\mathrm{d}t}\tilde{\rho}_\mathrm{S}(t) = -\frac{\alpha^2}{\hbar^2}\sum_{\beta,\beta'}\int_0^t \mathrm{d}t' \,\mathrm{Tr}\left\{\rho_\mathrm{B}\tilde{B}_\beta^\dagger(t)\tilde{B}_{\beta'}(t')\right\}\left[\tilde{A}_\beta^\dagger(t), \tilde{A}_{\beta'}(t')\tilde{\rho}_\mathrm{S}(t')\right] + \mathrm{h.c.}. \tag{3.42}$$

Above the trace term is the expectation value of the bath operator product at different times t and t':

$$\mathrm{Tr}\left\{\rho_\mathrm{B}\tilde{B}_\beta^\dagger(t)\tilde{B}_{\beta'}(t')\right\} = \left\langle \tilde{B}_\beta^\dagger(t)\tilde{B}_{\beta'}(t')\right\rangle. \tag{3.43}$$

Equation (3.43) is called the *reservoir correlation function* [31]. It tells us how much do the bath operators correlate with each other at two different times. Intuitively the time interval $t - t'$ should be the contributing factor here since we have assumed the environment to be stationary and not changing in time. Motivated by this reasoning let's change the time variable to $\tau = t - t'$. Using this new variable τ let's examine the correlation function (3.43) a bit closer.

The reservoir correlation function becomes

$$\left\langle \tilde{B}_\beta^\dagger(t)\tilde{B}_{\beta'}(t-\tau)\right\rangle = \mathrm{Tr}\left\{\rho_\mathrm{B}\tilde{B}_\beta^\dagger(t)\tilde{B}_{\beta'}(t-\tau)\right\}. \tag{3.44}$$

Let's apply here the definition for the interaction picture of the operators given by equation (3.22). Now U_0 is given by the free parts Hamiltonian $U_0 = \mathrm{e}^{-\mathrm{i}(H_\mathrm{S}+H_\mathrm{B})t/\hbar}$ but, since we are considering only bath operators in the interaction picture, the system Hamiltonian has no effect. This is because $\left[H_\mathrm{S}, B_\beta\right] = 0$ as the operators live in different Hilbert spaces. Therefore we get

$$\left\langle \tilde{B}_\beta^\dagger(t)\tilde{B}_{\beta'}(t-\tau)\right\rangle = \mathrm{Tr}\left\{\rho_\mathrm{B}\mathrm{e}^{\mathrm{i}H_\mathrm{B}t/\hbar}B_\beta^\dagger\mathrm{e}^{-\mathrm{i}H_\mathrm{B}t/\hbar}\mathrm{e}^{\mathrm{i}H_\mathrm{B}(t-\tau)/\hbar}B_{\beta'}\mathrm{e}^{-\mathrm{i}H_\mathrm{B}(t-\tau)/\hbar}\right\}. \tag{3.45}$$

Because the bath is stationary we have $\left[H_\mathrm{B}, \rho_\mathrm{B}\right] = 0$. This allows us to treat ρ_B and $\mathrm{e}^{\mathrm{i}H_\mathrm{B}t}$ as if they were scalars in the above. Using this and the cyclicity of trace we can move the factor $\mathrm{e}^{\mathrm{i}H_\mathrm{B}(t-\tau)}$ from the back to the right side of ρ_B and get

$$\left\langle \tilde{B}_\beta^\dagger(t)\tilde{B}_{\beta'}(t-\tau)\right\rangle = \mathrm{Tr}\left\{\rho_\mathrm{B}\mathrm{e}^{\mathrm{i}H_\mathrm{B}\tau/\hbar}B_\beta^\dagger\mathrm{e}^{-\mathrm{i}H_\mathrm{B}\tau/\hbar}B_{\beta}\right\} = \left\langle \tilde{B}_\beta^\dagger(\tau)\tilde{B}_{\beta'}(0)\right\rangle. \tag{3.46}$$

Thus the correlation function depends only on the time difference τ as guessed before.

Let's now use the change of variables $\tau = t - t'$ and equation (3.46) in equation (3.42) to get

$$\frac{\mathrm{d}}{\mathrm{d}t}\tilde{\rho}_\mathrm{S}(t) = -\frac{\alpha^2}{\hbar^2}\sum_{\beta,\beta'}\int_0^t \mathrm{d}\tau \left\langle \tilde{B}_\beta^\dagger(\tau)\tilde{B}_{\beta'}(0)\right\rangle\left[\tilde{A}_\beta^\dagger(t), \tilde{A}_{\beta'}(t-\tau)\tilde{\rho}_\mathrm{S}(t-\tau)\right] + \mathrm{h.c.}. \tag{3.47}$$

This form of the system time-evolution equation is still difficult to solve because the equation depends on the system evolution history due to the presence of $\tilde{\rho}_\mathrm{S}(t-\tau)$. Therefore it's time for another approximation.

3.2.2 MARKOV APPROXIMATION

Getting rid of the system state's history in equation (3.47) requires the use of *Markov approximation*. Let's say that the environment correlation function (3.46) decays in a time scale τ_B. This means that $|\langle \tilde{B}^\dagger_\beta(\tau)\tilde{B}_{\beta'}(0)\rangle| \propto e^{-t/\tau_B}$. Now we assume that this time scale τ_B is much smaller than the relevant time scale for the system dynamics τ_S in which the system state in the interaction picture changes appreciably, so $\tau_B \ll \tau_S$. Therefore, if we consider a time $t^* \gg \tau_B$ but which is still much smaller than τ_S, we can replace $\tilde{\rho}_S(t-\tau)$ by $\tilde{\rho}(t)$ in the integral (3.47) because the correlation function decays to zero at any appreciable time $\tau \sim t^* \gg \tau_B$ [49]. Effectively we assume the existence of a time scale t^* such that

$$\tau_B \ll t^* \ll \tau_S = \mathcal{O}(\hbar^2/\alpha^2), \tag{3.48}$$

with the system time scale being determined by the coupling between the system and its environment [49].

Using the above argument of correlation function being negligible for $\tau \gg \tau_B$ we can also extend the upper limit of integration to infinity and get

$$\frac{d}{dt}\tilde{\rho}_S(t) = -\frac{\alpha^2}{\hbar^2}\sum_{\beta,\beta'}\int_0^\infty d\tau \left\langle \tilde{B}^\dagger_\beta(\tau)\tilde{B}_{\beta'}(0)\right\rangle \left[\tilde{A}^\dagger_\beta(t), \tilde{A}_{\beta'}(t-\tau)\tilde{\rho}_S(t)\right] + \text{h.c.}. \tag{3.49}$$

The validity of moving from equation (3.47) to (3.49) is discussed in Ref. [39]. There it is shown that if the correlation functions decay even subexponentially[7], then the above approximation works.

Now we have a Markovian differential equation. In the literature, equation (3.49) is called the *Redfield equation*, but it does not warrant complete positivity [38, 49, 39], which is a requirement for the physical (CPTP)[8] evolution of density matrices. We now proceed to fix this issue.

Our next step is to move from the time domain to the frequency domain. This is done by introducing the so called *jump operators* (the naming will become evident soon) of the system. In essence we express the system operators $A_\beta(t)$ in frequency domain. This representation turns out to be convenient later.

We proceed by decomposing the system operators in the energy eigenbasis of the system. In this basis the system Hamiltonian H_S is diagonalized

$$H_S = \sum_i \epsilon_i |\epsilon_i\rangle\langle\epsilon_i| . \tag{3.50}$$

Here ϵ_i is the energy of the eigenstate $|\epsilon_i\rangle$ such that $H_S|\epsilon_i\rangle = \epsilon_i|\epsilon_i\rangle$. Then the system operators can be written as

$$A_\beta = \sum_{i,j}|\epsilon_i\rangle\langle\epsilon_i|A_\beta|\epsilon_j\rangle\langle\epsilon_j| = \sum_{i,j}\langle\epsilon_i|A_\beta|\epsilon_j\rangle|\epsilon_i\rangle\langle\epsilon_j| , \tag{3.51}$$

[7] Meaning that if the decay is of the form $|\langle \tilde{B}^\dagger_\beta(\tau)\tilde{B}_{\beta'}(0)\rangle| \propto e^{-(t/\tau_B)^k}$, then the Markov approximation is valid for $k > 0$, so k need not be even greater or equal to 1 [39].

[8] Completely Positive, Trace Preserving

where we used the fact that the energy eigenstates constitute a complete basis such that $\sum_i |\epsilon_i\rangle\langle\epsilon_i| = \mathbb{1}$. Let's now fix the energy difference between the two basis states to be $\epsilon_j - \epsilon_i = \hbar\omega$, with ω being the *Bohr frequency*. This gives us

$$A_\beta(\omega) = \sum_{\epsilon_j-\epsilon_i=\hbar\omega} \langle\epsilon_i|A_\beta|\epsilon_j\rangle\,|\epsilon_i\rangle\langle\epsilon_j|\,, \quad \text{with} \quad A_\beta = \sum_\omega A_\beta(\omega)\,. \tag{3.52}$$

What equation (3.52) does, is collecting all the elements of the matrix which contribute to the same Bohr frequency ω. These operators $A_\beta(\omega)$ are now the jump operators because they are responsible for changing the state energy level by the amount $\hbar\omega$ or, in other words, by jumping up/down in energy levels by that amount. The full operator A_β is then the sum over all possible frequencies of these jump operators. The meaning of equation (3.52) is also explained in figure 3.2, where we consider the matrix representation of the operator A_β. There the coloured diagonal beams correspond to different jump operators $A_\beta(\omega)$. Thus equation (3.52) essentially decomposes the matrix A_β into a sum of its k-diagonals, where $k = 0$ corresponds to the leading diagonal, $k = \pm 1$ to the super- and subdiagonals et cetera.

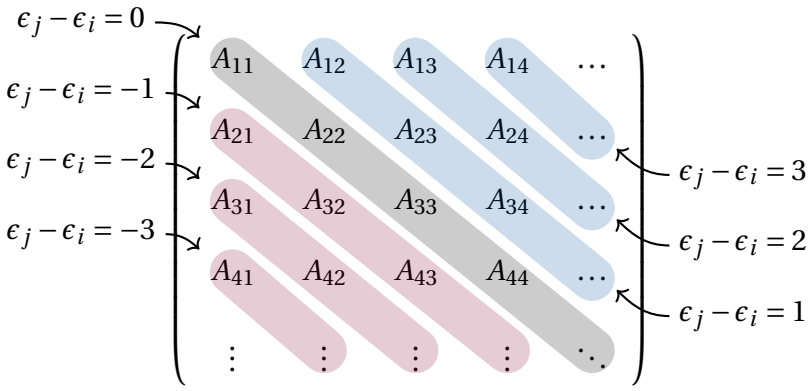

Figure 3.2: Pictorial representation of equation (3.52). The different jump operators correspond to different diagonal lines in the matrix form of operator A_β. The jump operator method therefore decomposes the matrix A_β to a sum of its different k-diagonals, which are represented in wide coloured beams in the figure.

Next we need to convert operators $A_\beta(\omega)$ to the interaction picture. Due to the definition (3.52) of the jump operators this is easy:

$$\begin{aligned}
\tilde{A}_\beta(\omega) &= U_0^\dagger A_\beta(\omega) U_0 \\
&= \sum_{\epsilon_j-\epsilon_i=\hbar\omega} \langle\epsilon_i|A_\beta|\epsilon_j\rangle\, \mathrm{e}^{\mathrm{i}H_S t/\hbar}\,|\epsilon_i\rangle\langle\epsilon_j|\,\mathrm{e}^{-\mathrm{i}H_S t/\hbar} \\
&= \mathrm{e}^{\mathrm{i}(\epsilon_i-\epsilon_j)t/\hbar} \sum_{\epsilon_j-\epsilon_i=\hbar\omega} \langle\epsilon_i|A_\beta|\epsilon_j\rangle\,|\epsilon_i\rangle\langle\epsilon_j| \\
&= \mathrm{e}^{-\mathrm{i}\omega t} A_\beta(\omega)\,.
\end{aligned} \tag{3.53}$$

From this we immediately get also the adjoint

$$\tilde{A}_\beta^\dagger(\omega) = \mathrm{e}^{\mathrm{i}\omega t} A_\beta^\dagger(\omega)\,. \tag{3.54}$$

From equations (3.53) and (3.54) we get the form for the interaction picture system operator $\tilde{A}_\beta(t)$ by summing over the frequencies (see Eq. (3.52))

$$\tilde{A}_\beta(t) = \sum_\omega e^{-i\omega t} A_\beta(\omega), \quad \text{and} \quad \tilde{A}^\dagger_\beta(t) = \sum_\omega e^{i\omega t} A^\dagger_\beta(\omega). \tag{3.55}$$

We can now use the above equation in the Markovian system state evolution equation (3.49):

$$\frac{d}{dt}\tilde{\rho}_S(t) = -\frac{\alpha^2}{\hbar^2}\sum_{\beta,\beta'}\int_0^\infty d\tau \left\langle \tilde{B}^\dagger_\beta(\tau)\tilde{B}_{\beta'}(0)\right\rangle \Big[\sum_\omega e^{i\omega t}A^\dagger_\beta(\omega), \sum_{\omega'} e^{-i\omega'(t-\tau)}A_{\beta'}(\omega')\tilde{\rho}_S(t)\Big] + \text{h.c.}. \tag{3.56}$$

After some algebra this becomes

$$\frac{d}{dt}\tilde{\rho}_S(t) = -\frac{\alpha^2}{\hbar^2}\sum_{\beta,\beta'}\sum_{\omega,\omega'} e^{i(\omega-\omega')t}\big[A^\dagger_\beta(\omega), A_{\beta'}(\omega')\tilde{\rho}_S(t)\big]\int_0^\infty d\tau \left\langle \tilde{B}^\dagger_\beta(\tau)\tilde{B}_{\beta'}(0)\right\rangle e^{i\omega'\tau} + \text{h.c.}. \tag{3.57}$$

It is notable that we have managed to separate all environment dependency (coming from the bath operators B_β) to the integral over the time interval τ. This is of course the effect of taking the partial trace over the environment. To clean up notation let's define

$$\Gamma_{\beta\beta'}(\omega') \equiv \int_0^\infty d\tau \left\langle \tilde{B}^\dagger_\beta(\tau)\tilde{B}_{\beta'}(0)\right\rangle e^{i\omega'\tau}. \tag{3.58}$$

This is the one sided Fourier transform of the bath correlation function. Applying this shorthand notation to (3.57) we arrive at

$$\frac{d}{dt}\tilde{\rho}_S(t) = -\frac{\alpha^2}{\hbar^2}\sum_{\beta,\beta'}\sum_{\omega,\omega'} e^{i(\omega-\omega')t}\Gamma_{\beta\beta'}(\omega')\big[A^\dagger_\beta(\omega), A_{\beta'}(\omega')\tilde{\rho}_S(t)\big] + \text{h.c.}. \tag{3.59}$$

This form is called the *Bloch-Redfield master equation*. This equation still does not guarantee complete positivity of the transformed density matrices due to the oscillating terms with $\omega \neq \omega'$ [39]. We will need one final approximation to obtain the desired form.

3.2.3 SECULAR APPROXIMATION

The *secular approximation*, also known as the *rotating wave approximation*, deals with the frequency difference $\omega - \omega'$ and the effect it has on the final state of the system. As can be seen from equation (3.59) the frequency difference appears in the exponential factor $e^{i(\omega-\omega')t}$, which is a rotation. The time scale of this rotation is clearly $|\omega-\omega'|^{-1}$. Let's now assume a time scale t^* satisfies [49]

$$\exists t^* \text{ such that } |\omega-\omega'|^{-1} \ll t^* \ll \tau_S = \mathcal{O}(\hbar^2/\alpha^2). \tag{3.60}$$

In this range the terms oscillating with frequency $\omega - \omega'$ will not give any significant contribution to the system dynamics, since by integrating (3.59) with respect to time these oscillations average out to zero [49, 39]. Note that equation (3.60) is a refinement of equation (3.48).

When neglecting the fast rotating terms we should be careful to check the validity of equation (3.60) as discussed in Ref. [49]. In some circumstances neglecting all terms with $\omega \neq \omega'$ is feasible, provided the difference in each frequency pair is large enough such that $|\omega - \omega'|^{-1} \ll \tau_S$ for all ω, ω' (called the *full* secular approximation). Then all of the rotating terms are oscillating so fast compared to the system evolution time scale that their contributions average out. However, if some frequency steps are close to the system time scale, $|\omega - \omega'|^{-1} \sim \tau_S$, then we cannot find a time scale t^* in between that would satisfy equation (3.60). In this case some of the slowly rotating terms with $\omega \neq \omega'$ would need to be kept (this is called the *partial* secular approximation).

For simplicity let us now assume the full secular approximation and neglect all the terms in equation (3.59) with $\omega \neq \omega'$. This gives us

$$\frac{\mathrm{d}}{\mathrm{d}t}\tilde{\rho}_S(t) = -\frac{\alpha^2}{\hbar^2}\sum_{\beta,\beta'}\sum_{\omega}\Big(\Gamma_{\beta\beta'}(\omega)\big[A^\dagger_\beta(\omega), A_{\beta'}(\omega)\tilde{\rho}_S(t)\big] + \Gamma^*_{\beta'\beta}(\omega)\big[\tilde{\rho}_S(t)A^\dagger_\beta(\omega), A_{\beta'}(\omega)\big]\Big), \quad (3.61)$$

where the Hermitian conjugate was written out explicitly.

Let's now decompose the one sided Fourier transform $\Gamma_{\beta\beta'}(\omega)$ to a real and imaginary parts as follows.

$$\Gamma_{\beta\beta'}(\omega) \equiv \frac{1}{2}\gamma_{\beta\beta'}(\omega) + \mathrm{i}S_{\beta\beta'}(\omega). \quad (3.62)$$

Then we have

$$\gamma_{\beta\beta'}(\omega) \equiv \Gamma_{\beta\beta'}(\omega) + \Gamma^*_{\beta'\beta}(\omega) = \int_{-\infty}^{\infty}\mathrm{d}\tau\,\big\langle \tilde{B}^\dagger_\beta(\tau)\tilde{B}_{\beta'}(0)\big\rangle \mathrm{e}^{\mathrm{i}\omega\tau}, \quad (3.63)$$

$$S_{\beta\beta'}(\omega) \equiv \frac{1}{2\mathrm{i}}\big(\Gamma_{\beta\beta'}(\omega) - \Gamma^*_{\beta'\beta}(\omega)\big). \quad (3.64)$$

We can notice that $\gamma_{\beta\beta'}(\omega)$ becomes the full Fourier transform of the bath correlation functions.

We can now use the decomposition (3.62) in equation (3.61). After a little bit of quite straightforward algebra we end up with the following form

$$\frac{\mathrm{d}}{\mathrm{d}t}\tilde{\rho}_S(t) = -\frac{\mathrm{i}}{\hbar}\big[H_{LS}, \tilde{\rho}_S(t)\big] + \frac{\alpha^2}{\hbar^2}\sum_{\beta,\beta'}\sum_{\omega}\gamma_{\beta\beta'}(\omega)\Big(A_{\beta'}(\omega)\tilde{\rho}_S(t)A^\dagger_\beta(\omega) - \frac{1}{2}\big\{A^\dagger_\beta(\omega)A_{\beta'}(\omega), \tilde{\rho}_S(t)\big\}\Big), \quad (3.65)$$

where we used the anticommutator $\{A, B\} = AB + BA$ and defined the *Lamb-shift* Hamiltonian H_{LS} as

$$H_{LS} = \frac{\alpha^2}{\hbar}\sum_{\beta,\beta'}\sum_{\omega}S_{\beta\beta'}(\omega)A^\dagger_\beta(\omega)A_{\beta'}(\omega). \quad (3.66)$$

This renormalizes the system energy levels due to the interaction with the environment, like in the case of the original Lamb shift encountered in the hydrogen atom energy levels [51].

Equation (3.65) is still in the interaction picture. Using the equation for Hamiltonian unitary transformation (3.27) we can move back to the Schrödinger picture with $U = \mathrm{e}^{\mathrm{i}H_0 t/\hbar}$.

Note that since the jump operators $A_\beta(\omega)$ commute with H_0, they are left invariant by U. When moving to Schrödinger picture the state operators change to $\tilde{\rho}_S(t) \to \rho_S(t)$ and the commutator term picks up the free Hamiltonian H_0. Finally we get

$$\dot{\rho}_S(t) = -\frac{i}{\hbar}\big[H_0 + H_{LS}, \rho_S(t)\big] + \frac{\alpha^2}{\hbar^2}\sum_{\beta,\beta'}\sum_{\omega}\gamma_{\beta\beta'}(\omega)\Big(A_{\beta'}(\omega)\rho_S(t)A_\beta^\dagger(\omega) - \frac{1}{2}\big\{A_\beta^\dagger(\omega)A_{\beta'}(\omega), \rho_S(t)\big\}\Big). \tag{3.67}$$

This equation is called the *GKSL-equation*, named after Gorini, Kossakowski, Sudarshan and Lindblad [52, 53], or just the *Lindblad equation*. It satisfies complete positivity, because the coefficients $\gamma_{\beta\beta'}$ can be shown to be positive [39]. Thus the Lindblad equation is a proper master equation that describes dynamics of a quantum system subject to effects of the environment. It can also be written, using the superoperator notation, as

$$\frac{d}{dt}\rho_S(t) = \mathscr{L}[\rho_S(t)], \tag{3.68}$$

just like in equation (3.11) for the Liouville-von Neumann equation but now with a more complex Liouvillian superoperator $\mathscr{L}$.

We can notice that the first term in the Lindblad equation looks a lot like the Liouville-von Neumann equation (3.10). This is no coincidence but a fact that shows that the theory works. Since (3.67) is an extension of the Liouville-von Neumann equation to open quantum systems, it should be contained within the more general equation. Indeed, we notice that in the limit of vanishingly weak coupling $\alpha \to 0$ we recover the Liouville-von Neumann equation since the Lamb-shift Hamiltonian as well as the α^2-term, called the *dissipator* and denoted as $\mathscr{D}[\rho]$, disappear and our Hamiltonian (3.28) reduces to just the free part H_0. Thus the environmental effects disappear and we are left with a closed quantum system.

3.2.4 THE ADJOINT MASTER EQUATION

Equation (3.67) is, as stated before, in Schrödinger picture and it was derived by going through the interaction picture (see Eq. (3.65)). In both of these pictures the states carry time dependence but sometimes it's useful to fully consider the time dependence of the operators. Thus we need a Heisenberg picture form of the Lindblad equation.

To arrive at the Heisenberg picture we again use the equivalence of the expectation values between the pictures as shown in equation (3.15). As we start from the Schrödinger picture, an arbitrary operator O acting on $\mathscr{H}_S$ is time independent and we can safely consider the time evolution of its expectation value using equation (3.67).

$$\begin{aligned}\frac{d}{dt}\operatorname{Tr}\{O\rho_S(t)\} = &-\frac{i}{\hbar}\operatorname{Tr}\Big\{O\big[H_0 + H_{LS}, \rho_S(t)\big]\Big\} \\ &+ \frac{\alpha^2}{\hbar^2}\sum_{\beta,\beta'}\sum_{\omega}\gamma_{\beta\beta'}(\omega)\operatorname{Tr}\Big\{O\Big(A_{\beta'}(\omega)\rho_S(t)A_\beta^\dagger(\omega) - \frac{1}{2}\big\{A_\beta^\dagger(\omega)A_{\beta'}(\omega), \rho_S(t)\big\}\Big)\Big\}.\end{aligned} \tag{3.69}$$

Let's consider first the unitary part of the equation. Let's simplify the notation by denoting

$H_0 + H_{\mathrm{LS}} \equiv H$ for now.

$$\begin{aligned}\mathrm{Tr}\Big\{O\big[H,\rho_{\mathrm{S}}(t)\big]\Big\} &= \mathrm{Tr}\{OH\rho_{\mathrm{S}}(t)\} - \mathrm{Tr}\{O\rho_{\mathrm{S}}(t)H\} = \mathrm{Tr}\{OH\rho_{\mathrm{S}}(t)\} - \mathrm{Tr}\{HO\rho_{\mathrm{S}}(t)\} \\ &= \mathrm{Tr}\Big\{\big[O,H\big]\rho_{\mathrm{S}}(t)\Big\} = -\mathrm{Tr}\Big\{\big[H,O\big]\rho_{\mathrm{S}}(t)\Big\}.\end{aligned}$$

Then let's compute the trace inside the dissipator.

$$\begin{aligned}\mathrm{Tr}\Big\{O\Big(A\rho_{\mathrm{S}}(t)A^\dagger - \frac{1}{2}\{A^\dagger A,\rho_{\mathrm{S}}(t)\}\Big)\Big\} &= \mathrm{Tr}\Big\{OA\rho_{\mathrm{S}}(t)A^\dagger - \frac{1}{2}OA^\dagger A\rho_{\mathrm{S}}(t) - \frac{1}{2}O\rho_{\mathrm{S}}(t)A^\dagger A\Big\} \\ &= \mathrm{Tr}\Big\{\Big(A^\dagger OA - \frac{1}{2}OA^\dagger A - \frac{1}{2}A^\dagger AO\Big)\rho_{\mathrm{S}}(t)\Big\} \\ &= \mathrm{Tr}\Big\{\Big(A^\dagger OA - \frac{1}{2}\{A^\dagger A,O\}\Big)\rho_{\mathrm{S}}(t)\Big\}.\end{aligned}$$

Using the above results we can write equation (3.69) as

$$\begin{aligned}\frac{\mathrm{d}}{\mathrm{d}t}\mathrm{Tr}\{O\rho_{\mathrm{S}}(t)\} &= \frac{\mathrm{i}}{\hbar}\mathrm{Tr}\Big\{\big[H_0 + H_{LS},O\big]\rho_{\mathrm{S}}(t)\Big\} \\ &\quad + \frac{\alpha^2}{\hbar^2}\sum_{\beta,\beta'}\sum_{\omega}\gamma_{\beta\beta'}(\omega)\,\mathrm{Tr}\Big\{\Big(A^\dagger_\beta(\omega)OA_{\beta'}(\omega) - \frac{1}{2}\{A^\dagger_\beta(\omega)A_{\beta'}(\omega),O\}\Big)\rho_{\mathrm{S}}(t)\Big\}. \quad (3.70)\end{aligned}$$

Now we can move the time dependency from the state ρ_{S} to the operator O. The expectation values stay the same between the Schrödinger and Heisenberg pictures if the time evolution of the operator $O(t)$ is given by the equation

$$\dot{O}(t) = \frac{\mathrm{i}}{\hbar}\big[H_0 + H_{\mathrm{LS}},O(t)\big] + \frac{\alpha^2}{\hbar^2}\sum_{\beta,\beta'}\sum_{\omega}\gamma_{\beta\beta'}(\omega)\Big(A^\dagger_\beta(\omega)O(t)A_{\beta'}(\omega) - \frac{1}{2}\{A^\dagger_\beta(\omega)A_{\beta'}(\omega),O(t)\}\Big). \quad (3.71)$$

This is called the *adjoint master equation*, the name referring to the fact that if we present (3.71) in the superoperator form like equation (3.68) we get

$$\frac{\mathrm{d}}{\mathrm{d}t}O(t) = \mathscr{L}^\dagger[O(t)], \quad (3.72)$$

showing the fact that the operator time evolution is generated by $\mathscr{L}^\dagger$, the adjoint superoperator.

3.3 LIOUVILLE SPACE FORMULATION

Having succesfully derived the Lindblad master equation (3.67) governing the quantum system dynamics the next obvious question is how to solve it. The formal solution is obtained by looking at the superoperator formulation (3.68), which gives us straight away that

$$\rho_S(t) = \mathrm{e}^{\mathscr{L}t}\rho_{\mathrm{S}}(0). \quad (3.73)$$

But this raises questions. How do we treat the superoperator $\mathscr{L}$? What does it mean to exponentiate it? What *is* $\mathscr{L}$ exactly? These questions are answered and the problem of

solving the master equation is made easier by moving to a *Liouville space*, where we are able to represent the state operators as vectors and superoperators as matrices acting on them. This allows us to utilize the powerful tools of linear algebra.

The discussion in this section follows Ref. [54] by Jerryman Gyamfi, where he describes the Liouville space formulation in detail. Here the most important and crucial steps in constructing the Liouville space formulation, as well as showing how to obtain the master equation in this formulation are provided. The finer mathematical details are left out but the reader can find them easily from the reference provided.

We begin by considering a density matrix of a two-level system to illustrate the mapping from matrices to vectors. The state operator can be written as

$$\rho(t) = |\psi(t)\rangle\langle\psi(t)| = \begin{pmatrix} a(t) \\ b(t) \end{pmatrix}\begin{pmatrix} a^*(t) & b^*(t) \end{pmatrix} = \begin{pmatrix} |a(t)|^2 & a(t)b^*(t) \\ a^*(t)b(t) & |b(t)|^2 \end{pmatrix}, \tag{3.74}$$

for some time dependent complex values $a(t)$ and $b(t)$. Now we define a so called *bra-flipper operator* $\mho$, which acts on operators $|a\rangle\langle b|$ the following way:

$$\mho\big[\,|a\rangle\langle b|\,\big] = |a\rangle \otimes |b\rangle^* \equiv |a,b\rangle\rangle\,, \tag{3.75}$$

with $|b\rangle^*$ being the complex conjugate of $|b\rangle$ and where both the bra-flipper operator and the operator $|a\rangle\langle b|$ live in the same space $\mathscr{O}_d$, which is the space of operators acting on $\mathscr{H}_d$. The resulting element $|a,b\rangle\rangle$ lives in the Liouville space $\mathscr{L}_d$ and is called a *superket*. Essentially the bra-flipper $\mho$ transforms the ordinary matrix product between vectors to a tensor product (effectively a Kronecker product) between the elements. Using this to equation (3.74) yields

$$\mho[\rho(t)] = \mho\big[\,|\psi(t)\rangle\langle\psi(t)|\,\big] = |\psi(t)\rangle \otimes |\psi(t)\rangle^*\,. \tag{3.76}$$

If we represent this as matrices we get

$$|\rho\rangle\rangle = \begin{pmatrix} a(t) \\ b(t) \end{pmatrix} \otimes \begin{pmatrix} a^*(t) \\ b^*(t) \end{pmatrix} = \begin{pmatrix} |a(t)|^2 \\ a(t)b^*(t) \\ b(t)a^*(t) \\ |b(t)|^2 \end{pmatrix}. \tag{3.77}$$

We can notice that when we define the bra-flipper as in equation (3.75) we are defining a mapping from matrices to vectors where the vector is obtained by stacking the rows of the matrix. This can clearly be seen by comparing equations (3.74) and (3.77). Of course the density matrix ρ does not have to be two dimensional, the same procedure generalizes for arbitrary density matrices.

The same procedure works also for any operators acting on $\mathscr{H}_d$. We can see this by decomposing an arbitrary operator A in some orthonormal basis $\{|i\rangle\}$

$$A = \sum_i^d \sum_j^d A_{ij}\,|i\rangle\langle j|\,, \quad A_{ij} = \langle i|A|j\rangle\,, \tag{3.78}$$

where we assumed the Hilbert space to have dimension $\dim(\mathscr{H}_d) = d$. Then we apply the bra-flipper operation to this decomposition:

$$\mho[A] = |A\rangle\rangle = \sum_i^d \sum_j^d A_{ij} \mho\big[\,|i\rangle\langle j|\,\big] = \sum_i^d \sum_j^d A_{ij} |i,j\rangle\rangle = \sum_\alpha^{d^2} A_\alpha |\alpha\rangle\rangle\,. \tag{3.79}$$

Here we denoted the basis elements $|i,j\rangle\rangle$ of the Liouville space by a single index $|\alpha\rangle\rangle$. This denotes a basis (or a *superbasis*) of the Liouville space. We can see that we have transformed the operator representation from a $d \times d$ dimensional matrix into a d^2 dimensional vector.

We skip now a lot of mathematical details about the Liouville space formulation, such that the existence of dual vectors called *superbras* $\langle\langle\alpha|$, orthonormality of the superbasis spanned by the superkets and the fact that $\mho$ is an isomorphism between the space of operators $\mathscr{O}_d$ (acting on the Hilbert space $\mathscr{H}_d$) and the Liouville space $\mathscr{L}_d$. Although these interesting results are required to give rigour to the formulation we don't need the exact details in order to proceed further and gain intuition on what is happening with this method. So let us continue.

We saw above that we are indeed able to transform operator representation from matrices to vectors. But this is just the first step in the formulation. How about superoperators? It would make sense that since operators acting on $\mathscr{H}_d$ become vectors in $\mathscr{L}_d$, then superoperators (which act on operators) would become matrices in $\mathscr{L}_d$ acting on the vectorized state operators. As we will soon discover, this is exactly what happens.

At this point we can see the striking similarities this approach has with Dirac notation. For example, equation (3.79) is essentially a decomposition of the operator A in the Liouville space with a superbasis $|\alpha\rangle\rangle$, just like we would write for a pure state the Hilbert space $\mathscr{H}_d$. Therefore we can argue that there exists superoperators acting on $\mathscr{L}_d$, living in space $\mathscr{S}_d$, which can be expressed in terms of the orthonormal superbasis $\{|\alpha\rangle\rangle\langle\langle\alpha|\}$ as

$$\mathfrak{B} = \sum_\alpha^{d^2} \sum_{\alpha'}^{d^2} \mathfrak{B}_{\alpha\alpha'} |\alpha\rangle\rangle\langle\langle\alpha'|\,, \quad \mathfrak{B}_{\alpha\alpha'} = \langle\langle\alpha|\mathfrak{B}|\alpha'\rangle\rangle\,, \tag{3.80}$$

for some superoperator $\mathfrak{B}$, just like in equation (3.78) for operators. We can also express the superbasis explicitly in terms of the original basis elements of the Hilbert space $\mathscr{H}_d$ (see equation (3.79) last step) to get

$$\mathfrak{B} = \sum_i^d \sum_j^d \sum_k^d \sum_l^d \mathfrak{B}_{ij,kl} |i,j\rangle\rangle\langle\langle k,l|\,, \quad \mathfrak{B}_{ij,kl} = \langle\langle i,j|\mathfrak{B}|k,l\rangle\rangle\,, \tag{3.81}$$

The above equation shows explicitly that for our d-dimensional Hilbert space $\mathscr{H}_d$ the superoperators are $d^2 \times d^2$ matrices in the Liouville space formulation.

We have now encountered four different spaces, namely the Hilbert space of quantum states $\mathscr{H}_d$, the space $\mathscr{O}_d$ of operators acting on said Hilbert space, the Liouville space $\mathscr{L}_d$ of vectorized operators and the space $\mathscr{S}_d$ of superoperators acting on the Liouville space.[9] The relation between these spaces is summarized in figure 3.3.

[9] Strictly mathematically all of the said spaces have Hilbert space structure so they are all Hilbert spaces. But for clarity we are referring only to the space $\mathscr{H}_d$ as Hilbert space just to give it a distinct name.

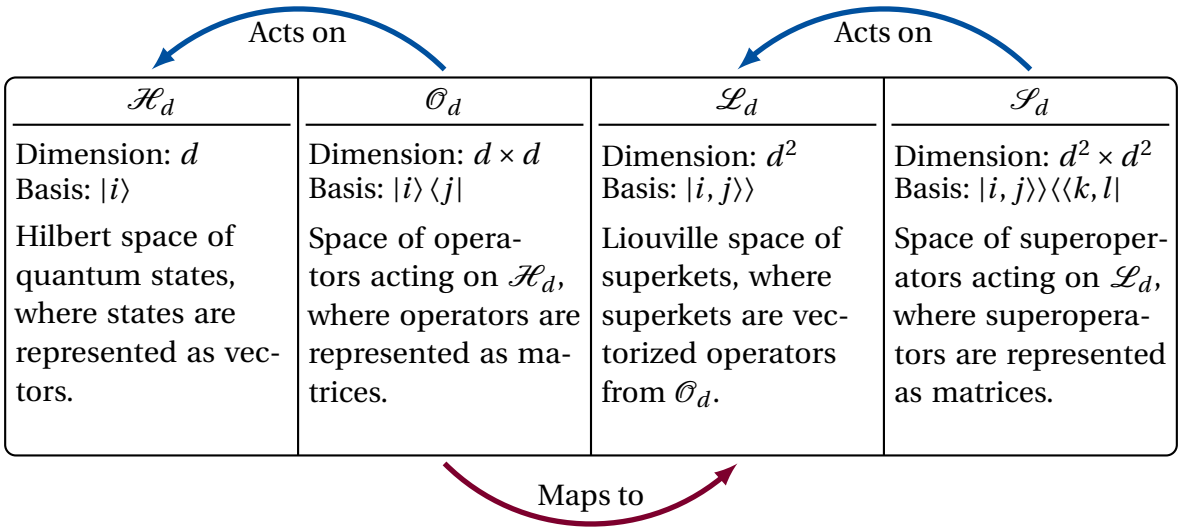

Figure 3.3: Structure of the Liouville space formalism discussed in this section. The spaces $\mathscr{H}_d$ and $\mathscr{L}_d$ are similar to each other as are spaces $\mathscr{O}_d$ and $\mathscr{S}_d$. The bridge between the representations is the isomorphism between $\mathscr{O}_d$ and $\mathscr{L}_d$ given by the bra-flipper operator.

Now that the full structure of the Liouville space formalism has been introduced, we can derive a result that is important for further treatment of the Lindblad master equation we derived in the last section. This result is called the *superket triple product identity*. Let us consider three operators A, B and C acting on $\mathscr{H}_d$ (and thus $A,B,C \in \mathscr{O}_d$). Their product is also an operator acting on $\mathscr{H}_d$. Applying the bra-flipper operator $\mho$ to the product ABC gives us the corresponding superket in $\mathscr{L}_d$, for which the superket triple product identity states that

$$|ABC\rangle\rangle = \left(A \otimes C^\top\right)|B\rangle\rangle\,. \tag{3.82}$$

What the above equation tells us is that the superket $|ABC\rangle\rangle \in \mathscr{L}_d$, corresponding to the operator $ABC \in \mathscr{O}_d$, can be written as a result of the superoperator $(A \otimes C^\top) \in \mathscr{S}_d$ acting on a superket $|B\rangle\rangle$. From (3.82) it is easy to derive two more results by adding an identity operator $\mathbb{1}_d$ either to the front or to the back of ABC:

$$|ABC\rangle\rangle = \left(AB \otimes \mathbb{1}_d\right)|C\rangle\rangle\,, \tag{3.83}$$

$$|ABC\rangle\rangle = \left(\mathbb{1}_d \otimes BC\right)|A\rangle\rangle\,. \tag{3.84}$$

The proof of equation (3.82) is given in the Appendix C.

Using the superket triple product identity we are able to deal with commutators. Let $A,B \in \mathscr{O}_d$. Mapping their commutator $\left[A,B\right] \in \mathscr{O}_d$ to the Liouville space $\mathscr{L}_d$ gives

$$\begin{aligned} |[A,B]\rangle\rangle &= |AB - BA\rangle\rangle = |AB\rangle\rangle - |BA\rangle\rangle = |AB\mathbb{1}_d\rangle\rangle - |\mathbb{1}_d BA\rangle\rangle \\ &= \left(A \otimes \mathbb{1}_d\right)|B\rangle\rangle - \left(\mathbb{1}_d \otimes A^\top\right)|B\rangle\rangle = \left(A \otimes \mathbb{1}_d - \mathbb{1}_d \otimes A^\top\right)|B\rangle\rangle \\ &= \left[\!\left[A, \mathbb{1}_d\right]\!\right]|B\rangle\rangle\,, \end{aligned} \tag{3.85}$$

where we defined the *supercommutator* between two superoperators

$$\left[\!\left[X, Y\right]\!\right] = X \otimes Y^\top - Y \otimes X^\top\,. \tag{3.86}$$

Similarly we can define a *superanticommutator* as

$$\{\{X,Y\}\} = X \otimes Y^\top + Y \otimes X^\top . \tag{3.87}$$

Now we have finally all the tools we need to transform the Lindblad master equation (3.67) to the Liouville space. Applying the bra-flipper to both sides of the equation gives

$$\begin{aligned}
|\dot{\rho}_S\rangle\rangle &= -\frac{i}{\hbar}|[H,\rho_S]\rangle\rangle + \frac{\alpha^2}{\hbar^2}\sum_{\beta,\beta'}\sum_{\omega}\gamma_{\beta\beta'}\Big(|A_{\beta'}\rho_S A_\beta^\dagger\rangle\rangle - \frac{1}{2}\big|\{A_\beta^\dagger A_{\beta'},\rho_S\}\big\rangle\big\rangle\Big) \\
&= -\frac{i}{\hbar}[\![H,\mathbb{1}]\!]|\rho_S\rangle\rangle + \frac{\alpha^2}{\hbar^2}\sum_{\beta,\beta'}\sum_{\omega}\gamma_{\beta\beta'}\Big(A_{\beta'}\otimes A_\beta^*|\rho_S\rangle\rangle - \frac{1}{2}\{\{A_\beta^\dagger A_{\beta'},\mathbb{1}\}\}|\rho_S\rangle\rangle\Big) \\
&= \Big[-\frac{i}{\hbar}[\![H,\mathbb{1}]\!] + \frac{\alpha^2}{\hbar^2}\sum_{\beta,\beta'}\sum_{\omega}\gamma_{\beta\beta'}\Big(A_{\beta'}\otimes A_\beta^* - \frac{1}{2}\{\{A_\beta^\dagger A_{\beta'},\mathbb{1}\}\}\Big)\Big]|\rho_S\rangle\rangle \\
&= \mathscr{L}|\rho_S\rangle\rangle ,
\end{aligned}$$

where the Liouvillian superoperator matrix $\mathscr{L}$ is given by

$$\mathscr{L} = -\frac{i}{\hbar}[\![H,\mathbb{1}]\!] + \frac{\alpha^2}{\hbar^2}\sum_{\beta,\beta'}\sum_{\omega}\gamma_{\beta\beta'}\Big(A_{\beta'}\otimes A_\beta^* - \frac{1}{2}\{\{A_\beta^\dagger A_{\beta'},\mathbb{1}\}\}\Big). \tag{3.88}$$

The main result of the Liouville space formulation now lies in front of us. We have managed to transform the abstract nature of the master equation (3.67) into something that can be computed using matrix calculus.

The solution to the master equation given by (3.73) is now understandable. We obtain the vectorized state of the system by computing the matrix exponential of (3.88) at time t. Then to represent the state again by a density matrix, we can perform an inverse operation to bra-flipper $\mho$. Thus, we jump to the Liouville space to make the computations easier and then jump back to the original space in order to be able to interpret the obtained results. Of course, solving the equation (3.73) is still difficult and cumbersome to do analytically for most cases but since we are now able to write the solution in terms of matrix operations, we can utilize computers to perform the tedious calculations.

◆ ◆ ◆

In this chapter we introduced the necessary tools and results of open quantum systems to compute their dynamics when a Hamiltonian describing the system is known. After a short reminder of basic quantum mechanics we moved on to derive the Lindblad master equation that gives the time evolution of our system. The derivation was quite long and several approximations had to be made in order to get to the final result. But all of the steps were physically motivated and gave some insight into the cases which we can analyze using these methods. The derivation left us with an abstract equation of operators and superoperators but in the final section we showed how we can map it into essentially a problem of matrix calculus, allowing us to later utilize computers in the final steps of solving the master equation.

As in chapter 2, the above was done in order to gain sufficient knowledge and understanding of the underlaying theory, to be able to compute the dynamics of an actual circuit, once its Hamiltonian has been found. Equipped with the tools of chapters 2 and 3, we are ready to deal with the actual matter of this thesis. How does the quantum state of a transmon qubit evolve in time when it is coupled to a resistive environment? This is the discussion ahead of us in the next chapter.

4 From Micrograph to Master Equation

Up to this point in this thesis we have discussed separately both the cQED architecture for building superconducting circuits and the theory of open quantum systems. We saw in chapter 2 that cQED gives us tools for finding the quantum Hamiltonian of a circuit. In chapter 3 we went through the process of deriving an equation of motion for an open quantum system when the total system Hamiltonian is already known and in a convenient form.

In this chapter we combine what we have learned so far to analyze an actual superconducting circuit with a transmon qubit coupled to a readout resonator and its drive line. The exact details of the qubit circuit can be found in [55]. In addition to just having a qubit and readout resonator in our model, we add a resistor into the qubit drive line, whose temperature can be modified. This *variable temperature noise source* [11] allows for characterization of thermal effects on the qubit state. The ultimate goal is indeed to gain theoretical knowledge on how the qubit state behaves as a function of temperature of this noise source.

We begin by considering the superconducting circuit of the qubit and other circuit elements. We draw its circuit diagram and using that infer the related energies of the system. That way we are able to first derive the classical Hamiltonian and then to quantize it to get an equation which can be used in the theory of open quantum systems. Using the derived quantum Hamiltonian we then derive a master equation which describes the time evolution of the qubit-readout resonator system.

4.1 Quantization of the circuit

As stated in the title of this chapter, we begin our journey from a micrograph picture of the qubit circuit. Figure 4.1 is an optical image of the qubit circuit we are interested in, taken from [55]. On the very top of the figure the qubit drive line is visible. Microwave signals intended to operate the qubit are send to the drive line. In the middle we can see the meandering readout resonator as a *coplanar waveguide* (CPW). This is used to read out the qubit state indirectly. On the bottom we can see the cross shape, which includes the qubit itself and its coupling to the readout resonator. The specific type of transmon in this geometry is called the *Xmon* qubit, the name motivated by its shape [56].

What is not visible in the figure is the resistor installed at the drive line, whose effect on the qubit's quantum state we actually want to analyze.

In order to quantize the circuit in question, we need to take the following steps:

1. Find the *lumped element circuit diagram* of the qubit circuit in figure 4.1.
2. Use the methods presented in chapter 2 to find the Lagrangian and the Hamiltonian of the circuit.
3. Quantize the resulting Hamiltonian.

Let's begin with the first step, which essentially parametrizes our problem mathematically, allowing for the use of theoretical tools in the rest of the analysis.

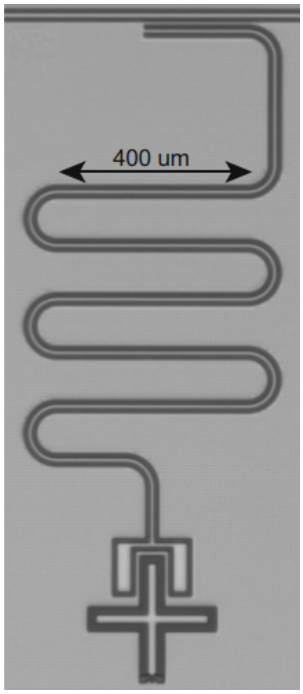

Figure 4.1: Qubit circuit micrograph. Figure cropped from original in Ref. [55] under license CC BY 4.0.

4.1.1 THE CIRCUIT DIAGRAM

The main difficulty in drawing the lumped element circuit diagram comes from the existence of the readout resonator. The methods of usual circuit analysis assume that the wavelength of the signals passing through the circuit are much smaller than the physical dimensions of the circuit itself [57]. In this case the circuit elements can be approximated as being discrete. However, the CPW resonators for qubit readout are manufactured such that their length is comparable to the wavelength of signals passing through them. Therefore we cannot trivially describe the readout resonator in a lumped element description. We need to use transmission line theory for their characterization.

An important distiction in considering the CPW resonators is whether they are $\lambda/4$ or $\lambda/2$ resonators. This means that whether the fundamental mode of the resonator has wavelength $\lambda = 4d$ or $\lambda = 2d$, where d is the total length of the CPW [57]. These different frequency modes are obtained by using different boundary conditions in the ends of the line. If both ends of the line are either short- or open-circuited, we recover a $\lambda/2$ resonator. If different boundary conditions are used on the ends, the line is a $\lambda/4$ resonator. See figure 4.2 for pictorial explanation on how the voltages and currents behave in each case. We are interested in a line that is open on the qubit end (giving capacitive coupling to qubit) and shorted on the drive line end (giving inductive coupling there), which makes it a $\lambda/4$ resonator.

A CPW resonator is a distributed device, whose capacitance and inductance can be modelled as being distributed along the whole length of the resonator [58]. Following the example of [7], we represent a transmission line as a combination of lumped elements, as shown in figure 4.3. In this model the self-inductance of the line is distributed along its whole length using small lumped element inductors L, as is the capacitance to ground with

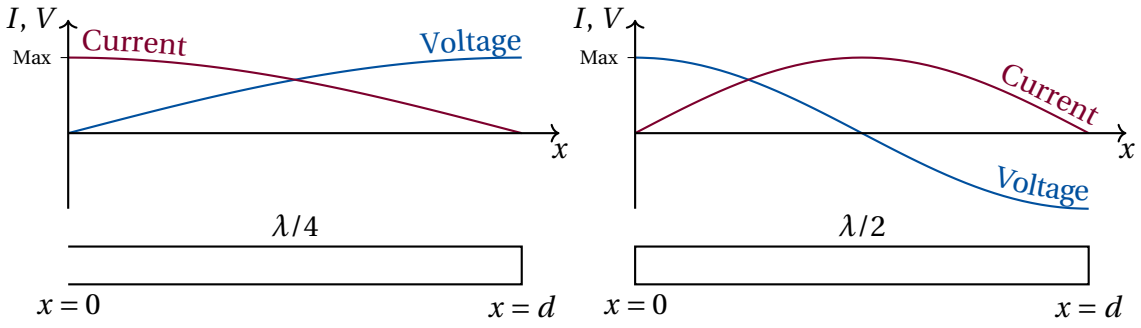

Figure 4.2: Differences between the two types of CPWs. On the left side we have a CPW with left end shorted (giving maximum current) and right end open (with maximum voltage). The right side CPW has both ends open so the current at the ends disappear. The $\lambda/4$ CPW depicted above will lead to an inductive coupling on its left end and to capacitive coupling on its right end.

lumped capacitors C [57]. In this *telegrapher model*, the different elements are separated by a small distance Δx from each other.

In Ref. [7] it is shown that the continuum limit $\Delta x \to 0$ of the telegrapher model in figure 4.3 leads into a continuous form Hamiltonian

$$H = \int_0^d \mathrm{d}x \Big[\frac{Q(x,t)^2}{2c_0} + \frac{1}{2l_0}\Big(\frac{\partial \Phi(x,t)}{\partial x}\Big)^2 \Big], \tag{4.1}$$

where c_0 and l_0 are respectively the distributed capacitance and inductance per unit length of the line. The function $Q(x,t)$ is the charge density field and $\Phi(x,t)$ the flux field. This Hamiltonian, together with the Hamilton equations lead into a wave equation for the flux field $\Phi(x,t)$:

$$v_0^2 \frac{\partial^2 \Phi(x,t)}{\partial x^2} - \frac{\partial^2 \Phi(x,t)}{\partial t^2} = 0, \tag{4.2}$$

with $v_0 = 1/\sqrt{l_0 c_0}$ being the speed of the signal. It is well known that the wave equation is separable and that a linear combination of solutions is also a solution [59] so we can write general form of the solution as

$$\Phi(x,t) = \sum_{m=0}^{\infty} \phi_m(t) u_m(x). \tag{4.3}$$

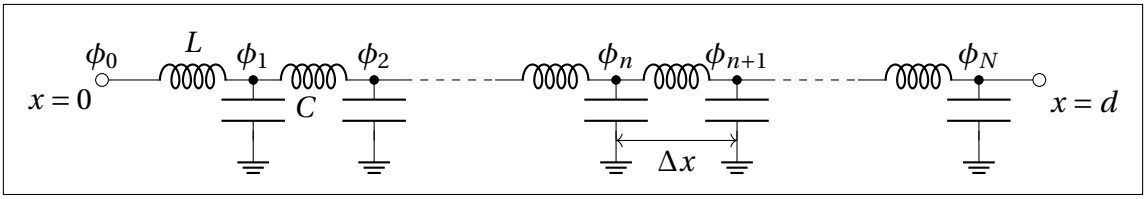

Figure 4.3: Telegrapher model of the transmission line. The line can be thought of as consisting of several lumped capacitors and inductors that are distributed along the whole length of the line. Figure adapted from [7].

The separability of the wave equation leads to two separate differential equations

$$u_m''(x) = -\frac{\omega_m^2}{v_0^2} u_m(x) \quad \text{and} \quad \ddot{\phi}_m(t) = -\omega_m^2 \phi_m(t) \tag{4.4}$$

for each mode m. We can concentrate on solving the spatial profile of the wave given by $u_m(x)$. The specific solution we are looking for $u_m(x)$ is determined by the boundary conditions of our problem. As our CPW resonator is open at one end (at $x = d$), we require that the current disappears there. On the shorted end (at $x = 0$) we require that the voltage disappears. These two boundary conditions can be presented via the following equations [7]

$$V(x=0,t) = \frac{\partial \Phi(x,t)}{\partial t}\Big|_{x=0} = 0\,, \tag{4.5}$$

$$I(x=d,t) = -\frac{1}{l_0}\frac{\partial \Phi(x,t)}{\partial x}\Big|_{x=d} = 0\,. \tag{4.6}$$

The voltage boundary condition is satisfied if $\Phi(x=0,t)=0$.[1] Using these two boundary conditions for the spatial profile we get

$$u_m(x) = A\sin\left(\frac{(2m+1)\pi}{2}\frac{x}{d}\right) = A\sin\left(k_m\frac{x}{d}\right), \tag{4.7}$$

where we defined $k_m \equiv (2m+1)\pi/2$. The coefficient A can be determined via a normalization condition [7]:

$$\frac{1}{d}\int_0^d u_n(x)u_m(x)\mathrm{d}x = \delta_{nm}\,. \tag{4.8}$$

Evaluating the above integral with the spatial profiles from equation (4.7) gives $A=\sqrt{2}$. We can now collect what we have found to gain an expression for the flux field $\Phi(x,t)$ in equation (4.3). We get

$$\Phi(x,t) = \sum_{m=0}^{\infty} \sqrt{2}\sin\left(k_m\frac{x}{d}\right)\phi_m(t)\,. \tag{4.9}$$

Note that we have not solved the time profile explicitly but that is not a problem as the explicit form is not needed. Now we can use the flux field solution above in the Hamiltonian (4.1). Noting that $Q(x,t)$ is the charge conjugate to the flux field given by $Q(x,t) = c_0\partial_t\Phi(x,t)$ we get

$$\begin{aligned} H &= \int_0^d \mathrm{d}x\left[\frac{1}{2}c_0\Big(\frac{\partial\Phi(x,t)}{\partial t}\Big)^2 + \frac{1}{2l_0}\Big(\frac{\partial\Phi(x,t)}{\partial x}\Big)^2\right] \\ &= \sum_{n,m}^{\infty}\left[\frac{1}{2}c_0\dot{\phi}_m(t)\dot{\phi}_n(t)\int_0^d u_m(x)u_n(x)\mathrm{d}x\right] + \frac{1}{2l_0}\int_0^d \Phi'(x,t)\Phi'(x,t)\mathrm{d}x\,. \end{aligned}$$

[1] Strictly the requirement given by equation (4.5) is that $\Phi(x=0,t)$ is constant in time. But since $\Phi(x,t)$ has explicit time dependence, we require that the spatial profile vanishes at this boundary, thus setting the constant to zero.

We can use integration by parts to the second term. The substitution term is zero due to the boundary conditions (4.5) and (4.6). To the remaining integral term with $\Phi''(x,t)$ we can use equation (4.4) and get

$$H = \sum_{n,m}^{\infty} \Big[\frac{1}{2} c_0 \dot{\phi}_m(t)\dot{\phi}_n(t) + \frac{1}{2l_0}\frac{\omega_m^2}{v_0^2}\phi_m(t)\phi_n(t) \Big] \underbrace{\int_0^d u_m(x)u_n(x)\mathrm{d}x}_{(4.8)}$$

$$= \sum_{m=0}^{\infty} \Big[\frac{1}{2} c_0 d\dot{\phi}_m^2 + \frac{d}{2l_0}\frac{\omega_m^2}{v_0^2}\phi_m^2 \Big] = \sum_{m=0}^{\infty} \Big[\frac{1}{2} C_\mathrm{f}\dot{\phi}_m^2 + \frac{1}{2} C_\mathrm{f}\omega_m^2\phi_m^2 \Big].$$

Above we defined the total capacitance $C_\mathrm{f} = dc_0$ and used the definition of v_0 to simplify the second term. Now we use the conjugate charge which was defined as $Q_m = C_\mathrm{f}\dot{\phi}_m$ (see chapter 2) to get

$$H = \sum_{m=0}^{\infty} \Big[\frac{Q_m^2}{2C_\mathrm{f}} + \frac{1}{2} C_\mathrm{f}\omega_m^2\phi_m^2 \Big]. \tag{4.10}$$

If we compare this to the Hamiltonian of a single parallel LC-oscillator (2.6) we can immediately notice that the CPW resonator can be modelled as an infinite sum of parallel LC-circuits with capacitance C_f and mode frequency ω_m. The infinity of the sum is a bit problematic but if we work in a frequency range that is close to the resonance frequency of the CPW resonator (and this is usually the case [7])[2], we can neglect all the other contributions other than the one arising from the $m = 0$ term. Therefore we can model the CPW resonator as a parallel LC-oscillator, with the capacitance defined by $C_\mathrm{f} = dc_0$ and inductance determinable from the frequency and capacitance as $L_\mathrm{f} = 1/(C_\mathrm{f}\omega_0^2)$.

So we have indeed managed to find a simple lumped element representation for the CPW. But there is one question that still remains. What is the capacitance C_f in our model and how do we obtain its value? We defined it to be the "total" distributed capacitance $C_\mathrm{f} = dc_0$ along the whole length d of the CPW. So the problem reduces essentially to determining the capacitance per unit length c_0. It turns out that c_0 is completely determinable from the geometry of the manufactured CPW, depending on the width of the conducting line and on the gaps between the central conductor and the surrounding ground plane [58]. Therefore, if we know the geometry of our CPW resonator we can find out the distributed capacitance and thus also the lumped element capacitance.

Now we are ready to draw the circuit diagram for the qubit circuit in the micrograph 4.1. This is shown in figure 4.4. We can see there in the left the qubit drive line with an additional resistor R whose effect to the qubit dynamics we ultimately want to model. Between the drive line and the readout resonator is an inductive coupling via a mutual inductance M. On the right side we have the transmon qubit with a coupling to the readout resonator via a capacitor C_g. The black dots represent different nodes of the circuit and the corresponding voltages are given by the time derivatives of the generalized fluxes.

[2] CPW resonators can be manufactured such that their fundamental mode resonance frequency f_0 is close to the qubit frequency, but also other regimes are possible. As the frequency responses of both the qubit and the resonator are very narrow (see for example [55, 58]), we can indeed work in a frequency range close to f_0 and ignore the other modes.

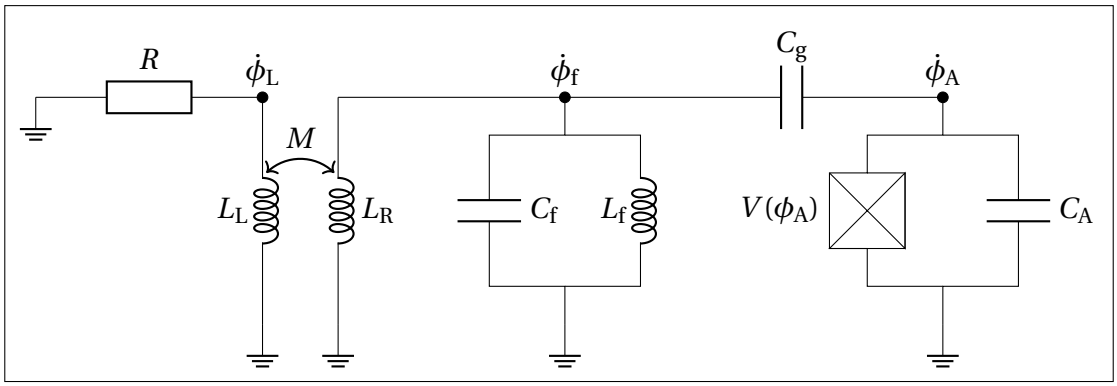

Figure 4.4: Lumped element circuit model of the micrograph in figure 4.1. On the left is the drive line with inductive coupling to the readout resonator, which in turn is capacitively coupled to the qubit.

4.1.2 CIRCUIT HAMILTONIAN

Now that we have obtained a lumped element model for the qubit circuit, we can apply the tools learned in chapter 2 to compute the Hamiltonian of the circuit. Our goal is to obtain a Hamiltonian that describes the free dynamics of the qubit and the readout resonator and the interaction between them. Additionally we want to see the interaction between the resistor and the qubit-resonator system. In essence, we are looking for a Hamiltonian which is in a form that resembles the starting point of interaction picture analysis. This allows us later to obtain a master equation describing the qubit dynamics.

We begin by considering the capacitive and inductive energies of the circuit in figure 4.4, writing them in terms of the generalized flux variables. In what follows we apply the Caldeira-Leggett model for the resistor, modelling it as an infinite series of parallel LC-oscillators.

The capacitive energy of the circuit is given by

$$E_C = \frac{1}{2}C_A\dot{\phi}_A^2 + \frac{1}{2}C_f\dot{\phi}_f^2 + \frac{1}{2}C_g(\dot{\phi}_A - \dot{\phi}_f)^2 + \sum_{\alpha=1}^{\infty}\frac{1}{2}C_\alpha\dot{\phi}_\alpha^2. \tag{4.11}$$

and the inductive energy is given by

$$E_L = V(\phi_A) + \frac{1}{2L_f}\phi_f^2 + \frac{1}{2L_R}\phi_f^2 + \frac{M}{L_L L_R}\phi_f\phi_L + \frac{1}{2L_L}\phi_L^2 + \sum_{\alpha=1}^{\infty}\frac{1}{2L_\alpha}\phi_\alpha^2. \tag{4.12}$$

The sums over α correspond to the resistor decomposition shown in chapter 2. Now we can apply Kirchoff's voltage law to notice that $\sum_\alpha^\infty \dot{\phi}_\alpha = \dot{\phi}_L$, so then it must hold that $\sum_\alpha^\infty \phi_\alpha = \phi_L + \phi_{ext}$, with some external flux ϕ_{ext}. Taking the external flux to be zero, we get from (4.12)

$$E_L = V(\phi_A) + \frac{1}{2L_f}\phi_f^2 + \frac{1}{2L_R}\phi_f^2 + \frac{M}{L_L L_R}\phi_f\Big(\sum_\alpha^\infty \phi_\alpha\Big) + \frac{1}{2L_L}\Big(\sum_\alpha^\infty \phi_\alpha\Big)^2 + \sum_{\alpha=1}^{\infty}\frac{1}{2L_\alpha}\phi_\alpha^2. \tag{4.13}$$

Looking at equations (4.11) and (4.13), we see that some terms describe coupling between certain variables while some other terms are free, describing only energy associated with a

single variable. We can better see this structure, if we represent these equations in matrix form. Let's therefore define a flux vector $\boldsymbol{\phi} = \left[\phi_\mathrm{A}, \phi_\mathrm{f}, \boldsymbol{\phi}_\alpha^\top\right]^\top$, with the vector $\boldsymbol{\phi}_\alpha^\top = \left[\phi_1, \phi_2, ...\right]$ collecting together the resonator fluxes. Using this convention, we can rewrite the energy equations as

$$E_\mathrm{C} = \frac{1}{2}\dot{\boldsymbol{\phi}}^\top \boldsymbol{C}\dot{\boldsymbol{\phi}}, \quad E_\mathrm{L} = \frac{1}{2}\boldsymbol{\phi}\boldsymbol{L}^{-1}\boldsymbol{\phi} + V(\phi_\mathrm{A}), \tag{4.14}$$

with the matrices $\boldsymbol{C}$ and $\boldsymbol{L}^{-1}$ given by

$$\boldsymbol{C} = \left[\begin{array}{cc|ccc} C_\mathrm{A}+C_\mathrm{g} & -C_\mathrm{g} & 0 & 0 & \dots \\ -C_\mathrm{g} & C_\mathrm{f}+C_\mathrm{g} & 0 & 0 & \\ \hline 0 & 0 & C_1 & 0 & \\ 0 & 0 & 0 & C_2 & \\ \vdots & & & & \ddots \end{array}\right], \boldsymbol{L}^{-1} = \left[\begin{array}{cc|ccc} 0 & 0 & 0 & 0 & \dots \\ 0 & L_\mathrm{f}^{-1}+L_\mathrm{R}^{-1} & \frac{M}{L_\mathrm{R}L_\mathrm{L}} & \frac{M}{L_\mathrm{R}L_\mathrm{L}} & \\ \hline 0 & \frac{M}{L_\mathrm{R}L_\mathrm{L}} & L_1^{-1}+L_\mathrm{L}^{-1} & L_\mathrm{L}^{-1} & \\ 0 & \frac{M}{L_\mathrm{R}L_\mathrm{L}} & L_\mathrm{L}^{-1} & L_2^{-1}+L_\mathrm{L}^{-1} & \\ \vdots & & & & \ddots \end{array}\right] \tag{4.15}$$

We can see that the matrices have a structure which describes the interaction between the circuit parts. The upper left corner describes the system comprised of the qubit and the readout resonator, while the lower right corner describes the resistor. The interactions between the qubit-resonator system with the resistor is included in the lower left and upper right blocks.

Let's now define a vector $\boldsymbol{a} = [0,1]^\top$ and $\boldsymbol{e}$ as a vector full of ones. Then we can write the above matrices in a more concise manner as

$$\boldsymbol{C} = \begin{bmatrix} \boldsymbol{S}_\mathrm{C} & 0 \\ 0 & \boldsymbol{C}_\alpha \end{bmatrix}, \quad \boldsymbol{L}^{-1} = \begin{bmatrix} \boldsymbol{S}_\mathrm{L} & \frac{M}{L_\mathrm{R}L_\mathrm{L}}\boldsymbol{a}\boldsymbol{e}^\top \\ \frac{M}{L_\mathrm{R}L_\mathrm{L}}\boldsymbol{e}\boldsymbol{a}^\top & \boldsymbol{L}_\alpha^{-1} + L_\mathrm{L}^{-1}\boldsymbol{e}\boldsymbol{e}^\top \end{bmatrix}. \tag{4.16}$$

The matrices $\boldsymbol{S}_\mathrm{C}$ and $\boldsymbol{S}_\mathrm{L}$ are the qubit-resonator system matrices given by the top left blocks in equation (4.15). $\boldsymbol{C}_\alpha$ and $\boldsymbol{L}_\alpha^{-1}$ are diagonal matrices with the values C_α and L_α^{-1} on their diagonals.

Now we can present the Lagrangian of our circuit as

$$\mathscr{L} = \frac{1}{2}\dot{\boldsymbol{\phi}}^\top \boldsymbol{C}\dot{\boldsymbol{\phi}} - \frac{1}{2}\boldsymbol{\phi}^\top \boldsymbol{L}^{-1}\boldsymbol{\phi} - V(\phi_\mathrm{A}), \tag{4.17}$$

with the matrices $\boldsymbol{C}$ and $\boldsymbol{L}^{-1}$ given by equation (4.16). In principle we could now do the Legendre transformation to obtain the Hamiltonian of the circuit. But that would be in a cumbersome form due to the existence of interaction between the different resistor modes α. We would lose a clear separation between system, environment, and resistor Hamiltonian. To get the Hamiltonian in a better form, we introduce a coordinate transformation (or a point transformation) of the flux vector $\boldsymbol{\phi}$ from Refs. [60, 10]:

$$\boldsymbol{Z} = \begin{bmatrix} \mathbb{1}_2 & 0 \\ 0 & M_0^{-1/2}\boldsymbol{M}_\alpha^{1/2} \end{bmatrix}, \quad \boldsymbol{M}_\alpha = \boldsymbol{L}_\alpha^{-1} + \xi\boldsymbol{e}\boldsymbol{e}^\top. \tag{4.18}$$

Here M_0 is a free constant with units of inverse inductance and ξ is a parameter we can choose freely.

Following the example of Cattaneo and Paraoanu [10], we apply the transformation $\boldsymbol{Z}$ giving us new coordinates $\boldsymbol{z} = \boldsymbol{Z}\boldsymbol{\phi}$. This forces the matrices to transform as $\boldsymbol{C}_z = \boldsymbol{Z}^{-1}\boldsymbol{C}\boldsymbol{Z}^{-1}$ and $\boldsymbol{L}_z^{-1} = \boldsymbol{Z}^{-1}\boldsymbol{L}^{-1}\boldsymbol{Z}^{-1}$. The transformed capacitance and inductance matrices are

$$\boldsymbol{C}_z = \begin{bmatrix} \boldsymbol{S}_{\mathrm{C}} & 0 \\ 0 & M_0 \boldsymbol{M}_\alpha^{-1/2} \boldsymbol{C}_\alpha \boldsymbol{M}_\alpha^{-1/2} \end{bmatrix}, \tag{4.19}$$

$$\boldsymbol{L}_z^{-1} = \begin{bmatrix} \boldsymbol{S}_{\mathrm{L}} & \frac{M}{L_{\mathrm{R}} L_{\mathrm{L}}} \boldsymbol{a}\boldsymbol{e}^\top \boldsymbol{M}_\alpha^{-1/2} M_0^{1/2} \\ \frac{M}{L_{\mathrm{R}} L_{\mathrm{L}}} M_0^{1/2} \boldsymbol{M}_\alpha^{-1/2} \boldsymbol{e}\boldsymbol{a}^\top & M_0 \boldsymbol{M}_\alpha^{-1/2} \big(\boldsymbol{L}_\alpha^{-1} + L_{\mathrm{L}}^{-1} \boldsymbol{e}\boldsymbol{e}^\top \big) \boldsymbol{M}_\alpha^{-1/2} \end{bmatrix}. \tag{4.20}$$

Using the definition of $\boldsymbol{M}_\alpha$ from equation (4.18) we can modify the bottom right element of the $\boldsymbol{L}_z^{-1}$ matrix to get

$$M_0 \boldsymbol{M}_\alpha^{-1/2} \big(\boldsymbol{L}_\alpha^{-1} + L_{\mathrm{L}}^{-1} \boldsymbol{e}\boldsymbol{e}^\top \big) \boldsymbol{M}_\alpha^{-1/2} = M_0 \mathbb{1} + (L_{\mathrm{L}}^{-1} - \xi) \boldsymbol{f}_\alpha \boldsymbol{f}_\alpha^\top ,$$

where we defined $\boldsymbol{f}_\alpha \equiv M_0^{1/2} \boldsymbol{M}_\alpha^{-1/2} \boldsymbol{e}$, called a coupling vector. Moreover, the above calculation presents us with an easy choice for the free parameter ξ. Setting $\xi = L_{\mathrm{L}}^{-1}$ makes the bottom right part of the $\boldsymbol{L}_z^{-1}$ matrix diagonal, which is what we are looking for. This choice of ξ also allows us to compute the inverse of $\boldsymbol{M}_\alpha$. For that we use the *Shermann-Morrison formula*, which states that if a matrix $\boldsymbol{A}$ can be written as a sum of some matrix $\boldsymbol{B}$ and a vector outerproduct $\boldsymbol{A} = \boldsymbol{B} + \boldsymbol{u}^\top \boldsymbol{v}$, its inverse is given by

$$(\boldsymbol{B} + \boldsymbol{u}^\top \boldsymbol{v})^{-1} = \boldsymbol{B}^{-1} - \frac{\boldsymbol{B}^{-1} \boldsymbol{u}^\top \boldsymbol{v} \boldsymbol{B}^{-1}}{1 + \boldsymbol{v}^\top \boldsymbol{B}^{-1} \boldsymbol{u}} . \tag{4.21}$$

The matrix $\boldsymbol{M}_\alpha$ is exactly of the form above. Thus its inverse is given by

$$\boldsymbol{M}_\alpha^{-1} = \boldsymbol{L}_\alpha - L_{\mathrm{R}}^{-1} \frac{\boldsymbol{L}_\alpha \boldsymbol{e}\boldsymbol{e}^\top \boldsymbol{L}_\alpha}{1 + L_{\mathrm{R}}^{-1} \boldsymbol{e}^\top \boldsymbol{L}_\alpha \boldsymbol{e}} \approx \boldsymbol{L}_\alpha . \tag{4.22}$$

The second term is negligible given that $L_\alpha \ll L_{\mathrm{R}}$ for all α, allowing us to do the approximation above.[3] The result in equation (4.22) is convenient because $\boldsymbol{L}_\alpha$ is a diagonal matrix, thus commuting with other diagonal matrices such as $\boldsymbol{C}_\alpha$.

Using the results above we can now write the transformed capacitance and inductance matrices from equations (4.19) and (4.20) as

$$\boldsymbol{C}_z = \begin{bmatrix} \boldsymbol{S}_{\mathrm{C}} & 0 \\ 0 & M_0 \boldsymbol{L}_\alpha \boldsymbol{C}_\alpha \end{bmatrix}, \quad \boldsymbol{L}_z^{-1} = \begin{bmatrix} \boldsymbol{S}_{\mathrm{L}} & \frac{M}{L_{\mathrm{R}} L_{\mathrm{L}}} \boldsymbol{a}\boldsymbol{f}_\alpha^\top \\ \frac{M}{L_{\mathrm{R}} L_{\mathrm{L}}} \boldsymbol{f}_\alpha \boldsymbol{a}^\top & M_0 \mathbb{1} \end{bmatrix}. \tag{4.23}$$

Now we can write the Lagrangian from equation (4.17) as

$$\begin{aligned} \mathscr{L} &= \frac{1}{2} \dot{\boldsymbol{\phi}}^\top \boldsymbol{C} \dot{\boldsymbol{\phi}} - \frac{1}{2} \boldsymbol{\phi}^\top \boldsymbol{L}^{-1} \boldsymbol{\phi} - V(z_{\mathrm{A}}) \\ &= \frac{1}{2} \dot{\boldsymbol{\phi}}^\top \boldsymbol{Z}\boldsymbol{Z}^{-1} \boldsymbol{C} \boldsymbol{Z}^{-1} \boldsymbol{Z} \dot{\boldsymbol{\phi}} - \frac{1}{2} \boldsymbol{\phi}^\top \boldsymbol{Z}\boldsymbol{Z}^{-1} \boldsymbol{L}^{-1} \boldsymbol{Z}^{-1} \boldsymbol{Z} \boldsymbol{\phi} - V(z_{\mathrm{A}}) \\ &= \frac{1}{2} \dot{\boldsymbol{z}}^\top \boldsymbol{C}_z \dot{\boldsymbol{z}} - \frac{1}{2} \boldsymbol{z}^\top \boldsymbol{L}_z^{-1} \boldsymbol{z} - V(z_{\mathrm{A}}) . \end{aligned} \tag{4.24}$$

[3] This is something that we assume to hold true. But we can see that it makes sense by looking at the form for the inductances of the resistor decomposition in equation (2.22). Taking the relevant frequencies ω_j to be in the order of GHz, as is usually the case in cQED, and $\Delta\omega$ small, then the approximation holds.

Defining the conjugate variable $\boldsymbol{p} = \partial\mathscr{L}/\partial\dot{\boldsymbol{z}}$ and performing the Legendre transformation gives us the matrix form Hamiltonian

$$H = \frac{1}{2}\dot{\boldsymbol{p}}^\top \boldsymbol{C}_z^{-1}\dot{\boldsymbol{p}} + \frac{1}{2}\boldsymbol{z}^\top \boldsymbol{L}_z^{-1}\boldsymbol{z} + V(z_\mathrm{A})\,. \tag{4.25}$$

Inverting $\boldsymbol{C}_z$ and opening the terms explicitly gives us the following Hamiltonian:

$$\begin{aligned} H = &\underbrace{\frac{p_\mathrm{A}^2}{2}\frac{C_\mathrm{f}+C_\mathrm{g}}{D} + V(z_\mathrm{A})}_{\text{Qubit}} + \underbrace{\frac{p_\mathrm{f}^2}{2}\frac{C_\mathrm{A}+C_\mathrm{g}}{D} + \frac{z_\mathrm{f}^2}{2}\left(\frac{1}{L_\mathrm{f}}+\frac{1}{L_\mathrm{R}}\right)}_{\text{Resonator}} + \underbrace{\sum_{\alpha=1}^{\infty}\left(\frac{p_\alpha^2}{2M_0}\frac{1}{L_\alpha C_\alpha} + \frac{M_0}{2}z_\alpha^2\right)}_{\text{Resistor}} \\ &+ \underbrace{p_\mathrm{A}p_\mathrm{f}\frac{C_\mathrm{g}}{D}}_{\substack{\text{Qubit-resonator}\\ \text{interaction}}} + \underbrace{\sum_{\alpha=1}^{\infty}\frac{M}{L_\mathrm{R}L_\mathrm{L}}f_\alpha z_\alpha z_\mathrm{f}}_{\substack{\text{Resistor-resonator}\\ \text{interaction}}}\,. \end{aligned} \tag{4.26}$$

Above we defined $D = C_\mathrm{A}C_\mathrm{f} + C_\mathrm{f}C_\mathrm{g} + C_\mathrm{g}C_\mathrm{A}$, which is the determinant of $\boldsymbol{S}_\mathrm{C}$ needed for computing $\boldsymbol{C}_z^{-1}$.

This Hamiltonian captures the energies of the circuit in figure 4.4. We can see the emergence of three free terms corresponding to the qubit, resonator and the resistor. These describe the energy associated with each of these elements separately. In addition to the free terms, two interaction terms emerge: qubit-resonator interaction and resonator-resistor interaction. The strength of these interactions are governed by the corresponding couplings between the elements. These are inductive coupling (via mutual inductance M) between the resistor and resonator, and capacitive coupling (via capacitance C_g) between the resonator and qubit. From the Hamiltonian we can notice that in the limit $C_\mathrm{g} \to 0$ and $M \to 0$ the interaction terms vanish and we are left with a free Hamiltonian.

Up to this point the treatment of circuit has been completely classical. To get a quantum description of the dynamics, we need to quantize the Hamiltonian (4.26). That is what we are going to do next.

4.1.3 HAMILTONIAN QUANTIZATION

In the Hamiltonian the terms for resonator and the resistor have the familiar harmonic oscillator dependency, namely they are of the form $p^2 + x^2$ for coordinate x and conjugate momentum p. Therefore we use the same method as in chapter 2 and try to find a way of quantizing them as quantum harmonic oscillators. The qubit part has an arbitrary potential $V(z_\mathrm{A})$, which we have not specified. Therefore the qubit is not in a harmonic oscillator form, but we will return to it a bit later.

Next we are going to quantize the resonator and resistor parts as quantum harmonic oscillators. This is done in the box below.

QHO:
The quantum harmonic oscillator of mass m and oscillation frequency ω is quantized, yielding

$$H_{\mathrm{QHO}} = \frac{p^2}{2m} + \frac{1}{2}m\omega^2 x^2 \quad \Rightarrow \quad x = \sqrt{\frac{\hbar}{2m\omega}}(a^\dagger + a), \qquad p = \mathrm{i}\sqrt{\frac{\hbar m\omega}{2}}(a^\dagger - a),$$

where $a^\dagger$ and a are the creation and annihilation operators respectively.

Resonator:
The resonator Hamiltonian is given by

$$H_{\mathrm{Resonator}} = \frac{p_{\mathrm{f}}^2}{2}\frac{C_{\mathrm{A}} + C_{\mathrm{g}}}{D} + \frac{z_{\mathrm{f}}^2}{2}\left(\frac{1}{L_{\mathrm{f}}} + \frac{1}{L_{\mathrm{R}}}\right). \tag{4.27}$$

Comparing this to the quantum harmonic oscillator case we can recognize its mass and frequency as

$$m = \frac{D}{C_{\mathrm{A}} + C_{\mathrm{g}}}, \qquad \omega_{\mathrm{f}}^2 = \frac{(C_{\mathrm{A}} + C_{\mathrm{g}})(L_{\mathrm{f}}^{-1} + L_{\mathrm{R}}^{-1})}{D}. \tag{4.28}$$

Therefore the (newly promoted) operators z_{f} and p_{f} can be written in terms of the ladder operators as

$$z_{\mathrm{f}} = \sqrt{\frac{\hbar(C_{\mathrm{A}} + C_{\mathrm{g}})}{2D\omega_{\mathrm{f}}}}(a^\dagger + a), \qquad p_{\mathrm{f}} = \mathrm{i}\sqrt{\frac{\hbar D\omega_{\mathrm{f}}}{2(C_{\mathrm{A}} + C_{\mathrm{g}})}}(a^\dagger - a). \tag{4.29}$$

Resistor:
The resistor Hamiltonian is given by

$$H_{\mathrm{Resistor}} = \sum_{\alpha=1}^{\infty}\left(\frac{p_\alpha^2}{2M_0}\frac{1}{L_\alpha C_\alpha} + \frac{M_0}{2}z_\alpha^2\right). \tag{4.30}$$

Comparing a single term with a fixed α to the QHO we can write the corresponding mass and frequency as

$$m_\alpha = M_0 L_\alpha C_\alpha, \qquad \omega_\alpha^2 = \frac{1}{L_\alpha C_\alpha}. \tag{4.31}$$

And these give the operators in terms of the ladder operators as

$$z_\alpha = \sqrt{\frac{\hbar\omega_\alpha}{2M_0}}(a^\dagger + a), \qquad p_\alpha = \mathrm{i}\sqrt{\frac{\hbar M_0}{2\omega_\alpha}}(a^\dagger - a). \tag{4.32}$$

Now most of the circuit Hamiltonian has been quantized, except for the qubit part. In order to do that, we need to set the inductive potential $V(z_{\mathrm{A}})$ to that of the transmon potential, which was discussed and derived in chapter 2 (see Eq. (2.52)). Neglecting the constant we

have

$$V(z_\mathrm{A}) = -E_\mathrm{J}\cos\left(2\pi\frac{z_\mathrm{A}}{\phi_0}\right), \tag{4.33}$$

with the Josephson energy E_J and magnetic flux quantum ϕ_0. We can now break this down into a Taylor series to get

$$V(z_\mathrm{A}) \approx -E_\mathrm{J} + \frac{E_\mathrm{J}}{2}\left(\frac{2\pi}{\phi_0}\right)^2 z_\mathrm{A}^2 - \frac{E_\mathrm{J}}{24}\left(\frac{2\pi}{\phi_0}\right)^4 z_\mathrm{A}^4. \tag{4.34}$$

We assume now that the manufactured transmon qubit has sufficient anharmonicity that we can confidently pick the computational subspace consisting of only the two lowest energy levels $|0\rangle$ and $|1\rangle$. Thus we can neglect also the z_A^4 term, because that would lead to terms proportional to $a^\dagger a^\dagger aa$, which would affect only higher energy levels [7, 36]. Once we drop also the constant $-E_\mathrm{J}$ for the same reason as always, the Hamiltonian equations being invariant with respect to addition of a constant, we get the qubit Hamiltonian as

$$H_\mathrm{Qubit} = \frac{p_\mathrm{A}^2}{2}\frac{C_\mathrm{f}+C_\mathrm{g}}{D} + V(z_\mathrm{A}) = \frac{p_\mathrm{A}^2}{2}\frac{C_\mathrm{f}+C_\mathrm{g}}{D} + \frac{E_\mathrm{J}}{2}\left(\frac{2\pi}{\phi_0}\right)^2 z_\mathrm{A}^2. \tag{4.35}$$

This is also in a form which resembles a harmonic oscillator. Repeating the same procedure as for the resonator and resistor above gives us the "mass" and frequency of the qubit as

$$m = \frac{D}{C_\mathrm{f}+C_\mathrm{g}}, \quad \omega_\mathrm{A}^2 = \frac{(C_\mathrm{f}+C_\mathrm{g})E_\mathrm{J}(2\pi)^2}{D\phi_0^2}, \tag{4.36}$$

which gives the operators z_A and p_A in terms of the ladder operators as

$$z_\mathrm{A} = \sqrt{\frac{\hbar(C_\mathrm{f}+C_\mathrm{g})}{2D\omega_\mathrm{A}}}(a_\mathrm{A}^\dagger + a_\mathrm{A}), \quad p_\mathrm{A} = \mathrm{i}\sqrt{\frac{\hbar D\omega_\mathrm{A}}{2(C_\mathrm{f}+C_\mathrm{g})}}(a_\mathrm{A}^\dagger - a_\mathrm{A}). \tag{4.37}$$

Now we need to remember that we are only interested in the two-level subspace of the qubit. The creation and annihilation operators live in an infinite dimensional Hilbert space, so we need to truncate them to two dimensions. We choose a basis where the ground state is $|g\rangle = [0\ 1]^\top$ and the excited state is $|e\rangle = [1\ 0]^\top$. This gives the following relations

$$a_\mathrm{A}^\dagger a_\mathrm{A}|g\rangle = 0, \ \ a_\mathrm{A}^\dagger a_\mathrm{A}|e\rangle = |e\rangle \quad \Rightarrow \quad a_\mathrm{A}^\dagger a_\mathrm{A} \sim \begin{bmatrix}1 & 0\\ 0 & 0\end{bmatrix} = \frac{\mathbb{1}+\sigma_z}{2} \propto \frac{1}{2}\sigma_z, \tag{4.38}$$

$$(a_\mathrm{A}^\dagger - a_\mathrm{A})|g\rangle = |e\rangle, \ \ (a_\mathrm{A}^\dagger - a_\mathrm{A})|e\rangle = -|g\rangle \quad \Rightarrow \quad (a_\mathrm{A}^\dagger - a_\mathrm{A}) \sim \begin{bmatrix}0 & 1\\ -1 & 0\end{bmatrix} = \mathrm{i}\sigma_y. \tag{4.39}$$

Above we wrote the truncation in terms of the Pauli sigma operators. Using now the quantized operators from equations (4.29), (4.32) and (4.37) in the circuit Hamiltonian (4.26) and applying the above truncation to the qubit operators yields us

$$\begin{aligned} H = &\underbrace{\frac{1}{2}\hbar\omega_\mathrm{A}\sigma_z}_{\text{Qubit}} + \underbrace{\hbar\omega_\mathrm{f}a_\mathrm{f}^\dagger a_\mathrm{f}}_{\text{Resonator}} + \underbrace{\sum_{\alpha=1}^{\infty}\hbar\omega_\alpha a_\alpha^\dagger a_\alpha}_{\text{Resistor}} - \underbrace{\frac{\mathrm{i}}{2}\hbar C_\mathrm{g}\sqrt{\frac{\omega_\mathrm{A}\omega_\mathrm{f}}{(C_\mathrm{f}+C_\mathrm{g})(C_\mathrm{A}+C_\mathrm{g})}}\sigma_y(a_\mathrm{f}^\dagger - a_\mathrm{f})}_{\text{Qubit-resonator interaction}} \\ &+ \underbrace{\frac{M}{L_\mathrm{L}}\sum_{\alpha=1}^{\infty}\sqrt{\frac{\hbar\omega_\alpha}{2}}\sqrt{\frac{\hbar(C_\mathrm{A}+C_\mathrm{g})}{2D\omega_\mathrm{f}}}\frac{\sqrt{L_\alpha}}{L_\mathrm{R}}(a_\alpha^\dagger + a_\alpha)(a_\mathrm{f}^\dagger + a_\mathrm{f})}_{\text{Resistor-resonator interaction}}. \end{aligned} \tag{4.40}$$

Above we used the definition of the coupling vector $\boldsymbol{f}_\alpha = \sqrt{M_o \boldsymbol{M}_\alpha^{-1}}\boldsymbol{e}$ to write the element of this vector as $f_\alpha = \sqrt{M_0 L_\alpha}$. Remember now that the inductances L_α were given by the Caldeira-Leggett model we derived in chapter 2. We can therefore use the derivation from there, more specifically equation (2.22) for the inductances and (2.36) for the spectrum of the resistor. Using these equations in the resistor-resonator interaction term in the quantized Hamiltonian (4.40) gives this term as

$$H_{\text{int}} = \frac{M}{L_L}\mu\sum_{k=1}^{\infty}\sqrt{\frac{\hbar\Delta\omega R\omega_{\text{c}}^2}{\pi\omega_k(\omega_{\text{c}}^2+\omega_k^2)L_{\text{R}}^2}}(a_k^\dagger + a_k)(a_{\text{f}}^\dagger + a_{\text{f}})\,, \tag{4.41}$$

where we switched the summation index to "dense" index k to comply with the literature [10] and introduced a factor μ as

$$\mu \equiv \sqrt{\frac{\hbar(C_{\text{A}}+C_{\text{g}})}{2D\omega_{\text{f}}}}\,. \tag{4.42}$$

The square root term in the sum in equation (4.41) describes the current fluctuations in the circuit for different frequencies ω_k. This allows us to define a coupling coefficient g_k that describes the interaction strength between the mode k of the resistor and the readout resonator as

$$g_k = \sqrt{\frac{\hbar\Delta\omega R\omega_{\text{c}}^2}{\pi\omega_k(\omega_{\text{c}}^2+\omega_k^2)}}\frac{\mu}{L_{\text{R}}}\,. \tag{4.43}$$

Using these definitions allows us to write the quantized Hamiltonian (4.40) as

$$H = \underbrace{\frac{1}{2}\hbar\omega_{\text{A}}\sigma_z}_{\text{Qubit}} + \underbrace{\hbar\omega_{\text{f}}a_{\text{f}}^\dagger a_{\text{f}}}_{\text{Resonator}} \underbrace{-\text{i}\hbar g_{\text{f}}\sigma_y(a_{\text{f}}^\dagger - a_{\text{f}})}_{\substack{\text{Qubit-resonator}\\ \text{interaction}}} + \underbrace{\sum_{k=1}^{\infty}\hbar\omega_k a_k^\dagger a_k}_{\text{Resistor}} + \underbrace{\frac{M}{L_{\text{L}}}\sum_{k=1}^{\infty}g_k(a_k^\dagger + a_k)(a_{\text{f}}^\dagger + a_{\text{f}})}_{\text{Resistor-resonator interaction}}\,, \tag{4.44}$$

where we defined the qubit-resonator coupling strength g_{f} as

$$g_f \equiv \frac{C_{\text{g}}}{2}\sqrt{\frac{\omega_{\text{A}}\omega_{\text{f}}}{(C_{\text{f}}+C_{\text{g}})(C_{\text{A}}+C_{\text{g}})}}\,. \tag{4.45}$$

One quantity we are interested in when considering the interaction between the bath and the system (so in this case the resistor and qubit-resonator combination) is the *spectral density* of the bath [31]. It tells how strongly does each frequency mode of the bath couple to the system. In our case we can compute it as

$$J(\omega) = \frac{1}{\hbar^2}\sum_{k=1}^{\infty}|g_k|^2\delta(\omega-\omega_k)\,. \tag{4.46}$$

Now the infinitesimal frequency gap $\Delta\omega$, originating from the Caldeira-Leggett model for the resistor, becomes useful because this allows us to represent the spectral density as an integral in the limit $\Delta\omega \to 0$. Plugging equation (4.43) into (4.46) and taking the continuum limit yields us

$$J(\omega) = \chi\frac{\omega_{\text{c}}^2}{\pi\omega(\omega_{\text{c}}^2+\omega^2)}\,, \tag{4.47}$$

where we introduced a factor $\chi = R\mu^2/(\hbar L_{\text{R}}^2)$.

4.2 DERIVATION OF THE MASTER EQUATION

Now that we have a fully quantized Hamiltonian (4.44) we are ready to start the process of finding the master equation that governs the qubit dynamics. As discussed in chapter 3, the open quantum systems approach allows us to compute the dynamics of a system coupled to some external bath. Therefore we need to choose now what parts of the Hamiltonian (4.44) do we regard as our system and what as the bath. We choose the qubit-resonator part to be our system and that leaves the resistor playing the role of the environment. Thus the Hamiltonian can be written as follows

$$H = H_{\text{System}} + H_{\text{Bath}} + H_{\text{Interaction}}\,, \tag{4.48}$$

where

$$H_{\text{System}} = \frac{1}{2}\hbar\omega_{\text{A}}\sigma_z + \hbar\omega_{\text{f}}a_{\text{f}}^\dagger a_{\text{f}} - \mathrm{i}\hbar g_{\text{f}}\sigma_y(a_{\text{f}}^\dagger - a_{\text{f}})\,, \tag{4.49}$$

$$H_{\text{Bath}} = \sum_{k=1}^{\infty}\hbar\omega_k a_k^\dagger a_k\,, \tag{4.50}$$

$$H_{\text{Interaction}} = \frac{M}{L_{\text{L}}}\sum_{k=1}^{\infty} g_k(a_k^\dagger + a_k)(a_{\text{f}}^\dagger + a_{\text{f}})\,. \tag{4.51}$$

This choice of system and bath makes intuitive sense but poses a problem for our calculations. In order to obtain the master equation describing the system dynamics, we need to have a basis where the system Hamiltonian is diagonal (see Eq. (3.50)). Looking at our chosen system Hamiltonian (4.49), we can see that it would be already in a diagonal form if the coupling strength $g_{\text{f}} = 0$.[4] However the inner interaction between the qubit and resonator complicates the situation. We need to look for a way to make H_{System} diagonal.

4.2.1 THE JAYNES-CUMMINGS HAMILTONIAN

Let's consider the state of the qubit in its two dimensional Hilbert space. It is either in its ground state $|g\rangle$ or its excited state $|e\rangle$. Similarly to the creation and annihilation operators $a^\dagger$ and a of infinite dimensional Hilbert spaces, we can say that there exists operators σ_+ and σ_- for the qubit such that $\sigma_+|g\rangle = |e\rangle$ and $\sigma_-|e\rangle = |g\rangle$. Writing these operators in terms of the qubit basis elements $|e\rangle$ and $|g\rangle$ we have

$$\sigma_+ = |e\rangle\langle g|\,, \quad \sigma_- = |g\rangle\langle e|\,. \tag{4.52}$$

We can express the Pauli operators in terms of these two operators as

$$\sigma_z = |e\rangle\langle e| - |g\rangle\langle g| = [\sigma_+, \sigma_-]\,, \tag{4.53}$$

$$\sigma_x = |e\rangle\langle g| + |g\rangle\langle e| = \sigma_+ + \sigma_-\,, \tag{4.54}$$

$$\sigma_y = \mathrm{i}(|g\rangle\langle e| - |e\rangle\langle g|) = \mathrm{i}(\sigma_- - \sigma_+)\,. \tag{4.55}$$

[4] If $g_{\text{f}} = 0$ the basis that diagonalizes H_{System} would be $|n_{\text{q}}\rangle \otimes |n_{\text{f}}\rangle$, where $n_{\text{q}} \in \{e, g\}$ and $|n_{\text{f}}\rangle$ is the Fock-basis of the resonator.

Using (4.55) in (4.49) gives us the following Hamiltonian

$$H_{\text{System}} = \frac{1}{2}\hbar\omega_{\text{A}}\sigma_z + \hbar\omega_{\text{f}}a_{\text{f}}^{\dagger}a_{\text{f}} + \hbar g_{\text{f}}(\sigma_- - \sigma_+)(a_{\text{f}}^{\dagger} - a_{\text{f}})\,. \tag{4.56}$$

If we now open up the interaction part we get terms proportional to $\sigma_- a_{\text{f}}^{\dagger}$, $\sigma_- a_{\text{f}}$, $\sigma_+ a_{\text{f}}^{\dagger}$ and $\sigma_+ a_{\text{f}}$. In the interaction picture these terms would oscillate at different frequencies with the following time dependence [61]

$$\begin{aligned}
\sigma_- a_{\text{f}}^{\dagger} &\sim \mathrm{e}^{-\mathrm{i}(\omega_{\text{A}}-\omega_{\text{f}})t} \\
\sigma_- a_{\text{f}} &\sim \mathrm{e}^{-\mathrm{i}(\omega_{\text{A}}+\omega_{\text{f}})t} \\
\sigma_+ a_{\text{f}}^{\dagger} &\sim \mathrm{e}^{\mathrm{i}(\omega_{\text{A}}+\omega_{\text{f}})t} \\
\sigma_+ a_{\text{f}} &\sim \mathrm{e}^{\mathrm{i}(\omega_{\text{A}}-\omega_{\text{f}})t}\,.
\end{aligned} \tag{4.57}$$

We can see that two terms oscillate faster compared to the other two. Moreover, the fast rotating terms do not conserve energy of the system because $\sigma_- a_{\text{f}}$ corresponds to both the qubit and resonator losing a quantum of energy while $\sigma_+ a_{\text{f}}^{\dagger}$ corresponds to both of them gaining a quantum of energy. Therefore we neglect the non energy conserving and fast rotating terms [61]. This is a valid approximation if $\omega_{\text{A}} + \omega_{\text{f}} \gg |\omega_{\text{A}} - \omega_{\text{f}}|$ which requires that the qubit and resonator frequencies are sufficiently close to each other [62]. Using this rotating wave approximation allows us to write the Hamiltonian as[5]

$$H_{\text{System}} = \frac{1}{2}\hbar\omega_{\text{A}}\sigma_z + \hbar\omega_{\text{f}}a_{\text{f}}^{\dagger}a_{\text{f}} + \hbar g_{\text{f}}(\sigma_- a_{\text{f}}^{\dagger} + \sigma_+ a_{\text{f}})\,. \tag{4.58}$$

This is called the *Jaynes-Cummings Hamiltonian*. It is used originally in quantum optics to describe the interaction between light and matter [65] but has found new ground in solid-state physics, for example in the research of superconducting qubits [62].

4.2.2 DISPERSIVE JAYNES-CUMMINGS MODEL

The Jaynes-Cummings Hamiltonian is still not in a diagonal form in equation (4.58). To get it into a diagonal form we move into a *dispersive regime*, where we assume that the coupling g_{f} between the qubit and the resonator is weak compared to the detuning $\Delta = |\omega_{\text{A}} - \omega_{\text{f}}|$ of resonance frequencies between the same elements. To accomplish this we introduce a *dispersive parameter* $\lambda = g_{\text{f}}/\Delta$ and require that $\lambda \ll 1$. Note that moving to the dispersive regime might seem contradictory with the application of the rotating wave approximation in deriving the Jaynes-Cummings Hamiltonian since there we required that ω_{A} and ω_{f} are sufficiently close to each other. However, our discussion is valid if both conditions are fulfilled, that is when [62]

$$g_{\text{f}} \ll |\omega_{\text{A}} - \omega_{\text{f}}| \ll \omega_{\text{A}} + \omega_{\text{f}}\,. \tag{4.59}$$

Following Ref. [62] we apply a unitary transformation U to the system Hamiltonian (4.58), where the transformation is parametrized by λ:

$$U = \mathrm{e}^{\lambda(\sigma_+ a_{\text{f}} - \sigma_- a_{\text{f}}^{\dagger})}\,. \tag{4.60}$$

[5] This is not the only way to arrive at the Hamiltonian (4.58). It can be shown that the Hamiltonian (4.56) can be represented as a continued fraction with respect to the coupling parameter g_{f} [63]. Therefore the rotating wave approximation is a correction of first order in g_{f}^2 and valid for $g_{\text{f}} \ll 1$ [63, 64], yielding (4.58).

Notice the crucial sign difference when compared to the interaction term of the Hamiltonian. Without the minus sign the transformation would not be unitary. Applying the transformation (see Eq. (3.27)) and using the Hadamard lemma we can write the Hamiltonian transformation as a series of commutators

$$H_{\text{Sys}}^{\text{D}} = U H_{\text{Sys}} U^\dagger = \mathrm{e}^{A} H_{\text{Sys}} \mathrm{e}^{-A} = H + \lambda\big[A, H\big] + \frac{\lambda^2}{2}\big[A, \big[A, H\big]\big] + \mathcal{O}(\lambda^3)\,, \tag{4.61}$$

where $A = \sigma_+ a_{\text{f}} - \sigma_- a_{\text{f}}^\dagger$. After a lot of tediuos algebra required to compute the commutators, we arrive at the dispersive Hamiltonian

$$H_{\text{Sys}}^{\text{D}} = \frac{1}{2}\hbar(\omega_{\text{A}} + 2g_{\text{f}}\lambda)\sigma_z + \hbar(\omega_{\text{f}} + g_{\text{f}}\lambda\sigma_z)a_{\text{f}}^\dagger a_{\text{f}} + \hbar g_{\text{f}}\lambda\sigma_- \sigma_+ + \mathcal{O}(\lambda^2)\,. \tag{4.62}$$

We can see that in this frame the qubit and resonator frequencies have changed a little bit. The new qubit frequency is $\omega_{\text{A}} \to \omega_{\text{A}}' = \omega_{\text{A}} + 2g_{\text{f}}\lambda$ and the resonator frequency becomes $\omega_{\text{f}} \to \omega_{\text{f}}' = \omega_{\text{f}} + g_{\text{f}}\lambda\sigma_z$. The remarkable thing is that the resonator frequency becomes now dependent on the state of the qubit. This allows for indirect, quantum nondemolition measurements of the qubit state via probing for the resonance frequency of the readout resonator [13, 66].

If we now neglect the terms of order $\mathcal{O}(\lambda^2)$ (because we set $\lambda \ll 1$) in equation (4.62), we have a Hamiltonian whose eigenstates are qubit-resonator product states. Therefore the Hamiltonian is diagonal in a basis $\{|e, n-1\rangle, |g, n\rangle\}$.[6] The eigenenergies of the dispersive Hamiltonian are given by

$$\begin{aligned} E_{g,n} &= \Big(n - \frac{1}{2}\Big)\hbar\omega_{\text{f}} - \frac{\hbar\Delta}{2} - n\hbar g_{\text{f}}\lambda\,, \\ E_{e,n-1} &= \Big(n - \frac{1}{2}\Big)\hbar\omega_{\text{f}} + \frac{\hbar\Delta}{2} + n\hbar g_{\text{f}}\lambda\,. \end{aligned} \tag{4.63}$$

We have now found a frame in which the system Hamiltonian (4.49) becomes diagonal. However, moving to the dispersive frame requires the unitary transformation (4.60) which applies also to other parts of the total Hamiltonian (4.48). In the total Hamiltonian the transformation changes the system-bath interaction term while leaving the bath term invariant:

$$H^{\text{D}} = U H_{\text{Sys}} U^\dagger + U H_{\text{Bath}} U^\dagger + U H_{\text{Int}} U^\dagger = H_{\text{Sys}}^{\text{D}} + H_{\text{Bath}} + U H_{\text{Int}} U^\dagger\,. \tag{4.64}$$

Therefore in order to obtain the full dispersive description, we need to evaluate the transformed interaction term. Just like in equation (4.61), we use the Hadamard lemma, neglect terms of order $\mathcal{O}(\lambda^2)$ and after some more tedious algebra end up with

$$H_{\text{Int}}^{\text{D}} = \frac{M}{L_{\text{L}}}(a_{\text{f}}^\dagger + a_{\text{f}} + \lambda\sigma_x)\sum_{k=1}^{\infty} g_k(a_k^\dagger + a_k)\,. \tag{4.65}$$

[6] Note that the basis was chosen such that the total number of quanta is conserved between the elements as required by the Jaynes-Cummings Hamiltonian. This choice also makes the eigenenergies match well as can be seen in equation (4.63).

The interaction part picked up an extra $\lambda\sigma_x$ term.

In conclusion, we have now the following Hamiltonian in the dispersive frame:

$$H^{\mathrm{D}} = H^{\mathrm{D}}_{\mathrm{Sys}} + H_{\mathrm{Bath}} + H^{\mathrm{D}}_{\mathrm{Int}}, \tag{4.66}$$

where

$$H^{\mathrm{D}}_{\mathrm{Sys}} = \frac{1}{2}\hbar(\omega_{\mathrm{A}} + 2g_{\mathrm{f}}\lambda)\sigma_z + \hbar(\omega_{\mathrm{f}} + g_{\mathrm{f}}\lambda\sigma_z)a^\dagger_{\mathrm{f}}a_{\mathrm{f}} + \hbar g_{\mathrm{f}}\lambda\sigma_-\sigma_+, \tag{4.67}$$

$$H_{\mathrm{Bath}} = \sum_{k=1}^{\infty}\hbar\omega_k a^\dagger_k a_k, \tag{4.68}$$

$$H^{\mathrm{D}}_{\mathrm{Int}} = \frac{M}{L_{\mathrm{L}}}(a^\dagger_{\mathrm{f}} + a_{\mathrm{f}} + \lambda\sigma_x)\sum_{k=1}^{\infty} g_k(a^\dagger_k + a_k). \tag{4.69}$$

Now we are ready to construct the master equation.

4.2.3 ARRIVING AT THE MASTER EQUATION

In the master equation derivation we needed the interaction Hamiltonian to be in the product form given by equation (3.37). Looking at equation (4.69) we can first notice that the interaction strength α is given by M/L_{L}. Then the interaction Hamiltonian is decomposed as

$$H^{\mathrm{D}}_{\mathrm{Int}} = \alpha A^{\mathrm{D}} \otimes B \quad \Rightarrow \quad A^{\mathrm{D}} = a^\dagger_{\mathrm{f}} + a_{\mathrm{f}} + \lambda\sigma_x, \quad B = \sum_{k=1}^{\infty} g_k(a^\dagger_k + a_k). \tag{4.70}$$

Now we need to write the system operator A^{D} in terms of the jump operators $A^{\mathrm{D}}(\omega)$ for different frequencies ω like in equation (3.51). This is done using the eigenstates $|g, n\rangle$ and $|e, n-1\rangle$ of the dispersive system Hamiltonian and its eigenenergies (4.63). A similar calculation has been done in Ref. [67]. In the calculations that follow we drop the superscript indicating dispersive frame for clarity of notation.

Case 1:
The qubit remains in its ground state:

$$A(E_{g,m} - E_{g,n}) = |g,n\rangle\langle g,n|A|g,m\rangle\langle g,m|.$$

The matrix element is

$$\langle g,n|A|g,m\rangle = \langle g,n|a^\dagger_{\mathrm{f}} + a_{\mathrm{f}} + \lambda\sigma_x|g,m\rangle = \sqrt{m+1}\delta_{n-1,m} + \sqrt{m}\delta_{n+1,m}.$$

So we have

$$A(E_{g,m} - E_{g,n}) = \left(\sqrt{m+1}\delta_{n-1,m} + \sqrt{m}\delta_{n+1,m}\right)|g,n\rangle\langle g,m|. \tag{4.71}$$

Case 2:

The qubit remains in its excited state:

$$A(E_{e,m-1} - E_{e,n-1}) = |e,n-1\rangle\langle e,n-1|A|e,m-1\rangle\langle e,m-1|\,.$$

The matrix element is

$$\langle e,n-1|A|e,m-1\rangle = \langle e,n-1|a_{\rm f}^\dagger + a_{\rm f} + \lambda\sigma_x|e,m-1\rangle = \sqrt{m}\delta_{n-1,m} + \sqrt{m-1}\delta_{n+1,m}\,.$$

So we have

$$A(E_{e,m-1} - E_{e,n-1}) = \left(\sqrt{m}\delta_{n-1,m} + \sqrt{m-1}\delta_{n+1,m}\right)|e,n-1\rangle\langle e,m-1|\,. \tag{4.72}$$

Case 3:
Qubit switches from ground state to excited state:

$$A(E_{g,m} - E_{e,n-1}) = |e,n-1\rangle\langle e,n-1|A|g,m\rangle\langle g,m|\,.$$

The matrix element is

$$\langle e,n-1|A|g,m\rangle = \langle e,n-1|a_{\rm f}^\dagger + a_{\rm f} + \lambda\sigma_x|g,m\rangle = \lambda\delta_{n-1,m}\,.$$

So we have

$$A(E_{g,m} - E_{e,n-1}) = \lambda\delta_{n-1,m}|e,n-1\rangle\langle g,m|\,. \tag{4.73}$$

Case 4:
Qubit drops from the excited state to the ground state. This is essentially the Hermitian conjugate of the above case, becoming

$$A(E_{e,m-1} - E_{g,n}) = \lambda\delta_{n+1,m}|g,n\rangle\langle e,m-1|\,. \tag{4.74}$$

Let's now collect the jump operators together from equations (4.71), (4.72), (4.73) and (4.74). We sum over m and fiddle with indices to get

$$A(E_{g,n} - E_{g,n+1}) = \sum_{n=0}^{\infty}\sqrt{n+1}\,|g,n+1\rangle\langle g,n| \equiv A(-\omega_{gg})\,, \tag{4.75}$$

$$A(E_{g,n+1} - E_{g,n}) = \sum_{n=0}^{\infty}\sqrt{n+1}\,|g,n\rangle\langle g,n+1| \equiv A(\omega_{gg})\,, \tag{4.76}$$

$$A(E_{e,n} - E_{e,n+1}) = \sum_{n=0}^{\infty}\sqrt{n+1}\,|e,n+1\rangle\langle e,n| \equiv A(-\omega_{ee})\,, \tag{4.77}$$

$$A(E_{e,n+1} - E_{e,n}) = \sum_{n=0}^{\infty}\sqrt{n+1}\,|e,n\rangle\langle e,n+1| \equiv A(\omega_{ee})\,, \tag{4.78}$$

$$A(E_{g,n} - E_{e,n}) = \lambda\sum_{n=0}^{\infty}|e,n\rangle\langle g,n| \equiv A(-\omega_{eg})\,, \tag{4.79}$$

$$A(E_{e,n} - E_{g,n}) = \lambda\sum_{n=0}^{\infty}|g,n\rangle\langle e,n| \equiv A(\omega_{eg})\,. \tag{4.80}$$

Equations (4.75) to (4.80) describe the possible jump operators for different frequencies. We should remember that according to equation (3.52), if we sum over all the possible frequencies we should get back the original operator of the system. In our case we should therefore find that the sum of equations (4.75) to (4.80) becomes $A = a_\mathrm{f}^\dagger + a_\mathrm{f} + \lambda\sigma_x$. That is indeed what we get, because the sum of (4.75) and (4.77) gives the matrix representation of $a_\mathrm{f}^\dagger$:

$$\begin{aligned} A(-\omega_{gg}) + A(-\omega_{ee}) &= \sum_{n=0}^{\infty} \left(\sqrt{n+1}\,|g,n+1\rangle\langle g,n| + \sqrt{n+1}\,|e,n+1\rangle\langle e,n| \right) \\ &= \Big(\underbrace{|e\rangle\langle e| + |g\rangle\langle g|}_{\mathbb{1}_2} \Big) \otimes \sum_{n=0}^{\infty} \sqrt{n+1}\,|n+1\rangle\langle n| = \mathbb{1}_2 \otimes a_\mathrm{f}^\dagger . \end{aligned} \tag{4.81}$$

Similarly the sum of the positive frequency components (4.76) and (4.78) gives the annihilation operator a_f. Then summing together (4.79) and (4.80) yields $\lambda\sigma_x$, so indeed the jump operators are correct.

Now, we need to consider how will we deal with the secular approximation in the derivation of the master equation (see subsection 3.2.3). Below are listed the frequencies we are dealing with. They are calculated by taking their definitions from equations (4.75) to (4.80) and using the eigenenergies of the dispersive Hamiltonian from equation (4.63):

$$\omega_{gg} = \omega_\mathrm{f} - g_\mathrm{f}\lambda\,, \tag{4.82}$$
$$\omega_{ee} = \omega_\mathrm{f} + g_\mathrm{f}\lambda\,, \tag{4.83}$$
$$\omega_{eg} = \omega_\mathrm{A} + (2n+1)g_\mathrm{f}\lambda\,. \tag{4.84}$$

The secular approximation deals with the frequency differences so let us compute the needed differences using the equations above.

$$|\omega_{gg} - \omega_{ee}| = 2g_\mathrm{f}\lambda\,, \tag{4.85}$$
$$|\omega_{gg} - \omega_{eg}| = \Delta + 2(n+1)g_\mathrm{f}\lambda\,, \tag{4.86}$$
$$|\omega_{ee} - \omega_{eg}| = \Delta + 2ng_\mathrm{f}\lambda\,. \tag{4.87}$$

Since we are working in the dispersive limit where Δ is taken to be sufficiently large, we can safely say that crossterms of the master equation dissipator with $A(\omega_{gg/ee})\rho A(\omega_{eg})$ are negligible and can be disregarded.[7] However, we need to be more careful with the other crossterms of the forms $A(\omega_{gg})\rho A(\omega_{ee})$. These cannot be disregarded as the timescale determined by equation (4.85) is quite large since λ is small.

To obtain a valid master equation we now briefly set $\lambda = 0$. This approach gives us a *local master equation*[8], which will provide us a valid approximation of the system dynamics if the

[7] Same is true for the crossterm with $A(\pm\omega_{gg/ee})\rho A(\mp\omega_{gg/ee})$.

[8] The local versus global approach to master equations is discussed in detail in Ref. [49]. In short, the local master equation sets the inner system coupling to zero, detaching the qubit from the resistor in our case when deriving the jump operators. The coupling is then reintroduced afterwards. In our case the assumption of locality does not actually affect the jump operator derivation (terms where λ appears will eventually be of the order λ^2 and can thus be neglected, see Eq. (4.93)) so we are not losing anything by doing it.

coupling between the qubit and resonator is sufficiently small [49]. This sets the frequencies $\omega_{gg} = \omega_{ee} = \omega_\mathrm{f}$ and thus $\omega_{gg} - \omega_{ee} = 0$, which gets rid of the rotation term in the master equation (see Eq. (3.59)). Note that even though now $\omega_{gg} = \omega_{ee}$, we still **cannot** neglect the cross terms $A(\omega_{gg})\rho A(\omega_{ee})$ because they correspond to different jump operators and their effect is not negligible. We now write the master equation into the following form:[9]

$$\begin{aligned}\dot{\rho}_\mathrm{Sys} = -\frac{\mathrm{i}}{\hbar}\left[H_\mathrm{Sys} + H_\mathrm{LS}, \rho_\mathrm{Sys}\right] + \frac{\alpha^2}{\hbar^2}\Big(&\mathscr{D}_{(\omega_{gg},\omega_{gg})}\left[\rho_\mathrm{Sys}\right] + \mathscr{D}_{(-\omega_{gg},-\omega_{gg})}\left[\rho_\mathrm{Sys}\right] \\ &+ \mathscr{D}_{(\omega_{ee},\omega_{ee})}\left[\rho_\mathrm{Sys}\right] + \mathscr{D}_{(-\omega_{ee},-\omega_{ee})}\left[\rho_\mathrm{Sys}\right] \\ &+ \mathscr{D}_{(\omega_{gg},\omega_{ee})}\left[\rho_\mathrm{Sys}\right] + \mathscr{D}_{(-\omega_{gg},-\omega_{ee})}\left[\rho_\mathrm{Sys}\right] \\ &+ \mathscr{D}_{(\omega_{ee},\omega_{gg})}\left[\rho_\mathrm{Sys}\right] + \mathscr{D}_{(-\omega_{ee},-\omega_{gg})}\left[\rho_\mathrm{Sys}\right] \\ &+ \mathscr{D}_{(\omega_{eg},\omega_{eg})}\left[\rho_\mathrm{Sys}\right] + \mathscr{D}_{(-\omega_{eg},-\omega_{eg})}\left[\rho_\mathrm{Sys}\right]\Big).\end{aligned} \tag{4.88}$$

This master equation is currently in a similar form as presented in [67], where they discussed the coherent frequency condition. The dissipators are given as

$$\mathscr{D}_{(\omega_{gg},\omega_{gg})}\left[\rho_\mathrm{Sys}\right] = \gamma(\omega_\mathrm{f})\left[A(\omega_{gg})\rho_\mathrm{Sys}A^\dagger(\omega_{gg}) - \frac{1}{2}\left\{A^\dagger(\omega_{gg})A(\omega_{gg}),\ \rho_\mathrm{Sys}\right\}\right], \tag{4.89}$$

$$\mathscr{D}_{(\omega_{ee},\omega_{ee})}\left[\rho_\mathrm{Sys}\right] = \gamma(\omega_\mathrm{f})\left[A(\omega_{ee})\rho_\mathrm{Sys}A^\dagger(\omega_{ee}) - \frac{1}{2}\left\{A^\dagger(\omega_{ee})A(\omega_{ee}),\ \rho_\mathrm{Sys}\right\}\right], \tag{4.90}$$

$$\mathscr{D}_{(\omega_{gg},\omega_{ee})}\left[\rho_\mathrm{Sys}\right] = \gamma(\omega_\mathrm{f})\left[A(\omega_{gg})\rho_\mathrm{Sys}A^\dagger(\omega_{ee}) - \frac{1}{2}\left\{A^\dagger(\omega_{ee})A(\omega_{gg}),\ \rho_\mathrm{Sys}\right\}\right], \tag{4.91}$$

$$\mathscr{D}_{(\omega_{ee},\omega_{gg})}\left[\rho_\mathrm{Sys}\right] = \gamma(\omega_\mathrm{f})\left[A(\omega_{ee})\rho_\mathrm{Sys}A^\dagger(\omega_{gg}) - \frac{1}{2}\left\{A^\dagger(\omega_{gg})A(\omega_{ee}),\ \rho_\mathrm{Sys}\right\}\right], \tag{4.92}$$

$$\mathscr{D}_{(\omega_{eg},\omega_{eg})}\left[\rho_\mathrm{Sys}\right] = \lambda^2\gamma(\omega_\mathrm{A})\left[A(\omega_{eg})\rho_\mathrm{Sys}A^\dagger(\omega_{eg}) - \frac{1}{2}\left\{A^\dagger(\omega_{eg})A(\omega_{eg}),\ \rho_\mathrm{Sys}\right\}\right]. \tag{4.93}$$

The dissipators with negative frequencies switch the place of conjugate transpose between the jump operators. We can notice that the last dissipator is proportional to λ^2 and can thus be neglected.[10]

To make some sense of the above master equation (4.88) with the dissipators (4.89) to (4.93), we use the jump operator definitions in equations (4.75) to (4.80). We can show after some straighforward algebra that the sum of the positive frequency dissipators becomes

$$\sum_{i,j\in\{\omega_{gg},\omega_{ee}\}} \mathscr{D}_{(i,j)}\left[\rho_\mathrm{Sys}\right] = \gamma(\omega_\mathrm{f})\left[a_\mathrm{f}\rho_\mathrm{Sys}a_\mathrm{f}^\dagger - \frac{1}{2}\left\{a_\mathrm{f}^\dagger a_\mathrm{f}, \rho_\mathrm{Sys}\right\}\right]. \tag{4.94}$$

The sum over the negative frequency dissipators gives a form where the conjugate transpose has switched its place:

$$\sum_{i,j\in\{-\omega_{gg},-\omega_{ee}\}} \mathscr{D}_{(i,j)}\left[\rho_\mathrm{Sys}\right] = \gamma(-\omega_\mathrm{f})\left[a_\mathrm{f}^\dagger\rho_\mathrm{Sys}a_\mathrm{f} - \frac{1}{2}\left\{a_\mathrm{f}a_\mathrm{f}^\dagger, \rho_\mathrm{Sys}\right\}\right]. \tag{4.95}$$

[9] Here we are already in the Schrödinger picture, with H_Sys given by (4.67). Therefore we have reintroduced λ in the unitary part of the master equation.

[10] The λ^2 dependency comes from the jump operator (4.79).

Using the above two equations in (4.88) we get the master equation as

$$\begin{aligned}\dot{\rho}_{\mathrm{Sys}} = -\frac{\mathrm{i}}{\hbar}\big[H_{\mathrm{Sys}} + H_{\mathrm{LS}}, \rho_{\mathrm{Sys}}\big] + \frac{\alpha^2}{\hbar^2}\gamma(\omega_{\mathrm{f}})\Big[a_{\mathrm{f}}\rho_{\mathrm{Sys}}a_{\mathrm{f}}^\dagger - \frac{1}{2}\big\{a_{\mathrm{f}}^\dagger a_{\mathrm{f}}, \rho_{\mathrm{Sys}}\big\}\Big] \\ + \frac{\alpha^2}{\hbar^2}\gamma(-\omega_{\mathrm{f}})\Big[a_{\mathrm{f}}^\dagger\rho_{\mathrm{Sys}}a_{\mathrm{f}} - \frac{1}{2}\big\{a_{\mathrm{f}}a_{\mathrm{f}}^\dagger, \rho_{\mathrm{Sys}}\big\}\Big].\end{aligned} \tag{4.96}$$

This is almost the final form for the master equation. What is left to do is to compute the coefficients $\gamma(\omega_{\mathrm{f}})$ and find out the form of the Lamb-shift Hamiltonian in the dispersive frame H_{LS}.

To compute $\gamma(\omega)$, we need to calculate the bath correlation function $\langle\tilde{B}^\dagger(\tau)\tilde{B}(0)\rangle$, where the bath operator B is shown in equation (4.70). Moving to the interaction picture via the unitary transformation $U = \mathrm{e}^{\mathrm{i}(H_{\mathrm{Sys}}+H_{\mathrm{Bath}})t/\hbar}$ gives us

$$\tilde{B}(t) = \sum_{k=0}^{\infty} g_k(a_k^\dagger \mathrm{e}^{\mathrm{i}\omega_k t} + a_k\mathrm{e}^{-\mathrm{i}\omega_k t}). \tag{4.97}$$

Let's now compute the bath correlation function.

The bath correlation function is defined the expectation value between the bath operators with a certain time interval τ. Using the bath operator in the interaction picture we get

$$\begin{aligned}\big\langle\tilde{B}^\dagger(\tau)\tilde{B}(0)\big\rangle &= \Big\langle \sum_{k,l=0}^{\infty} g_k g_l\big(a_k\mathrm{e}^{-\mathrm{i}\omega_k\tau} + a_k^\dagger\mathrm{e}^{\mathrm{i}\omega_k\tau}\big)\big(a_l^\dagger + a_l\big)\Big\rangle \\ &= \mathrm{Tr}\Big[\sum_{k,l=0}^{\infty} g_k g_l\big(a_k a_l^\dagger\mathrm{e}^{-\mathrm{i}\omega_k\tau} + a_k^\dagger a_l^\dagger\mathrm{e}^{\mathrm{i}\omega_k\tau} + a_k a_l\mathrm{e}^{-\mathrm{i}\omega_k\tau} + a_k^\dagger a_l\mathrm{e}^{\mathrm{i}\omega_k\tau}\big)\rho_{\mathrm{B}}\Big] \\ &= \sum_{k,l=0}^{\infty} g_k g_l\Big(\mathrm{Tr}\big[a_k a_l^\dagger\rho_{\mathrm{B}}\big]\mathrm{e}^{-\mathrm{i}\omega_k\tau} + \mathrm{Tr}\big[a_k^\dagger a_l^\dagger\rho_{\mathrm{B}}\big]\mathrm{e}^{\mathrm{i}\omega_k\tau} \\ &\qquad + \mathrm{Tr}\big[a_k a_l\rho_{\mathrm{B}}\big]\mathrm{e}^{-\mathrm{i}\omega_k\tau} + \mathrm{Tr}\big[a_k^\dagger a_l\rho_{\mathrm{B}}\big]\mathrm{e}^{\mathrm{i}\omega_k\tau}\Big).\end{aligned} \tag{4.98}$$

Assuming that the bath is in a thermal state given by equation (3.35) the traces become

$$\mathrm{Tr}\big[a_k^\dagger a_l^\dagger\rho_{\mathrm{B}}\big] = \mathrm{Tr}\big[a_k a_l\rho_{\mathrm{B}}\big] = 0, \tag{4.99}$$

$$\mathrm{Tr}\big[a_k a_l^\dagger\rho_{\mathrm{B}}\big] = \delta_{kl}\big(1 + \bar{n}(\omega_k)\big), \tag{4.100}$$

$$\mathrm{Tr}\big[a_k^\dagger a_l\rho_{\mathrm{B}}\big] = \delta_{kl}\bar{n}(\omega_k), \tag{4.101}$$

where $\bar{n}(\omega_k)$ is the expected number of quanta of frequency ω_k given by the Bose-Einstein distribution. Using the above equations for the traces in (4.98) we get

$$\big\langle\tilde{B}^\dagger(\tau)\tilde{B}(0)\big\rangle = \sum_{k=1}^{\infty} g_k^2\big[\big(1 + \bar{n}(\omega_k)\big)\mathrm{e}^{-\mathrm{i}\omega_k\tau} + \bar{n}(\omega_k)\mathrm{e}^{\mathrm{i}\omega_k\tau}\big] \tag{4.102}$$

Now we use the definition of the spectral density (see Eq. (4.46)) to turn the sum into an integral as

$$J(\omega) = \frac{1}{\hbar^2}\sum_{k=1}^{\infty}|g_k|^2\delta(\omega-\omega_k) \quad\Rightarrow\quad \sum_{k=1}^{\infty}|g_k|^2 = \hbar^2\int_0^\infty J(\omega)\mathrm{d}\omega. \tag{4.103}$$

Thus we can write equation (4.102) as

$$\left\langle \tilde{B}^{\dagger}(\tau)\tilde{B}(0)\right\rangle = \hbar^2 \int_0^{\infty} J(\omega_k)\left[\left(1+\bar{n}(\omega_k)\right)\mathrm{e}^{-\mathrm{i}\omega_k\tau} + \bar{n}(\omega_k)\mathrm{e}^{\mathrm{i}\omega_k\tau}\right]\mathrm{d}\omega_k\,. \tag{4.104}$$

Using this we can calculate the coefficients $\gamma(\omega_\mathrm{f})$ of the master equation (4.96), which can be found by computing the Fourier transform of the bath correlation functions as shown in equation (3.63). We get

$$\begin{aligned}\gamma(\omega_\mathrm{f}) &= \hbar^2 \int_{-\infty}^{\infty}\mathrm{d}\tau \int_0^{\infty}\mathrm{d}\omega_k J(\omega_k)\left[\left(1+\bar{n}(\omega_k)\right)\mathrm{e}^{-\mathrm{i}\omega_k\tau} + \bar{n}(\omega_k)\mathrm{e}^{\mathrm{i}\omega_k\tau}\right]\mathrm{e}^{\mathrm{i}\omega_\mathrm{f}\tau} \\ &= \hbar^2 \int_{-\infty}^{\infty}\mathrm{d}\tau \int_0^{\infty}\mathrm{d}\omega_k J(\omega_k)\left[\left(1+\bar{n}(\omega_k)\right)\mathrm{e}^{-\mathrm{i}(\omega_k-\omega_\mathrm{f})\tau} + \bar{n}(\omega_k)\mathrm{e}^{\mathrm{i}(\omega_k+\omega_\mathrm{f})\tau}\right].\end{aligned} \tag{4.105}$$

We use the definition of the Dirac delta function

$$\delta(x-y) = \frac{1}{2\pi}\int_{-\infty}^{\infty}\mathrm{e}^{\mathrm{i}p(x-y)}\mathrm{d}p \tag{4.106}$$

in the time integrals in equation (4.105) to get

$$\gamma(\omega_\mathrm{f}) = 2\pi\hbar^2 \int_0^{\infty}\mathrm{d}\omega_k J(\omega_k)\left[\left(1+\bar{n}(\omega_k)\right)\delta(\omega_\mathrm{f}-\omega_k) + \bar{n}(\omega_k)\delta(\omega_\mathrm{f}+\omega_k)\right]. \tag{4.107}$$

We can see from the above that we get a different result for positive and negative values of ω_f. For $\omega_\mathrm{f} > 0$ we get $\gamma(\omega_\mathrm{f}) = 2\pi\hbar^2 J(\omega_f)(1+\bar{n}(\omega_\mathrm{f}))$ and for $\omega_\mathrm{f} < 0$ we have $\gamma(\omega_\mathrm{f}) = 2\pi\hbar^2 J(-\omega_f)\bar{n}(-\omega_\mathrm{f})$. Using these results in the master equation (4.96) we get the following:

$$\begin{aligned}\dot{\rho}_\mathrm{Sys} = -\frac{\mathrm{i}}{\hbar}\left[H_\mathrm{Sys}+H_\mathrm{LS},\rho_\mathrm{Sys}\right] &+ \gamma\bar{n}\left(a_\mathrm{f}^{\dagger}\rho_\mathrm{Sys}a_\mathrm{f} - \frac{1}{2}\left\{a_\mathrm{f}a_\mathrm{f}^{\dagger},\rho_\mathrm{Sys}\right\}\right) \\ &+ \gamma(1+\bar{n})\left(a_\mathrm{f}\rho_\mathrm{Sys}a_\mathrm{f}^{\dagger} - \frac{1}{2}\left\{a_\mathrm{f}^{\dagger}a_\mathrm{f},\rho_\mathrm{Sys}\right\}\right).\end{aligned} \tag{4.108}$$

This form of the master equation is studied for example in Ref. [68] in the case of zero temperature and more generally in [69].

Above we defined the coefficient $\gamma = \alpha^2 2\pi J(\omega_\mathrm{f})$ with the spectral density $J(\omega)$ given by equation (4.47) and the system Hamiltonian is the dispersive Jaynes-Cummings Hamiltonian from equation (4.67). The Lamb-shift Hamiltonian H_LS renormalizes the resonator frequency but does not affect the qubit. Its effect on the resonator is very small so in practice we could disregard it completely. The Lamb-shift is studied more closely in Appendix D.

The master equation (4.108) describes thermally induced emission and absorbtion processes [31]. The absorbtion is governed by the $\gamma\bar{n}$ term and the emission by the $\gamma(1+\bar{n})$ term. Since $\bar{n}$ is the Bose-Einstein distribution we get $\bar{n} = 0$ at the absolute zero $T = 0$. There only the emission term survives, which makes sense. The resonator is able to emit out the quanta that are left in but not to absorb anything. Note that the emission and absorbtion rates depend on the temperature of the resistor, which we took to be our bath.

◆ ◆ ◆

We started this chapter by analyzing the micrograph 4.1 of the superconducting circuit with the qubit and the readout resonator. We were able to represent the distributed element CPW in a lumped element approximation and thus were able to draw the circuit diagram describing the superconducting circuit. We then managed to obtain the Hamiltonian of the circuit and quantize it by noticing that essentially all of the components of the circuit became quantum harmonic oscillators. Having derived the quantum Hamiltonian of the circuit we moved on to analyze it using the theory of open quantum systems. After a lot of calculations and some approximations we managed to derive the master equation (4.108) describing the dispersive dynamics of the qubit-resonator system coupled to a resistor on the drive line.

Just as the chapter title states, we made our way from micrograph to master equation. The obtained equation describes the dynamics of our quantum system and allows us to infer a very general behaviour directly from its form. But in order to obtain the fine details of the qubit dynamics we need to solve the said equation.

5 Solving for Qubit Dynamics

In the previous chapter, we first derived the Hamiltonian describing the energies of the superconducting circuit and then the master equation describing the time evolution of the qubit-resonator system. In order to gain specific knowledge on how the qubit's state behaves in time we have to solve the said master equation. Doing this analytically is cumbersome due to the appearance of large dimensional matrices. Therefore, we resort to numerical methods.

In order to understand the solutions we eventually obtain from the master equation, we need to understand the two different processes that characterize the qubit time evolution. Therefore we start this chapter by talking about *dissipation* and *decoherence*, gaining knowledge on what they mean, what is their effect on the qubit's state and where do they arise from. We also introduce the time scales that characterize these phenomena.

After talking about the underlying phenomena that we should observe, we move on to calculating analytical solutions of specific, solvable, cases of the master equation. We consider the unitary dynamics to gain understanding on how the qubit superposition sate evolves in time when no dissipators are present. This allows us to better understand the results obtained from solving the full system dynamics later. The assumption of unitarity simplifies our calculations significantly as it gets rid of the open system effects that we are ultimately interested in. Introducing back the dissipators, we are again left with the full master equation. This is much more difficult to solve, but we are able to analytically compute the steady state of the dynamics.

The final step in our analytical calculations is to map the master equation to the Liouville space. This not only allows us to compute the expectation values of the Pauli operators analytically as a decomposition into the eigenstates of the Liouvillian, but gives us a form of the master equation that we can solve numerically using a computer.

Finally, after the analytical considerations, we arrive at the numerical solutions, where we show how the qubit state behaves in time. We show the dynamics for the circuit we have been studying in this thesis by giving the circuit elements real numerical values that are determined during its manufacturing process. We also examine some other parameter regimes where different behaviours arise. Finally we show the main result of this thesis, answering how does the qubit decoherence time behave as a function of temperature.

5.1 ABOUT DISSIPATION AND DECOHERENCE

As soon as the quantum state of the qubit is prepared, it is subject to the time evolution determined by its Hamiltonian. If it were to be in a closed system we would be able to predict its state at any time in the future. But as stated multiple times already the qubit is an open quantum system, interacting with the circuitry around it and most notably the resistor in its drive line. This introduces coupling to uncontrollable degrees of freedom in the bath, or noise in short [8]. The presence of noise changes the state of the qubit in such a way that after a sufficiently long time the state is lost and we cannot know what was the original quantum state subject to the noise.

Two properties of quantum states of qubits that interest us are its energy or the *state population* and the superposition of the state or the *state coherence*.[1] External noise on the qubit can cause loss of energy of the qubit called dissipation or loss of superposition called decoherence. The effect of noise can be analyzed in the density matrix level by examining the time evolution of its elements. The diagonal entries of the qubit density matrix are called populations and they describe the energy eigenstates of the qubit. Therefore dissipation is seen as a decay of the matrix element corresponding to the excited state. The off-diagonal entries of the density matrix are called coherences and they describe the superposition nature of the quantum state. Thus decoherence is observed as the decay of the off-diagonal elements in the density matrix [8].

Whether our quantum system experiences dissipation or decoherence or both, stems from its Hamiltonian and the couplings present there. This is discussed in Ref. [8], where it is stated that dissipation arises from noise coupling that is *transverse* to the qubit quantization and *dephasing* (leading to decoherence) arises from *longitudinal* coupling. The term "longitudinal" refers to the direction of qubit quantization axis, which is the $\hat{z}$ axis in the Bloch sphere. Therefore any noise that couples to the operator σ_z in the qubit Hamiltonian induces dephasing and thus decoherence. Similarly any noise that couples to either σ_x or σ_y (those being transverse to qubit quantization) induces dissipation, thus pulling energy out from the qubit.[2] The effect of both decoherence and dissipation in the Bloch sphere representation is shown in figure 5.1.

Both dissipation and decoherence have their own time scales, which determine how fast these phenomena happen. We can describe them as *longitudinal relaxation rates* Γ_1 and *transverse relaxation rate* Γ_2 [8]:

$$\Gamma_1 \equiv \frac{1}{T_1}, \quad \Gamma_2 \equiv \frac{1}{T_2} = \frac{\Gamma_1}{2} + \Gamma_\phi, \tag{5.1}$$

where Γ_ϕ is the pure dephasing rate. It describes the time scale of dephasing where the quantum state rotates around the Bloch sphere. In figure 5.1 this is seen on the left, where the superposition state travels around the sphere as it is slowly losing its coherence and becoming a maximally mixed state.

[1] The superposition is between the energy eigenstates $|g\rangle$ and $|e\rangle$ of the qubit.

[2] Intuitively this can be understood as arising from the fact that both σ_x and σ_y change the state they operate on: $\sigma_x|g\rangle = |e\rangle$, $\sigma_x|e\rangle = |g\rangle$ and similarly for σ_y.

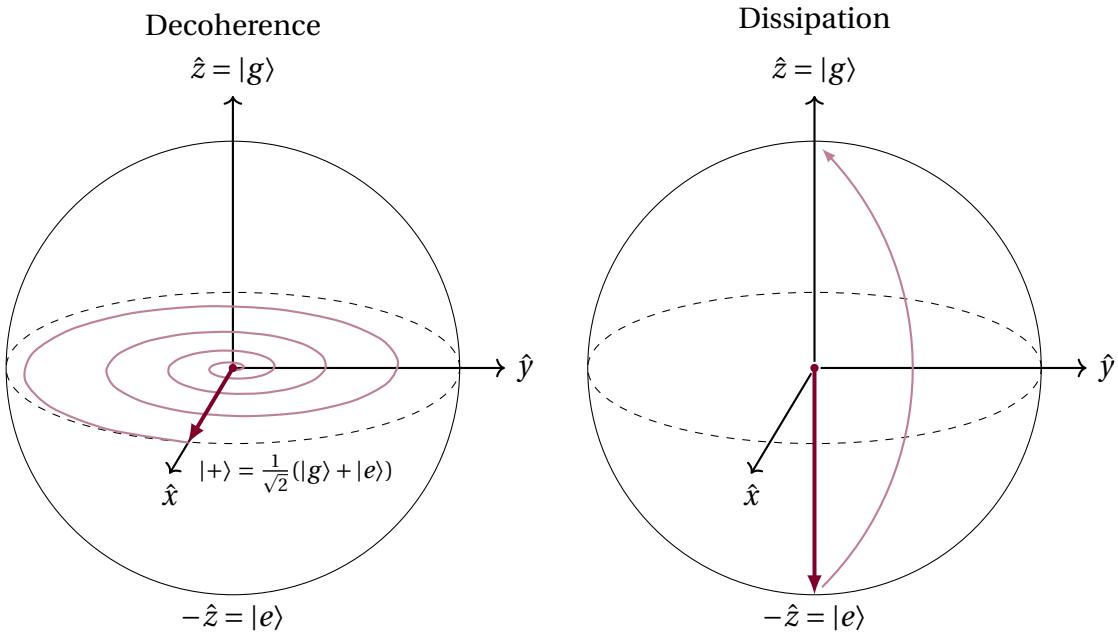

Figure 5.1: Decoherence and dissipation presented on a Bloch sphere. On the left a superposition state $|+\rangle$ experiences decoherence due to longitudinal noise. It loses its superposition and decays to the maximally mixed state $\mathbb{1}/2$ after a sufficiently long amount of time. On the right the excited state experiences dissipation due to transverse noise and loses its energy. After a sufficiently long amount of time it decays to the ground state $|g\rangle$.

The way to actually see dissipation and decoherence in the calculations is to compute expectation values of the Pauli operators. When we compute the expectation values we are actually computing the projection of the qubit's quantum state on the corresponding axis in the Bloch sphere representation. Thus $\langle\sigma_z\rangle$ projects the quantum state to the z-axis for example. Looking at figure 5.1 this measurement would yield 0 for $|+\rangle$ state and -1 for $|e\rangle$ state. Indeed, computing $\langle\sigma_z\rangle$ gives us knowledge about the qubit's mean energy.

To quantify coherence, we use an l_1-norm as a measure of coherence [70]

$$C(\rho) = \sum_{\substack{i,j \\ i\neq j}} |\rho_{ij}|\,. \tag{5.2}$$

This computes the sum of the norms of the off-diagonal matrix elements of the density matrix. In the case of a qubit this can be written in terms of the expectation values of the σ_x and σ_y operators as

$$C(\rho_{\mathrm{Q}}) = \sum_{\substack{i,j \\ i\neq j}} |\rho_{ij}| = |\rho_{01}| + |\rho_{10}| = 2|\rho_{01}| = 2\left|\frac{1}{2}\big(\langle\sigma_x\rangle - \mathrm{i}\langle\sigma_y\rangle\big)\right| = \sqrt{\langle\sigma_x\rangle^2 + \langle\sigma_y\rangle^2}\,. \tag{5.3}$$

So in order to completely describe the qubit time evolution we need to compute the expectation values of the Pauli operators.

In our case the qubit is coupled dispersively to the readout resonator and the resonator is coupled to the resistor. The qubit-resonator Hamiltonian was given by equation (4.67). From that Hamiltonian we can see that we are dealing with a longitudinal coupling to σ_z and no transverse coupling.[3] Therefore we could expect to see no dissipation when we solve the master equation (4.108) for the qubit dynamics but we should see decoherence as the qubit is interacting with the resonator via σ_z.

The absence of dissipation in our system can already be seen from the system Hamiltonian. However, we want to prove it rigorously. This in mind, we will consider the adjoint master equation of the one we derived in the end of the previous chapter. To get the exact time evolution of the coherence and more specifically how it changes as a function of temperature we need to solve the said master equation. In the next section we try to go as far as possible using analytical methods to gain insight on how the system behaves.

5.2 ANALYTICAL SOLUTIONS

The master equation describing the qubit-resonator system and its coupling to the resistor is given by

$$\begin{aligned}\dot{\rho}_{\text{Sys}} = -\frac{\mathrm{i}}{\hbar}[H_{\text{Sys}}, \rho_{\text{Sys}}] + \gamma\bar{n}\left(a_{\text{f}}^{\dagger}\rho_{\text{Sys}}a_{\text{f}} - \frac{1}{2}\{a_{\text{f}}a_{\text{f}}^{\dagger}, \rho_{\text{Sys}}\}\right) \\ + \gamma(1+\bar{n})\left(a_{\text{f}}\rho_{\text{Sys}}a_{\text{f}}^{\dagger} - \frac{1}{2}\{a_{\text{f}}^{\dagger}a_{\text{f}}, \rho_{\text{Sys}}\}\right),\end{aligned} \tag{5.4}$$

with the system Hamiltonian given by

$$H_{\text{Sys}} = \frac{1}{2}\hbar(\omega_{\text{A}} + 2g_{\text{f}}\lambda)\sigma_z + \hbar(\omega_{\text{f}} + g_{\text{f}}\lambda\sigma_z)a_{\text{f}}^{\dagger}a_{\text{f}} + \hbar g_{\text{f}}\lambda\sigma_{-}\sigma_{+}. \tag{5.5}$$

The Lamb-shift term was incorporated into the resonator frequency ω_{f} as it does not affect the qubit (see Appendix D).

We begin solving the master equation (5.4) by considering the time-evolution of σ_z. As argued in the last section the result should be simply that σ_z stays constant in time as there is no dissipation on the qubit. To show this rigorously, we apply the adjoint master equation (see Eq. (3.71)) which in our case reads

$$\begin{aligned}\dot{O}(t) = \frac{\mathrm{i}}{\hbar}[H_{\text{Sys}}, O(t)] + \gamma\bar{n}\left(a_{\text{f}}O(t)a_{\text{f}}^{\dagger} - \frac{1}{2}\{a_{\text{f}}a_{\text{f}}^{\dagger}, O(t)\}\right) \\ + \gamma(1+\bar{n})\left(a_{\text{f}}^{\dagger}O(t)a_{\text{f}} - \frac{1}{2}\{a_{\text{f}}^{\dagger}a_{\text{f}}, O(t)\}\right).\end{aligned} \tag{5.6}$$

Let's then set $O = \sigma_z$. We can immediately see that the dissipators vanish because σ_z commutes with the ladder operators. What we then have to do is to compute the commutator

[3] To be precise, if we look at equation (4.69) we see that the qubit is coupled transversely to the resistor via σ_x. However, this coupling is mediated by λ, which became λ^2 when computing the dissipators of the master equation (see Eq. (4.93)). Therefore we were able to neglect its contribution. Note that this term is exactly the one driving transitions $|g\rangle \leftrightarrow |e\rangle$, thus associated with dissipation.

between the system Hamiltonian and σ_z.

$$\begin{aligned}\left[H_{\text{Sys}}, \sigma_z(t)\right] &= \frac{1}{2}\hbar(\omega_\text{A} + 2g_\text{f}\lambda)\underbrace{\left[\sigma_z, \sigma_z\right]}_{=0} + \hbar\omega_\text{f}\underbrace{\left[a_\text{f}^\dagger a_\text{f}, \sigma_z\right]}_{=0} + \hbar g_\text{f}\lambda\underbrace{\left[\sigma_z a_\text{f}^\dagger a_\text{f}, \sigma_z\right]}_{=0} + \hbar g_\text{f}\lambda\left[\sigma_-\sigma_+, \sigma_z\right] \\ &= \hbar g_\text{f}\lambda\left[\sigma_-\sigma_+, \sigma_z\right] = \hbar g_\text{f}\lambda\left[\,|g\rangle\langle g|\,, |e\rangle\langle e| - |g\rangle\langle g|\,\right] = 0\,.\end{aligned}$$

So indeed we can see that $\dot{\sigma}_z(t) = 0$. Therefore σ_z is a constant in time. This means that the energy of the qubit does not change and dissipation does not occur in our system.

Computing the time evolution of the other Pauli operators is more complicated as we cannot use the adjoint master equation directly.[4] We need to resort either to simple regimes, where analytical solutions are possible, or to numerical methods. The numerical solutions are discussed later but let's now concentrate for a moment on a case with no environmental interaction. This gives the unitary dynamics of our system.

5.2.1 $\gamma = 0$: UNITARY DYNAMICS

Let's now consider a situation where the qubit-resonator system does not interact with the resistor in any way. This sets $\gamma = 0$ in the master equation (5.4) thus getting rid of the dissipator terms. Physically this means that the coupling mutual inductance M between the inductors in figure 4.4 is zero.[5]

As the dissipator terms disappear we are left with

$$\dot{\rho}_{\text{Sys}} = -\frac{\mathrm{i}}{\hbar}\left[H_{\text{Sys}}\,, \rho_{\text{Sys}}\right], \tag{5.7}$$

which is the Liouville-von Neumann equation governing the unitary dynamics of the system. Although the unitary dynamics do not represent the open quantum system situation, we can still gain useful knowledge by solving the unitary Liouville-von Neumann equation in some specially selected initial value conditions. These solutions help us to understand how the unitary part affects the solutions of the full master equation that we encounter later.

As shown in equation (3.13) the solution to the Liouville-von Neumann equation depends on the initial conditions for the density matrix ρ. As H_{Sys} is the dispersive Hamiltonian given by equation (5.5), we know its eigenstates and energy eigenvalues (see subsection 4.2.2). The Hamiltonian is diagonal in the product basis $|\Psi\rangle = |\Psi_\text{Q}\rangle \otimes |\Psi_\text{R}\rangle$, where $|\Psi_\text{Q}\rangle$ is the qubit state and $|\Psi_\text{R}\rangle$ the resonator state, so if we represent the state $|\Psi\rangle$ in terms of the eigenstates, solving the Liouville-von Neumann equation becomes easier.

In the calculations that follow we assume that the qubit begins in a superposition state $|\Psi_\text{Q}\rangle = |+\rangle = \frac{1}{\sqrt{2}}(|e\rangle + |g\rangle)$ like in figure 5.1. This choice sets the initial coherence to $C(\rho) = 1$ and allows us to track how it evolves in time.

[4] The problem with calculating σ_x and σ_y using the adjoint master equation is that we get terms such as $a^\dagger a\sigma_y(t)$, where the time dependency concerns the whole operator. We cannot separate $a^\dagger a\sigma_y(t) \rightarrow a^\dagger a(t)\sigma_y(t)$ so we would have to apply the adjoint master equation for $a^\dagger a\sigma_y(t)$ and so on. This leads to an infinite series of differential equations, which we do not want to deal with.

[5] Remember that we defined $\gamma = \alpha^2 2\pi J(\omega_\text{f})$ in deriving the master equation (4.108), where $\alpha = M/L_\text{L}$.

The part that we change between the different calculations is the initial state of the resonator. Let's first consider a case where the resonator starts in a Fock-state $|\Psi_R\rangle = |n\rangle$. Then the full state of the qubit-resonator system is

$$|\Psi\rangle = |\Psi_Q\rangle \otimes |\Psi_R\rangle = \frac{1}{\sqrt{2}}(|e\rangle + |g\rangle) \otimes |n\rangle = \frac{1}{\sqrt{2}}(|e,n\rangle + |g,n\rangle)\,. \tag{5.8}$$

Since the Liouville-von Neumann equation can be solved as $\rho(t) = e^{-iHt/\hbar}\rho(0)e^{iHt/\hbar}$, we get the density matrix as

$$\begin{aligned}\rho_{Sys}(t) &= e^{-iH_{Sys}t/\hbar}\,|\Psi\rangle\langle\Psi|\,e^{iH_{Sys}t/\hbar} \\ &= \frac{1}{2}\Big[e^{-iH_{Sys}t/\hbar}\,|g,n\rangle\langle g,n|\,e^{iH_{Sys}t/\hbar} + e^{-iH_{Sys}t/\hbar}\,|g,n\rangle\langle e,n|\,e^{iH_{Sys}t/\hbar} \\ &\quad + e^{-iH_{Sys}t/\hbar}\,|e,n\rangle\langle g,n|\,e^{iH_{Sys}t/\hbar} + e^{-iH_{Sys}t/\hbar}\,|e,n\rangle\langle e,n|\,e^{iH_{Sys}t/\hbar}\Big]\,.\end{aligned} \tag{5.9}$$

Since $|e,n\rangle$ and $|g,n\rangle$ are the energy eigenstates of the Hamiltonian H_{Sys} with energies $E_{e,n}$ and $E_{g,n}$ respectively (see equation (4.63)), we can use them directly in the above equation to obtain

$$\rho_{Sys}(t) = \frac{1}{2}\Big[\,|g,n\rangle\langle g,n| + |e,n\rangle\langle e,n| + e^{i(E_{e,n}-E_{g,n})t/\hbar}\,|g,n\rangle\langle e,n| + e^{-i(E_{e,n}-E_{g,n})t/\hbar}\,|e,n\rangle\langle g,n|\,\Big]\,. \tag{5.10}$$

Taking the partial trace over the resonator Hilbert space and computing the energy difference $E_{e,n} - E_{g,n}$ yields

$$\rho_Q(t) = \mathrm{Tr}_R\left(\rho_{Sys}(t)\right) = \frac{1}{2}\Big[\,|g\rangle\langle g| + |e\rangle\langle e| + e^{i(\omega_A + g_f\lambda(2n+1))t}\,|g\rangle\langle e| + e^{-i(\omega_A + g_f\lambda(2n+1))t}\,|e\rangle\langle g|\,\Big]\,. \tag{5.11}$$

Computing now the coherence measure $C(\rho_Q)$ we see that it is exactly one for all times:

$$C(\rho_Q(t)) = 2|\rho_{01}| = \left|e^{i(\omega_A + g_f\lambda(2n+1))t}\right| = 1\,. \tag{5.12}$$

The above calculation shows that if the resonator is in a single Fock state $|n\rangle$, then the qubit state just rotates around the Bloch sphere with a modified frequency that depends on the qubit-resonator coupling. However, the qubit does not lose its superposition. This is a useful result for later, when we analyze the qubit dynamics in the limit of zero temperature.

Since there is no effect on qubit coherences when the resonator stays in a determined state $|n\rangle$, let's change the resonator state into a superposition of Fock states. Letting the resonator start our at $|\Psi_R\rangle = \frac{1}{\sqrt{2}}(|n\rangle + |m\rangle)$, where $n \neq m$, we have an initial density matrix of

$$\begin{aligned}\rho_{Sys}(0) = \frac{1}{4}\Big(&|g,n\rangle\langle g,n| + \cancel{|g,n\rangle\langle g,m|} + |g,n\rangle\langle e,n| + \cancel{|g,n\rangle\langle e,m|} \\ &+ \cancel{|g,m\rangle\langle g,n|} + |g,m\rangle\langle g,m| + \cancel{|g,m\rangle\langle e,n|} + |g,m\rangle\langle e,m| \\ &+ |e,n\rangle\langle g,n| + \cancel{|e,n\rangle\langle g,m|} + |e,n\rangle\langle e,n| + \cancel{|e,n\rangle\langle e,m|} \\ &+ \cancel{|e,m\rangle\langle g,n|} + |e,m\rangle\langle g,m| + \cancel{|e,m\rangle\langle e,n|} + |e,m\rangle\langle e,m|\Big)\,.\end{aligned} \tag{5.13}$$

The terms that are crossed over can be neglected. Since $n \neq m$ they vanish when we take the partial trace over the environment. Computing the time evolved density matrix like previously gives us the following

$$\rho_{\mathrm{Q}}(t) = \frac{1}{4}\Big[2\,|g\rangle\langle g| + 2\,|e\rangle\langle e| + \Big(\mathrm{e}^{\mathrm{i}(\omega_{\mathrm{A}}+g_{\mathrm{f}}\lambda(2n+1))t} + \mathrm{e}^{\mathrm{i}(\omega_{\mathrm{A}}+g_{\mathrm{f}}\lambda(2m+1))t}\Big)\,|g\rangle\langle e| \\ + \Big(\mathrm{e}^{-\mathrm{i}(\omega_{\mathrm{A}}+g_{\mathrm{f}}\lambda(2n+1))t} + \mathrm{e}^{-\mathrm{i}(\omega_{\mathrm{A}}+g_{\mathrm{f}}\lambda(2m+1))t}\Big)\,|e\rangle\langle g|\Big]. \tag{5.14}$$

After some algebra we find the coherence measure to become

$$C(\rho_{\mathrm{Q}}(t)) = 2|\rho_{01}| = \frac{1}{2}\Big|\mathrm{e}^{\mathrm{i}(\omega_{\mathrm{A}}+g_{\mathrm{f}}\lambda(2n+1))t} + \mathrm{e}^{\mathrm{i}(\omega_{\mathrm{A}}+g_{\mathrm{f}}\lambda(2m+1))t}\Big| = \ldots = \Big|\cos\big(g_{\mathrm{f}}\lambda(n-m)\,t\big)\Big|. \tag{5.15}$$

We can see that the coherence measure in the equation above is now not constant in time as it was previously. Clearly the fact that the resonator started out in some superposition state allows the qubit and resonator to exchange coherences, leading to non-trivial behaviour of the qubit's quantum state. This $|\cos(x)|$ dependency is plotted in figure 5.2. We can see an oscillatory behaviour, which resembles the fact that the qubit dynamics are reversible, due to the unitary nature of the time evolution given by the Liouville-von Neumann equation.

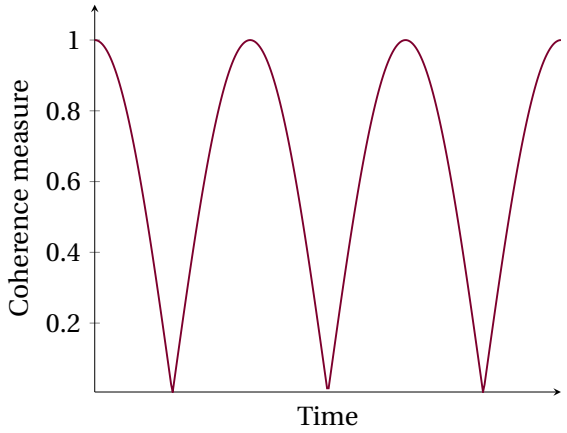

Figure 5.2: Plot of the general behaviour of the coherence measure in equation (5.15).

Now that we have analyzed the resonator starting in a simple superposition state of two Fock states, we can move to a more complex example, which is also more natural. Let's next discuss the case where the resonator starts out in a *coherent state* given by a superposition of an infinite number of Fock states

$$|\Psi_{\mathrm{R}}\rangle = |\alpha\rangle = \mathrm{e}^{-\frac{1}{2}|\alpha|^2}\sum_{n=0}^{\infty}\frac{\alpha^n}{\sqrt{n!}}\,|n\rangle\,. \tag{5.16}$$

The coherent states are regarded as the "most classical" quantum states of the harmonic oscillator [61]. Their distinguishing feature is that they are the eigenstates of the annihilation operator, satisfying $a\,|\alpha\rangle = \alpha\,|\alpha\rangle$.

Letting the resonator start out in a coherent state and the qubit in the superposition state $|+\rangle$ as usual, the initial density matrix is given by

$$\rho_{\mathrm{Sys}}(0) = \frac{1}{2}\mathrm{e}^{-|\alpha|^2}\sum_{n,m=0}^{\infty}\frac{\alpha^n\alpha^m}{\sqrt{n!m!}}\big(|g,n\rangle\langle g,m| + |g,n\rangle\langle e,m| + |e,n\rangle\langle g,m| + |e,n\rangle\langle e,m|\big). \tag{5.17}$$

We can again neglect terms where $n \neq m$ in the bra and in the ket because those terms would vanish when taking the trace over the resonator states. This effectively gets rid of the

sum over m, setting $m = n$ in the above equation. Then evolving the density matrix in time and taking the partial trace gives us

$$\rho_{\mathrm{Q}}(t) = \frac{1}{2}\mathrm{e}^{-|\alpha|^2}\Bigg[\sum_{n=0}^{\infty}\frac{|\alpha|^{2n}}{n!}\big(|g\rangle\langle g| + |e\rangle\langle e|\big) + \sum_{n=0}^{\infty}\frac{|\alpha|^{2n}}{n!}\mathrm{e}^{\mathrm{i}(\omega_{\mathrm{A}}+g_{\mathrm{f}}\lambda(2n+1))t}|g\rangle\langle e| + \sum_{n=0}^{\infty}\frac{|\alpha|^{2n}}{n!}\mathrm{e}^{-\mathrm{i}(\omega_{\mathrm{A}}+g_{\mathrm{f}}\lambda(2n+1))t}|e\rangle\langle g|\Bigg]. \tag{5.18}$$

We can use the definition of the exponential as $\exp(x) = \sum_{n=0}^{\infty}\frac{x^n}{n!}$ to the first sum. From the second and third terms we can pull out $\mathrm{e}^{\pm\mathrm{i}(\omega_{\mathrm{A}}+g_{\mathrm{f}}\lambda)t}$ from the sums. This process yields

$$\rho_{\mathrm{Q}}(t) = \frac{1}{2}\mathrm{e}^{-|\alpha|^2}\Bigg[\mathrm{e}^{|\alpha|^2}\big(|g\rangle\langle g| + |e\rangle\langle e|\big) + \mathrm{e}^{\mathrm{i}(\omega_{\mathrm{A}}+g_{\mathrm{f}}\lambda)t}\sum_{n=0}^{\infty}\frac{(|\alpha|^2\mathrm{e}^{\mathrm{i}2ng_{\mathrm{f}}\lambda t})^n}{n!}|g\rangle\langle e| + \mathrm{e}^{-\mathrm{i}(\omega_{\mathrm{A}}+g_{\mathrm{f}}\lambda)t}\sum_{n=0}^{\infty}\frac{(|\alpha|^2\mathrm{e}^{-\mathrm{i}2ng_{\mathrm{f}}\lambda t})^n}{n!}|e\rangle\langle g|\Bigg]. \tag{5.19}$$

Using the exponential definition in the remaining sums and multiplying in the exponential term $\mathrm{e}^{-|\alpha|^2}$ yields us

$$\rho_{\mathrm{Q}}(t) = \frac{1}{2}\Big[|g\rangle\langle g| + |e\rangle\langle e| + \mathrm{e}^{\mathrm{i}(\omega_{\mathrm{A}}+g_{\mathrm{f}}\lambda)t}\mathrm{e}^{|\alpha|^2(\mathrm{e}^{\mathrm{i}2ng_{\mathrm{f}}\lambda t}-1)}|g\rangle\langle e| + \mathrm{e}^{-\mathrm{i}(\omega_{\mathrm{A}}+g_{\mathrm{f}}\lambda)t}\mathrm{e}^{|\alpha|^2(\mathrm{e}^{-\mathrm{i}2ng_{\mathrm{f}}\lambda t}-1)}|e\rangle\langle g|\Big]. \tag{5.20}$$

From this we get the following coherence measure:

$$\begin{aligned} C(\rho_{\mathrm{Q}}(t)) &= \left|\mathrm{e}^{\mathrm{i}(\omega_{\mathrm{A}}+g_{\mathrm{f}}\lambda)t}\mathrm{e}^{|\alpha|^2(\mathrm{e}^{\mathrm{i}2ng_{\mathrm{f}}\lambda t}-1)}\right| \\ &= \left|\mathrm{e}^{|\alpha|^2(\mathrm{e}^{\mathrm{i}2ng_{\mathrm{f}}\lambda t}-1)}\right| \\ &= \mathrm{e}^{-2|\alpha|^2\sin^2(g_{\mathrm{f}}\lambda t)}. \end{aligned} \tag{5.21}$$

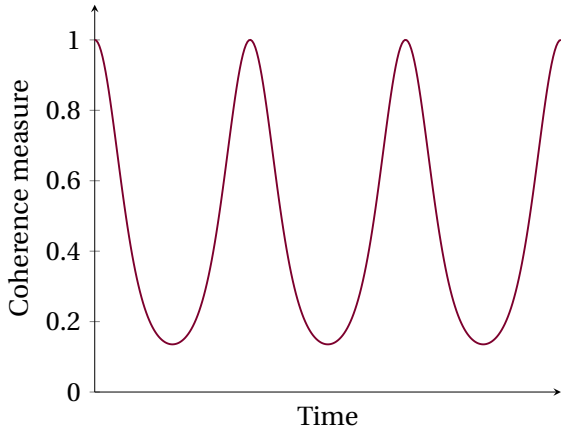

Figure 5.3: Plot of the general behaviour of the coherence measure in equation (5.21).

We see again non-trivial behaviour in the qubit coherences but something that is noticeably different from equation (5.15). When we plot the general behaviour of the coherence $\mathrm{e}^{-2\sin^2(x)}$, we can see that this time some of the qubit coherence is always preserved. Also just like in the previous case there is the same kind of reversible behaviour as in figure 5.2. The qubit first loses coherence but after some time gains it back and this process continues indefinitely.

The last unitary case that we are studying is the situation where the resonator starts out in a thermal state. This case is physically interesting if we assume that initially the system is at thermal equilibrium. As the density matrix of the thermal state is given by equation (3.35), the initial density matrix of the qubit-resonator system becomes

$$\rho_{\mathrm{Sys}}(0) = \frac{1}{2}\frac{1}{1+\bar{n}}\sum_{n=0}^{\infty}\left(\frac{\bar{n}}{1+\bar{n}}\right)^n\big[|g,n\rangle\langle g,n| + |g,n\rangle\langle e,n| + |e,n\rangle\langle g,n| + |e,n\rangle\langle e,n|\big]. \tag{5.22}$$

Applying the time-evolution and taking the trace over the resonator states gives

$$\rho_{\mathrm{Q}}(t)=\frac{1}{2}\frac{1}{1+\bar{n}}\sum_{n=0}^{\infty}\left(\frac{\bar{n}}{1+\bar{n}}\right)^{n}\left[\,|g\rangle\langle g|+\mathrm{e}^{\mathrm{i}(\omega_{\mathrm{A}}+g_{\mathrm{f}}\lambda(2n+1))t}|g\rangle\langle e|+\mathrm{e}^{-\mathrm{i}(\omega_{\mathrm{A}}+g_{\mathrm{f}}\lambda(2n+1))t}|e\rangle\langle g|+|e\rangle\langle e|\,\right]. \tag{5.23}$$

Next let's bring the sum inside the parenthesis. The diagonal terms have no dependency on n so we can evaluate the sum on its own there. We have a geometric sum $\sum_{n=0}^{\infty}\left(\frac{\bar{n}}{1+\bar{n}}\right)^{n}=\sum_{n=0}^{\infty}\left(\frac{1}{1+1/\bar{n}}\right)^{n}=1+\bar{n}$. From the off-diagonal terms we can pull out a rotation term which is not proportional to n. This gives

$$\begin{aligned}\rho_{\mathrm{Q}}(t)=\frac{1}{2}\frac{1}{1+\bar{n}}\Bigg[(1+\bar{n})\big(|g\rangle\langle g|+|e\rangle\langle e|\big)+\mathrm{e}^{\mathrm{i}(\omega_{\mathrm{A}}+g_{\mathrm{f}}\lambda)t}\sum_{n=0}^{\infty}\left(\frac{1}{1+\frac{1}{\bar{n}}}\mathrm{e}^{\mathrm{i}2g_{\mathrm{f}}\lambda t}\right)^{n}|g\rangle\langle e|\\ +\mathrm{e}^{-\mathrm{i}(\omega_{\mathrm{A}}+g_{\mathrm{f}}\lambda)t}\sum_{n=0}^{\infty}\left(\frac{1}{1+\frac{1}{\bar{n}}}\mathrm{e}^{-\mathrm{i}2g_{\mathrm{f}}\lambda t}\right)^{n}|e\rangle\langle g|\Bigg].\end{aligned} \tag{5.24}$$

The sum is again a geometric sum, which becomes

$$\sum_{n=0}^{\infty}\left(\frac{1}{1+\frac{1}{\bar{n}}}\mathrm{e}^{\mathrm{i}2g_{\mathrm{f}}\lambda t}\right)^{n}=\frac{1+\frac{1}{\bar{n}}}{1+\frac{1}{\bar{n}}-\mathrm{e}^{\mathrm{i}2g_{\mathrm{f}}\lambda t}}. \tag{5.25}$$

Using this in the qubit density matrix equation we get

$$\begin{aligned}\rho_{\mathrm{Q}}(t)=\frac{1}{2}\Bigg[|g\rangle\langle g|+|e\rangle\langle e|+\mathrm{e}^{\mathrm{i}(\omega_{\mathrm{A}}+g_{\mathrm{f}}\lambda)t}\frac{1+\frac{1}{\bar{n}}}{1+\frac{1}{\bar{n}}-\mathrm{e}^{\mathrm{i}2g_{\mathrm{f}}\lambda t}}|g\rangle\langle e|\\ +\mathrm{e}^{-\mathrm{i}(\omega_{\mathrm{A}}+g_{\mathrm{f}}\lambda)t}\frac{1+\frac{1}{\bar{n}}}{1+\frac{1}{\bar{n}}-\mathrm{e}^{-\mathrm{i}2g_{\mathrm{f}}\lambda t}}|e\rangle\langle g|\Bigg].\end{aligned} \tag{5.26}$$

From the above equation we can obtain the coherence measure as usual by taking the absolute value of the $|g\rangle\langle e|$ element. This time the calculation involves quite a lot of algebra. After the computations we ultimately get the coherence measure as

$$C\big(\rho_{\mathrm{Q}}(t)\big)=\frac{1}{\sqrt{2}}\frac{1}{\bar{n}}\frac{1}{\sqrt{1+\frac{1}{\bar{n}}+\frac{1}{2\bar{n}^{2}}-\cos\big(2g_{\mathrm{f}}\lambda t\big)\big(1+\frac{1}{\bar{n}}\big)}}. \tag{5.27}$$

Indeed, also the thermal state gives rise to non-trivial coherence behaviour. However, this time the coherence measure depends also on temperature, since the Bose-Einstein distribution $\bar{n}$ depends on temperature. The general behaviour of the coherence of the form $\frac{1}{\sqrt{2}}\frac{1}{\sqrt{5/2-2\cos(x)}}$ is again plotted in figure 5.4. We can see that the shape is quite close to what we show in figure 5.3 but this time the minimum level of remaining coherences is higher and it can be modified by changing the temperature. Also in this case we can notice the oscillatory behaviour coming from the reversible nature of the equation of motion we are solving.

In conclusion, we have analyzed the evolution of qubit coherences in four distinct cases.

We saw that if the resonator starts out in a precisely known Fock state, then coherences do not evolve in time (see Eq. (5.12)). After the introduction of a simple superposition between two Fock states the coherences start to behave in a non-trivial manner as seen in equation (5.15). Thus it is required that the resonator is initially in some superposition state in order for the qubit to exchange its coherences with the resonator. We also saw that in the case of initial coherent state and thermal state the qubit coherences behave non-trivially but in oscillatory fashion (see equations (5.21) and (5.27) respectively).

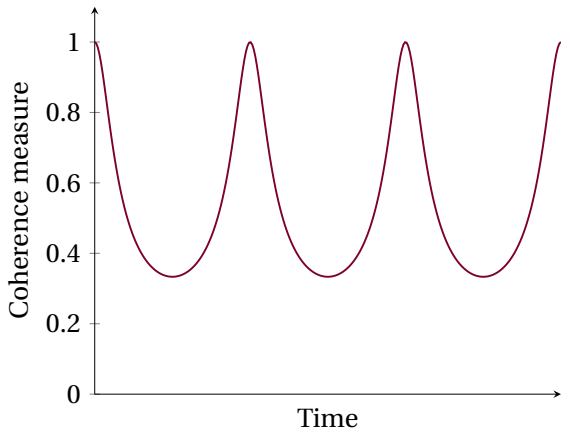

Figure 5.4: Plot of the general behaviour of the coherence measure in equation (5.27).

5.2.2 THE STEADY STATE

When solving for the dynamics of any system in physics, one particular interesting point is the possible existence of an equilibrium or steady state. In our case the steady state refers to the combined qubit-resonator state that does not change in time and towards which the system will evolve if it is not initially in such a state.

In finding the steady state we are looking for a solution to the equation

$$\rho_{\text{Sys}}(t) = \mathrm{e}^{\mathscr{L}t}\rho_{\text{Sys}}(0) = \rho_{\text{Sys}}(0) \;\forall\; t\,, \tag{5.28}$$

where $\mathscr{L}$ is now the Liouvillian superoperator corresponding to master equation (5.4) given by

$$\mathscr{L} = -\frac{\mathrm{i}}{\hbar}\big[H_{\text{Sys}}, \cdot\big] + \mathscr{D}[\cdot]\,. \tag{5.29}$$

The dissipator part of the master equation is now denoted by $\mathscr{D}[\cdot]$. Essentially we want to find a state ρ_{S} such that

$$\mathscr{L}\rho_{\text{S}} = -\frac{\mathrm{i}}{\hbar}\big[H_{\text{Sys}}, \rho_{\text{S}}\big] + \mathscr{D}[\rho_{\text{S}}] = 0\,. \tag{5.30}$$

It should be noted that the qubit state does not affect the dissipators at all because the dissipator is constructed only of operators acting on the resonator Hilbert space. Equation (5.30) is thus satisfied for a state, which is separable to the qubit and resonator contributions and where the both parts commute with the system Hamiltonian H_{Sys} and where the resonator contribution is the steady state of the dissipator. Let's now concentrate on the latter part. An educated guess for the dissipator's steady state, based on statistical mechanical considerations, would be the thermal state, since it is the thermal equilibrium state of a quantum system [31]. See also the discussion in Appendix B. Now we need to check if it is indeed the stationary state of the dissipator.

The dissipator with the thermal state is given by

$$\mathscr{D}[\rho_{\mathrm{Th}}] = \gamma\bar{n}\Big(\underbrace{a_{\mathrm{f}}^{\dagger}\rho_{\mathrm{Th}}a_{\mathrm{f}}}_{1.} - \underbrace{\frac{1}{2}\{a_{\mathrm{f}}a_{\mathrm{f}}^{\dagger},\rho_{\mathrm{Th}}\}}_{2.}\Big) + \gamma(1+\bar{n})\Big(\underbrace{a_{\mathrm{f}}\rho_{\mathrm{Th}}a_{\mathrm{f}}^{\dagger}}_{3.} - \underbrace{\frac{1}{2}\{a_{\mathrm{f}}^{\dagger}a_{\mathrm{f}},\rho_{\mathrm{Th}}\}}_{4.}\Big). \tag{5.31}$$

Using the definition for the thermal state from equation (3.35), the four different parts of the dissipator are given by

$$1.)\ a_{\mathrm{f}}^{\dagger}\rho_{\mathrm{Th}}a_{\mathrm{f}} = \frac{1}{1+\bar{n}}\sum_{n=0}^{\infty}\left(\frac{\bar{n}}{1+\bar{n}}\right)^{n}(n+1)\,|n+1\rangle\langle n+1| \tag{5.32}$$

$$2.)\ \frac{1}{2}\{a_{\mathrm{f}}a_{\mathrm{f}}^{\dagger},\rho_{\mathrm{Th}}\} = \frac{1}{1+\bar{n}}\sum_{n=0}^{\infty}\left(\frac{\bar{n}}{1+\bar{n}}\right)^{n}(n+1)\,|n\rangle\langle n| \tag{5.33}$$

$$3.)\ a_{\mathrm{f}}\rho_{\mathrm{Th}}a_{\mathrm{f}}^{\dagger} = \frac{1}{1+\bar{n}}\sum_{n=0}^{\infty}\left(\frac{\bar{n}}{1+\bar{n}}\right)^{n}n\,|n-1\rangle\langle n-1| \tag{5.34}$$

$$4.)\ \frac{1}{2}\{a_{\mathrm{f}}^{\dagger}a_{\mathrm{f}},\rho_{\mathrm{Th}}\} = \frac{1}{1+\bar{n}}\sum_{n=0}^{\infty}\left(\frac{\bar{n}}{1+\bar{n}}\right)^{n}n\,|n\rangle\langle n|\,. \tag{5.35}$$

If we now plug in the different terms to the dissipator and play with the summation indices it turns out that eventually the 2nd and 3rd term cancel eachother as will the 1st and 4th term. This of course gives then

$$\mathscr{D}[\rho_{\mathrm{Th}}] = 0\,, \tag{5.36}$$

confirming that the thermal state is the stationary state of the dissipator.

The thermal state being the stationary state of the dissipator is convenient, because it also commutes with the system Hamiltonian.

When it comes to the qubit part of the steady state, by looking at the Hamiltonian (5.5) it is evident that initial states $|e\rangle\langle e|$ or $|g\rangle\langle g|$ of the qubit commute with the system Hamiltonian due to the lack of σ_x terms. Thus any linear combination of them stays invariant under the dynamics governed by H_{Sys}. We can thus conclude that the most general steady state of the master equation (5.4) is

$$\rho_{\mathrm{Steady}} = a\,|e\rangle\langle e| \otimes \rho_{\mathrm{Th}} + (1-a)\,|g\rangle\langle g| \otimes \rho_{\mathrm{Th}}\,, \tag{5.37}$$

where $a \in [0,1]$.

Now we know how the qubit evolves under unitary conditions and what is the equilibrium state of the system towards which it evolves in time. However, we are of course interested in what happens in the middle, before the system reaches equilibrium and also how long the relaxation takes. For that we need to solve the full master equation (5.4) with non-zero γ.

As already discussed, the time evolution of the qubit can be decomposed into the computation of the time evolution of the Pauli operators. In our case computing $\langle\sigma_z(t)\rangle$ is trivial as it's a constant of motion. However, computing $\langle\sigma_x(t)\rangle$ and $\langle\sigma_y(t)\rangle$ is definitely not trivial.

This needs to be done on a computer but in order to gain qualitative understanding of how the different parts of the master equation affect the time evolution of coherences, we are going to go as far as possible using analytical methods.

5.2.3 EXPECTATION OF σ_x

In order to compute the expectation value of $\sigma_x(t)$ (and similarly of $\sigma_y(t)$) we will consider the master equation (5.4) in the Liouville space, which was discussed and introduced in section 3.3. As a reminder, this formulation allows us to represent the $d \times d$ dimensional quantum state operators as d^2 dimensional vectors, while the superoperators acting on them become $d^2 \times d^2$ matrices.

Applying the isomorphism to our master equation (5.4), as given in equation (3.88), transforms the Liouvillian superoperator to the following form:

$$\begin{aligned}\mathscr{L} = -\frac{\mathrm{i}}{\hbar}\left(H_{\mathrm{Sys}} \otimes \mathbb{1} - \mathbb{1} \otimes H_{\mathrm{Sys}}^{\top}\right) + \gamma\bar{n}\left(a_{\mathrm{f}}^{\dagger} \otimes a_{\mathrm{f}}^{\dagger} - \frac{1}{2}a_{\mathrm{f}}a_{\mathrm{f}}^{\dagger} \otimes \mathbb{1} - \frac{1}{2}\mathbb{1} \otimes a_{\mathrm{f}}a_{\mathrm{f}}^{\dagger}\right) \\ + \gamma(1+\bar{n})\left(a_{\mathrm{f}} \otimes a_{\mathrm{f}} - \frac{1}{2}a_{\mathrm{f}}^{\dagger}a_{\mathrm{f}} \otimes \mathbb{1} - \frac{1}{2}\mathbb{1} \otimes a_{\mathrm{f}}^{\dagger}a_{\mathrm{f}}\right).\end{aligned} \tag{5.38}$$

Here we used the definitions for the supercommutator and -anticommutator in equations (3.86) and (3.87) and the fact that $a^{\dagger} = a^{\top}$ and $a^{*} = a$ since the ladder operators are real matrices (see Eq. (4.81)).

As the Liouvillian can be represented as a matrix, it is not suprising that the eigenvalues and eigenvectors of said matrix play an important role in the computation of the associated dynamics. However, finding the eigenvalues and eigenvectors of a $d^2 \times d^2$ matrix can be challenging even numerically when d grows large, let alone in the ideal case of infinite dimensional Hilbert space.[6] Fortunately we can exploit some symmetries of the Liouvillian superoperator to get a more manageable form for the matrix. These symmetries were formulated in [71] by Albert and Jiang and recently refined and discussed in detail in [72] by Cattaneo, Giorgi, Maniscalco and Zambrini.

Motivated by the work done in Ref. [72], we will examine the observable responsible for the total number of particles in a system. In our case we need to compute separately the qubit quanta and the resonator quanta. Since the number operator in the two dimensional truncation of the qubit Hilbert space is σ_z (see Eq. (4.38)), we have the total number of particles operator N as

$$N = \sigma_z + a_{\mathrm{f}}^{\dagger}a_{\mathrm{f}}. \tag{5.39}$$

From the above we can define the superoperator $\mathscr{N} = [N, \cdot]$, which can be written using the supercommutator (3.86) as

$$\mathscr{N} = N \otimes \mathbb{1} - \mathbb{1} \otimes N. \tag{5.40}$$

What we need to compute next is the commutator between the superoperators $\mathscr{L}$ and $\mathscr{N}$. If

[6] In our case $d = 2d'$, where d' is dimension of the resonator Hilbert space and the factor 2 comes from the qubit Hilbert space. Therefore we need to find a suitable truncation for the resonator Hilbert space.

they commute,[7] then we can exploit the symmetries of the Liouvillian superoperator related to this total number of particles superoperator $\mathcal{N}$ [72]. The commutator is calculated in the box below.

The commutator between the superoperators can be decomposed into the following parts:

$$\begin{aligned}[\mathscr{L},\mathcal{N}] = &-\frac{\mathrm{i}}{\hbar}\underbrace{\left[H_{\mathrm{Sys}}\otimes\mathbb{1}-\mathbb{1}\otimes H_{\mathrm{Sys}}^{\top},\mathcal{N}\right]}_{1.}\\ &+\gamma\bar{n}\Big(\underbrace{\left[a_{\mathrm{f}}^{\dagger}\otimes a_{\mathrm{f}}^{\dagger},\mathcal{N}\right]}_{2.}-\frac{1}{2}\underbrace{\left[a_{\mathrm{f}}a_{\mathrm{f}}^{\dagger}\otimes\mathbb{1},\mathcal{N}\right]}_{3.}-\frac{1}{2}\underbrace{\left[\mathbb{1}\otimes a_{\mathrm{f}}a_{\mathrm{f}}^{\dagger},\mathcal{N}\right]}_{4.}\Big)\\ &+\gamma(1+\bar{n})\Big(\underbrace{\left[a_{\mathrm{f}}\otimes a_{\mathrm{f}},\mathcal{N}\right]}_{5.}-\frac{1}{2}\underbrace{\left[a_{\mathrm{f}}^{\dagger}a_{\mathrm{f}}\otimes\mathbb{1},\mathcal{N}\right]}_{6.}-\frac{1}{2}\underbrace{\left[\mathbb{1}\otimes a_{\mathrm{f}}^{\dagger}a_{\mathrm{f}},\mathcal{N}\right]}_{7.}\Big).\end{aligned}\tag{5.41}$$

Now we can compute the commutators separately. The first one is clearly zero because H_{Sys} in equation (5.5) consists only of σ_z, $a_{\mathrm{f}}^{\dagger}a_{\mathrm{f}}$, and $\sigma_-\sigma_+$, all of which commute separately with $\mathcal{N}$ in equation (5.40).

The second commutator needs to be computed more carefully:

$$\begin{aligned}\left[a_{\mathrm{f}}^{\dagger}\otimes a_{\mathrm{f}}^{\dagger},\mathcal{N}\right] &= \left[a_{\mathrm{f}}^{\dagger}\otimes a_{\mathrm{f}}^{\dagger},a_{\mathrm{f}}^{\dagger}a_{\mathrm{f}}\otimes\mathbb{1}\right]-\left[a_{\mathrm{f}}^{\dagger}\otimes a_{\mathrm{f}}^{\dagger},\mathbb{1}\otimes a_{\mathrm{f}}^{\dagger}a_{\mathrm{f}}\right]\\ &= \left(a_{\mathrm{f}}^{\dagger}\otimes a_{\mathrm{f}}^{\dagger}\right)\left(a_{\mathrm{f}}^{\dagger}a_{\mathrm{f}}\otimes\mathbb{1}-\mathbb{1}\otimes a_{\mathrm{f}}^{\dagger}a_{\mathrm{f}}\right)-\left(a_{\mathrm{f}}^{\dagger}a_{\mathrm{f}}\otimes\mathbb{1}-\mathbb{1}\otimes a_{\mathrm{f}}^{\dagger}a_{\mathrm{f}}\right)\left(a_{\mathrm{f}}^{\dagger}\otimes a_{\mathrm{f}}^{\dagger}\right)\\ &= a_{\mathrm{f}}^{\dagger}a_{\mathrm{f}}^{\dagger}a_{\mathrm{f}}\otimes a_{\mathrm{f}}^{\dagger}-a_{\mathrm{f}}^{\dagger}\otimes a_{\mathrm{f}}^{\dagger}a_{\mathrm{f}}^{\dagger}a_{\mathrm{f}}-a_{\mathrm{f}}^{\dagger}a_{\mathrm{f}}a_{\mathrm{f}}^{\dagger}\otimes a_{\mathrm{f}}^{\dagger}+a_{\mathrm{f}}^{\dagger}\otimes a_{\mathrm{f}}^{\dagger}a_{\mathrm{f}}a_{\mathrm{f}}^{\dagger}\\ &= a_{\mathrm{f}}^{\dagger}\otimes\left[a_{\mathrm{f}}^{\dagger}a_{\mathrm{f}},a_{\mathrm{f}}^{\dagger}\right]-\left[a_{\mathrm{f}}^{\dagger}a_{\mathrm{f}},a_{\mathrm{f}}^{\dagger}\right]\otimes a_{\mathrm{f}}^{\dagger}=a_{\mathrm{f}}^{\dagger}\otimes a_{\mathrm{f}}^{\dagger}-a_{\mathrm{f}}^{\dagger}\otimes a_{\mathrm{f}}^{\dagger}\\ &= 0.\end{aligned}\tag{5.42}$$

Above we used the fact that $[N,a^{\dagger}]=a^{\dagger}$. In a similar manner we can show that commutator number 5 is also zero. Last piece that we need to compute carefully is the third commutator (6. and 7. are trivially zero and 4. is similar to 3.):

$$\begin{aligned}\left[a_{\mathrm{f}}a_{\mathrm{f}}^{\dagger}\otimes\mathbb{1},\mathcal{N}\right] &= \left[a_{\mathrm{f}}a_{\mathrm{f}}^{\dagger}\otimes\mathbb{1},a_{\mathrm{f}}^{\dagger}a_{\mathrm{f}}\otimes\mathbb{1}\right]-\left[a_{\mathrm{f}}a_{\mathrm{f}}^{\dagger}\otimes\mathbb{1},\mathbb{1}\otimes a_{\mathrm{f}}^{\dagger}a_{\mathrm{f}}\right]\\ &= \left(a_{\mathrm{f}}a_{\mathrm{f}}^{\dagger}\otimes\mathbb{1}\right)\left(a_{\mathrm{f}}^{\dagger}a_{\mathrm{f}}\otimes\mathbb{1}-\mathbb{1}\otimes a_{\mathrm{f}}^{\dagger}a_{\mathrm{f}}\right)-\left(a_{\mathrm{f}}^{\dagger}a_{\mathrm{f}}\otimes\mathbb{1}-\mathbb{1}\otimes a_{\mathrm{f}}^{\dagger}a_{\mathrm{f}}\right)\left(a_{\mathrm{f}}a_{\mathrm{f}}^{\dagger}\otimes\mathbb{1}\right)\\ &= a_{\mathrm{f}}a_{\mathrm{f}}^{\dagger}a_{\mathrm{f}}^{\dagger}a_{\mathrm{f}}\otimes\mathbb{1}-\cancel{a_{\mathrm{f}}a_{\mathrm{f}}^{\dagger}\otimes a_{\mathrm{f}}^{\dagger}a_{\mathrm{f}}}-a_{\mathrm{f}}^{\dagger}a_{\mathrm{f}}a_{\mathrm{f}}a_{\mathrm{f}}^{\dagger}\otimes\mathbb{1}+\cancel{a_{\mathrm{f}}a_{\mathrm{f}}^{\dagger}\otimes a_{\mathrm{f}}^{\dagger}a_{\mathrm{f}}}\\ &= -\left[a_{\mathrm{f}}^{\dagger}a_{\mathrm{f}},a_{\mathrm{f}}a_{\mathrm{f}}^{\dagger}\right]\otimes\mathbb{1}\\ &= 0.\end{aligned}\tag{5.43}$$

[7] In reference [72] it is proved that $\mathscr{L}$ and $\mathcal{N}$ do commute if in the derivation of the master equation the partial secular approximation is used. About the symmetry of the Liouvillian they state that "*the symmetry arises only when considering a global master equation, while it may not be valid anymore when using a local one.*" Since we had to assume locality when deriving the jump operators in section 4.2.3 we cannot just blindly use the results from the referenced article, but have to carefully make sure that the superoperators do indeed commute.

Above we used the fact that $[a^\dagger a,\, aa^\dagger] = 0$, which is easy to prove using some arbitrary state $|n\rangle$ as an aid.

The above calculation shows that indeed $[\mathscr{L},\mathscr{N}] = 0$. It is stated in Ref. [72] that since the Liouvillian and the total number of particles superoperator commute, it generates a symmetry on the Liouvillian level that allows us to block diagonalise the Liouvillian matrix. In the block form each of the blocks may give insight about certain physical phenomena of interest, which allows us to focus our efforts in analyzing this one block instead of the whole matrix.

The block diagonalisation arises from the choice and ordering of a correct basis in which to represent the Liouvillian $\mathscr{L}$. It is notable that the number of particles operator N is diagonal in the same basis which we used in the derivation of the Liouvillian, namely the $\{|g,n\rangle,\, |e,n-1\rangle\}$ basis. The eigenvectors of the corresponding superoperator $\mathscr{N}$ are given by the tensor product of the referenced basis elements with itself.

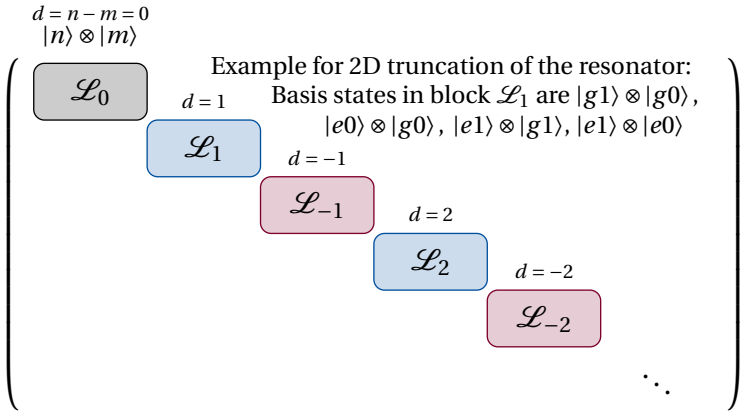

Figure 5.5: Block structure of the Liouvillian superoperator in the Liouville space. The exact order of the blocks can vary, what is important is that each block is labeled by d and contains only basis elements where the difference in quanta between the basis element kets is d. In the given example the resonator is truncated to 2D giving access only to states $|0\rangle$ and $|1\rangle$. The qubit ground $|g\rangle$ corresponds to 0 and excited state $|e\rangle$ to 1. In block $\mathscr{L}_1$ all the left side kets have one quanta more compared to the right side kets.

Let's now consider the eigenvalues of $\mathscr{N}$ and label them d. These eigenvalues show the difference in the number of quanta between the basis elements of the Liouville space, namely those of $|i,n\rangle \otimes |j,m\rangle$, where $i,j \in \{e,g\}$. The corresponding eigenvectors are the basis elements of the Liouvillian. If we now regroup the Liouvillian matrix such that the basis elements corresponding to the same eigenvalue d are next to each other, we see that the form of the Liouvillian becomes block diagonal as can be seen in figure 5.5. Mathematically we can express the block diagonal form of the Liouvillian as a direct sum of the sub-matrices

$$\mathscr{L} = \bigoplus_d \mathscr{L}_d\,. \tag{5.44}$$

It is noteworthy that the blocks with negative d can be trivially obtained from the blocks with positive d due to the relation $\mathscr{L}_d = \mathscr{L}^*_{-d}$ [72].

As we have found a way to describe the Liouvillian in a block form, we can concentrate on the specific blocks of interest for different physical phenomena. For example the steady state of the system lives in the $\mathscr{L}_0$ block [72]. It is therefore the only block with an eigenvalue 0. Later it turns out that our interest lies mainly in the block $\mathscr{L}_{\pm 1}$ because these blocks

contribute to the expectation value of the Pauli σ_x and σ_y operators. But in order to be able to compute the expectation value, we need to be able to consider the representation for an arbitrary quantum state in the Liouville space, where the Liouvillian is block diagonal. To represent the density matrix in terms of the eigenvectors of the block-diagonal Liouvillian, we follow references [73] and [74].

Our Liouvillian matrix is in a block diagonal form depicted in figure 5.5. Let us consider the eigenvectors and eigenvalues of some block $\mathscr{L}_d$. This block has in total $\sqrt{\dim(\mathscr{L}_d)}$ eigenvalues and -vectors.[8] Let us denote the i:th eigenvalue of the block $\mathscr{L}_d$ by $\lambda_i^{(d)}$ and the corresponding (right) eigenvector by $|v_i^{(d)}\rangle\rangle$. Then the (vectorized) density matrix can now be written as a linear combination of these eigenvectors:

$$\left|\rho_{\text{Sys}}\right\rangle\rangle = \sum_d \sum_i c_i^{(d)} \left|v_i^{(d)}\right\rangle\rangle, \tag{5.45}$$

where d goes over all possible blocks of the Liouvillian and i runs from 1 to $\sqrt{\dim(\mathscr{L}_d)}$, denoting the index of the eigenvector of a specific block. The coefficient $c_i^{(d)}$ is the projection of $|\rho_{\text{Sys}}\rangle\rangle$ to the eigenvector $\left|v_i^{(d)}\right\rangle\rangle$:

$$c_i^{(d)} = \left\langle\left\langle \tilde{v}_i^{(d)}\right|\rho_{\text{Sys}}\right\rangle\rangle = \text{Tr}\left[\rho_{\text{Sys}}\left(\tilde{v}_i^{(d)}\right)^\dagger\right]. \tag{5.46}$$

Here $\langle\langle\tilde{v}_i^{(d)}|$ denotes the i:th *left* eigenvector of the block $\mathscr{L}_d$.[9] The eigenvectors are taken to be normalized such that $\langle\langle\tilde{v}_i^{(d)}|v_j^{(d)}\rangle\rangle = \delta_{ij}$.

We know that the quantum state evolves as $\rho(t) = \mathrm{e}^{\mathscr{L}t}\rho(0)$. If we now represent the initial state $\rho(0)$ as a linear combination of the eigenvectors of the Liouvillian, as in equation (5.45), we obtain[10]

$$\begin{aligned}\left|\rho_{\text{Sys}}(t)\right\rangle\rangle &= \mathrm{e}^{\mathscr{L}t}\left|\rho_{\text{Sys}}(0)\right\rangle\rangle = \mathrm{e}^{\mathscr{L}t}\sum_d\sum_i c_i^{(d)}\left|v_i^{(d)}\right\rangle\rangle \\ &= \sum_d\sum_i c_i^{(d)}\mathrm{e}^{\mathscr{L}t}\left|v_i^{(d)}\right\rangle\rangle = \sum_d\sum_i c_i^{(d)}\mathrm{e}^{\lambda_i^{(d)}t}\left|v_i^{(d)}\right\rangle\rangle,\end{aligned} \tag{5.47}$$

where we used the fact $\mathscr{L}|v_i^{(d)}\rangle\rangle = \lambda_i^{(d)}|v_i^{(d)}\rangle\rangle$. The coefficients $c_i^{(d)}$ give us now the initial conditions.

Now that we have solved for the time evolution of the quantum state in terms of the eigenstates of the Liouvillian, we can consider the expectation value of σ_x. That was defined as $\langle\sigma_x(t)\rangle = \text{Tr}[\sigma_x\rho(t)] = \langle\langle\sigma_x|\rho(t)\rangle\rangle$. We know what is $|\rho(t)\rangle\rangle$ due to equation (5.47). The matrix form of σ_x is given as

$$\begin{aligned}\sigma_x &= \left(|g\rangle\langle e| + |e\rangle\langle g|\right)\otimes\mathbb{1}_n = \left(|e\rangle\langle g| + |g\rangle\langle e|\right)\otimes\left(|0\rangle\langle 0| + |1\rangle\langle 1| + |2\rangle\langle 2| + \ldots + |n\rangle\langle n|\right) \\ &= |g0\rangle\langle e0| + |g1\rangle\langle e1| + |g2\rangle\langle e2| + \ldots + |e0\rangle\langle g0| + |e1\rangle\langle g1| + |e2\rangle\langle g2| + \ldots.\end{aligned}$$

[8] Let's say that $\mathscr{L}_d$ is a $m \times m$ matrix, thus it has m eigenvalues and -vectors.

[9] The Liouvillian blocks (and the full Liouvillian itself) are not necessarily normal, which is a requirement for the left and right eigenvectors being equal. Therefore we need to distinguish between them.

[10] An important thing to note is that even though the linear combination of the eigenvectors of the Liouvillian is a valid density matrix, the eigenvectors themselves are *not* density matrices. The only eigenvector of the Liouvillian that is also a valid density matrix is the ground state [73].

From this we get the vectorized form as

$$\begin{aligned}\Rightarrow |\sigma_x\rangle\rangle = &\underbrace{|g0\rangle\rangle \otimes |e0\rangle\rangle + |g1\rangle\rangle \otimes |e1\rangle\rangle + |g2\rangle\rangle \otimes |e2\rangle\rangle + \ldots}_{d=-1} \\ &+ \underbrace{|e0\rangle\rangle \otimes |g0\rangle\rangle + |e1\rangle\rangle \otimes |g1\rangle\rangle + |e2\rangle\rangle \otimes |g2\rangle\rangle + \ldots}_{d=1}.\end{aligned} \tag{5.48}$$

We can notice that the vectorized form contains only the basis elements from the $\mathscr{L}_{\pm 1}$ blocks. Therefore, in studying the decoherence of the qubit we can concentrate only to these two blocks and forget the rest. Let's take now the inner product with the quantum state in order to compute the expectation value:

$$\begin{aligned}\langle \sigma_x(t)\rangle = \langle\langle \sigma_x|\rho(t)\rangle\rangle &= \sum_d \sum_i c_i^{(d)} e^{\lambda_i^{(d)} t} \left\langle\left\langle \sigma_x \middle| \nu_i^{(d)}\right\rangle\right\rangle \\ &= \sum_i \left[c_i^{(1)} e^{\lambda_i^{(1)} t} \left\langle\left\langle \sigma_x \middle| \nu_i^{(1)}\right\rangle\right\rangle + c_i^{(-1)} e^{\lambda_i^{(-1)} t} \left\langle\left\langle \sigma_x \middle| \nu_i^{(-1)}\right\rangle\right\rangle \right].\end{aligned} \tag{5.49}$$

From the equivalence between the Liouvillian blocks, $\mathscr{L}_d = \mathscr{L}_{-d}^*$ it follows that $c_i^{(d)} = c_i^{(-d)*}$ and $\langle\langle \sigma_x|\nu_i^{(d)}\rangle\rangle = \langle\langle \sigma_x|\nu_i^{(-d)}\rangle\rangle^*$. Also the eigenvalues λ_i^d follow the same kind of logic, and thus they can be written as $\lambda_i^{(\pm d)} = \mathrm{Re}[\lambda_i^{(d)}] \pm i\mathrm{Im}[\lambda_i^{(d)}]$. Using these results in equation (5.49) allows us to write it in the following way:

$$\langle \sigma_x(t)\rangle = \sum_i \left[c_i \left\langle\left\langle \sigma_x \middle| \nu_i\right\rangle\right\rangle e^{\mathrm{Re}[\lambda_i] t} e^{i\mathrm{Im}[\lambda_i] t} + c_i^* \left\langle\left\langle \sigma_x \middle| \nu_i\right\rangle\right\rangle^* e^{\mathrm{Re}[\lambda_i] t} e^{-i\mathrm{Im}[\lambda_i] t} \right]. \tag{5.50}$$

The superscripts denoting block $d = 1$ were dropped to clean up notation. We just need to remember that the sum is over the eigenspace of $\mathscr{L}_1$.

Now the factor $c_i\langle\langle \sigma_x|\nu_i\rangle\rangle$ is just some complex number with magnitude $|c_i\langle\langle \sigma_x|\nu_i\rangle\rangle|$ and some argument. Denoting $\langle\langle \sigma_x|\nu_i\rangle\rangle \equiv p_i$, we can write equation (5.50) as

$$\begin{aligned}\langle \sigma_x(t)\rangle &= \sum_i \left[|c_i p_i| e^{i\mathrm{Arg}[c_i p_i]} e^{\mathrm{Re}[\lambda_i] t} e^{i\mathrm{Im}[\lambda_i] t} + |c_i p_i| e^{-i\mathrm{Arg}[c_i p_i]} e^{\mathrm{Re}[\lambda_i] t} e^{-i\mathrm{Im}[\lambda_i] t} \right] \\ &= \sum_i |c_i p_i| e^{\mathrm{Re}[\lambda_i] t} \left(e^{i(\mathrm{Im}[\lambda_i] t + \mathrm{Arg}[c_i p_i])} + e^{-i(\mathrm{Im}[\lambda_i] t + \mathrm{Arg}[c_i p_i])} \right) \\ &= \sum_i 2|c_i p_i| e^{\mathrm{Re}[\lambda_i] t} \cos\left(\mathrm{Im}[\lambda_i] t + \mathrm{Arg}[c_i p_i]\right).\end{aligned} \tag{5.51}$$

The expectation value $\langle \sigma_y(t)\rangle$ is given by an equation equivalent to the above, the only difference is that the coefficient p_i becomes in that case $p_i \equiv \langle\langle \sigma_y|\nu_i\rangle\rangle$.

Equation (5.51) essentially decomposes the time evolution of σ_x into a sum of different modes. The oscillation of the different modes is driven by the imaginary part of the corresponding eigenvalue, while the real part is responsible for the decay of the mode.[11] Thus we

[11] The real part indeed is responsible for the decay, since the eigenvalues of the Liouvillian has always a negative or zero real part [71]. If one eigenvalue would have a strictly positive real part that would be bad news for our solution since that mode would grow exponentially in time.

can see that if some eigenvalue is purely real, that induces pure decay for the corresponding mode without any oscillations. An opposite case is a purely imaginary eigenvalue, where we see no decay and only oscillations of the coherence. The eigenvalue 0 of the Liouvillian corresponds to the steady state, but it is not found in the $\mathscr{L}_{\pm 1}$ blocks considered above but in the $\mathscr{L}_0$ block.

Now that we have a formula for the expectation value of σ_x and σ_y, we are able to compute the coherence measure $C(\rho(t)) = \sqrt{\langle\sigma_x\rangle^2 + \langle\sigma_y\rangle^2}$. In general this needs to be done on a computer because the expressions for the eigenvalues λ_i of the Liouvillian block $\mathscr{L}_1$ are cumbersome already for truncation to two dimensions for the resonator Hilbert space. But computing the coherence measure is not the only thing that equation (5.51) allows us to do. Using it we can estimate the decoherence times of the qubit with respect to temperature.

The qubit loses its coherence in time, as explained in the first section of this chapter. Since the expectation value of σ_x is decomposed as a sum of different modes, some modes die off quicker than others. From equation (5.51) we can see that the time scale associated with this loss of coherence is given by $\mathrm{Re}[\lambda_i]$. Therefore we define the *thermalization time scale*, describing how fast the qubit loses all of its coherences, to be the one which has minimum absolute value of the real part of the eigenvalue, or

$$\Gamma_2 = \min_i \left(\left|\mathrm{Re}\left[\lambda_i^{(1)}\right]\right|\right). \tag{5.52}$$

This thermalization rate is exactly the decoherence rate if the readout resonator is thermalized. This can be seen later in section 5.3.3. However, decoherence can happen also at a faster time scale if the resonator is not in a thermal state.

The eigenvalues $\lambda_i^{(1)}$ in equation (5.52) depend on all of the circuit parameters we used in deriving the circuit Hamiltonian and the master equation. In addition, they depend also on the temperature of the environment, so we can find the temperature dependency of the decoherence time by computing the eigenvalues $\lambda_i^{(1)}$ for different temperatures and using equation (5.52) to pick the one that describes slowest decay.

We have now come as far as we can analytically. To continue from here we need to resort to numerical methods in solving the master equation (5.4). This is the topic of the next section.

5.3 NUMERICAL SOLUTIONS

5.3.1 TRUNCATION OF HILBERT SPACE

To be able to solve the master equation numerically, we begin with the Liouvillian in equation (5.38). As discussed, here all the elements can be represented as matrices and the solution for some arbitary time t can be obtained by exponentiating the Liouvillian matrix $\rho(t) = \mathrm{e}^{\mathscr{L}t}\rho(0)$. However, one question that arises is how to treat the ladder operators a_f and $a_\mathrm{f}^\dagger$? Ideally they operate on an infinite dimensional Hilbert space as infinite dimensional matrices, which of course is not possible to be implemented in a program that solves the qubit dynamics. Therefore we need to truncate the Hilbert space to some number M.

Let's try to get some intuitive understanding on what is the effect of the truncation on the system. The truncation M effectively sets the upper limit for the resonator excitations. For example, by choosing $M = 2$, we restrict the resonator to behave like a qubit, only having access to states $|0\rangle$ and $|1\rangle$. This is of course not very ideal, because at any temperature higher than absolute zero the resonator is likely to populate also higher energy states in its steady state, the thermal state. This brings us to the method of determining M: truncation M should always be large enough such that the resonator can get close enough to its ideal steady state.

The equation for the steady state is given by (3.35). In a matrix form it looks like the following:

$$\rho_{\mathrm{Th}} = \begin{bmatrix} \frac{1}{1+\bar{n}(\omega_{\mathrm{f}},T)} & 0 & 0 & \dots \\ 0 & \frac{\bar{n}(\omega_{\mathrm{f}},T)}{(1+\bar{n}(\omega_{\mathrm{f}},T))^2} & 0 & \\ 0 & 0 & \frac{\bar{n}(\omega_{\mathrm{f}},T)^2}{(1+\bar{n}(\omega_{\mathrm{f}},T))^3} & \\ \vdots & & & \ddots \end{bmatrix}. \tag{5.53}$$

And the Bose-Einstein distribution is given by[12]

$$\bar{n}(\omega_{\mathrm{f}}, T) = \frac{1}{\mathrm{e}^{\hbar\omega_{\mathrm{f}}/k_{\mathrm{B}}T} - 1}. \tag{5.54}$$

We can see from equation (5.53) that the values become smaller when moving down along the diagonal, representing the fact that the probability of observing a state with higher energy becomes smaller. If temperature T is small, such that $\bar{n}(\omega_{\mathrm{f}}, T)$ is small, then we can use relatively small truncation M because the factors on the diagonal of the thermal state become negligible for rather small values of M. In the extreme case of $T = 0$ and therefore $\bar{n}(\omega_{\mathrm{f}}, T) = 0$, we can use truncation $M = 2$, because only the term corresponding to the ground state does not vanish. In practice for $T > 0$ we choose the truncation M such that the terms of the thermal state corresponding to states above the truncated value correspond to probability of 10^{-7} or less.

5.3.2 NUMERICAL VALUES FOR THE PARAMETERS

The analysis we did was based on the qubit chip shown in the micrograph 4.1, which was taken from [55]. All the numerical values that we need are coming from the circuit diagram 4.4, which sets our analysis concretely to the real world implementation of the qubit circuit. The values are listed in table 5.1.

The inductances L_{L} and L_{R} are estimated from the micrograph figure 4.1 by calculating the length of the part of the CPW that couples the drive line to the read out resonator and using the formula for an inductance of a straight wire. The mutual inductance is estimated by doing a numerical simulation and making the resonance frequency of the resonator match the values given in [55].

[12] Note that the frequency is set to the resonance frequency of the readout resonator ω_{f} in the derivation of the master equation.

$R(\Omega)$	L_L(pH)	L_R(pH)	M	C_f(fF)	C_g(fF)	C_A(fF)	ω_f(GHz)	ω_A(GHz)
50	80	80	$0.025L_R$	800	5	90	$2\pi \cdot 6.1$	$2\pi \cdot 4$

Table 5.1: Numerical values for all the needed circuit parameters used in the calculations. These values are approximate, obtained using crude estimations. They are used to obtain some numerical values for the solutions presented later.

The capacitance of the readout resonator C_f can be calculated as discussed in section 4.1.1. The distributed capacitance c_0 can be obtained from the geometry of the CPW by using the w and s parameters [58]. For us these are $w = 12\,\mu$m and $s = 6\,\mu$m. These give capacitance per unit length as $1.6 \cdot 10^{-10}$ F/m. Estimating the length of the CPW to be about 5 mm yields $C_f \approx 800$ fF.

The coupling capacitance C_g and qubit capacitance to ground C_A are values obtained from discussion with the authors of reference [55]. The frequencies are angular frequencies (therefore multiplied by 2π) obtained from the bare frequencies of the transition rates.

The values listed in table 5.1 determine the dynamics of the qubit as the qubit-resonator coupling g_f and the environmental coupling parameter γ are completely determined as a function of the circuit parameters. Collecting the results from the previous chapters of the thesis we have g_f as (see Eq. (4.45)):

$$g_f = \frac{C_g}{2}\sqrt{\frac{\omega_A\omega_f}{(C_f+C_g)(C_A+C_g)}} \approx 0{,}281\,\text{GHz} \quad \Rightarrow \quad g_f' = \frac{g_f}{\omega_A} \approx 0{,}0112 \tag{5.55}$$

and $\gamma = \alpha^2 2\pi J(\omega_f)$ can be opened up as (see Eqs. (4.47), (4.42) and (4.26) for the definition of D)

$$\gamma = 2\pi\left(\frac{M}{L_L}\right)^2 \frac{R\hbar(C_A+C_g)}{2(C_AC_f+C_fC_g+C_gC_A)\omega_f\hbar L_R^2}\frac{\omega_c^2}{\pi\omega_f(\omega_c^2+\omega_f^2)} \approx 4{,}12\,\text{GHz} \quad \Rightarrow \quad \gamma' = \frac{\gamma}{\omega_A} \approx 0{,}164\,. \tag{5.56}$$

The dimensionless values are normalized with respect to the qubit frequency ω_A. This allows us to see the how the different coupling parameters compare to each other. The cut-off frequency ω_c is set to be 1 THz in the above.

5.3.3 SIMULATED DYNAMICS

We solve the master equation with the help of QuTiP, the Quantum Toolbox in Python, which is a Python library specifically designed for solving dynamics of open quantum systems [75].

As discussed, the starting point of the numerical solution is the Liouville space master equation (5.4). We can code a program that builds the Liouvillian matrix and then exponentiates it. Then we are able to get the solutions at any time t by multiplying the initial density matrix by the exponentiated Liouvillian matrix at that time. It is noteworthy that the we do not need to set a time step in order to solve the master equation, contrary to the usual

methods of solving differential equations numerically. This is because of the quantum dynamical semigroup property [39]

$$e^{\mathscr{L}t}e^{\mathscr{L}t'} = e^{\mathscr{L}(t+t')}. \tag{5.57}$$

Thus only the initial condition affects the evolution of the master equation, not the size of the time step applied. The simulation of the dynamical semigroup is therefore computationally exact.

For the initial conditions we set the qubit to be in the superposition state $|\Psi_Q\rangle = |+\rangle = \frac{1}{\sqrt{2}}\big(|g\rangle + |e\rangle\big)$ and the resonator $|\Psi_R\rangle$ in either the thermal state with the given temperature or in a coherent state. This will be separately specified in each case studied. The total state of the qubit-resonator system is initially the product state $|\Psi\rangle = |\Psi_Q\rangle \otimes |\Psi_R\rangle$.

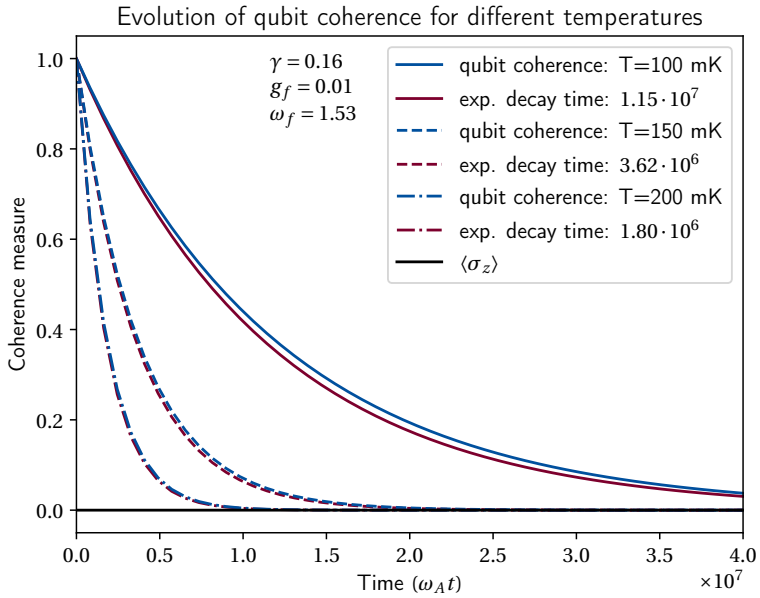

Figure 5.6: Qubit decoherence due to the thermal noise emanating from the resistor for different resistor temperatures. In blue the qubit coherence measure $C = \sqrt{\langle\sigma_x\rangle^2 + \langle\sigma_y\rangle^2}$ is plotted. In red is the exponential decay of the form e^{-t/T_2}, where the decay times T_2 are obtained from equation (5.52) for each temperature. We can see that the blue and red curves match each other very well. In black is the qubit population, which stays constant in time. The initial state of the resonator is the thermal state for each temperature considered. The parameters listed in the figure annotation, as well as the time scale of the figure, are normalized with respect to the qubit frequency.

We solve for the qubit coherence with the parameters given in table 5.1, giving the coupling rates shown in equations (5.55) and (5.56). The results for the coherence decay are shown in blue in figure 5.6 for three different resistor temperatures $T = 100\,\text{mK}$, $T = 150\,\text{mK}$ and $T = 200\,\text{mK}$. We can also predict the thermalization times for these three different temperatures by computing the Liouvillian matrices for the three temperatures and using

the block diagonalization method discussed in section 5.2.3. Applying equation (5.52) gives the predicted thermalization rates. The exponential decay of coherence of the form e^{-t/T_2} is plotted in red in figure 5.6 for the three temperatures. The initial state of the resonator is the thermal state.

We can notice that the qubit coherence decays in time, where the time scale is affected by the choice of temperature of the resistor. As suspected, the qubit coherence decays faster for higher temperatures due to the addition of thermal noise coming from the resistor. We also can see that the qubit population does not vary in time, as predicted in the beginning of section 5.2.

We can also see that the qubit decay follows closely the prediction of exponential decay shown in red. This confirms that our choice to express the relaxation time of the qubit coherences as in equation (5.52) makes sense, at least for the case of thermalized resonator. In other cases faster decoherence modes are present, as we will see soon.

Figure 5.6 shows the time evolution of the qubit for a specific case, where the parameters driving the evolution are fixed. Next we will consider different cases where the coupling parameters are varied. Changing γ, g_f and ω_f allows us to study regimes where more complex time evolution is present and to predict how these different parameters affect the qubit dynamics. This is done in the simulations which give the results in figure 5.7.

We choose values for the parameters γ, g_f and ω_f such that the decay times are relatively fast. This allows us to see also the direct oscillatory evolution of $\langle\sigma_x\rangle$, which comes from the qubit rotating around the Bloch sphere (see figure 5.1). This is the reason why the time scale changes when moving from 5.6 to 5.7. In these figures we also plot the expected number of quanta in the resonator $\langle a_\mathrm{f}^\dagger a_\mathrm{f}\rangle$, which gives us information on how the quantum state of the resonator evolves in time.

Figure 5.7a shows the qubit decoherence when the initial state of the resonator is thermal. We can see steady decrease in the coherence, while the number of quanta stays constant in time. This is a sign that the resonator is indeed in a steady state. The value for the expected number of quanta is in this case $\bar{n}(\omega_\mathrm{f} = 4\omega_\mathrm{A}, T = 0{,}3\,\mathrm{K}) \approx 0{,}083$, where ω_A is taken from table 5.1.

In the next figure 5.7b we change the initial state of the resonator into a coherent state with $\alpha = 1$, while keeping everything else unchanged. In this case we notice that in the beginning the qubit decoheres quite rapidly, while the resonator is moving towards its steady state. This can be interpreted with the help of equation (5.51), which showed that the coherence evolution can be decomposed into parts using the eigenstates of the Liouvillian. At times $t < 20$ the modes corresponding to large $|\mathrm{Re}(\lambda_i)|$ decay away, which is seen as the rapid decrease of qubit coherence. After that the modes that are left are decaying steadily. It is notable that this shift from fast decoherence to slower one happens at the same time when the resonator reaches its steady state.

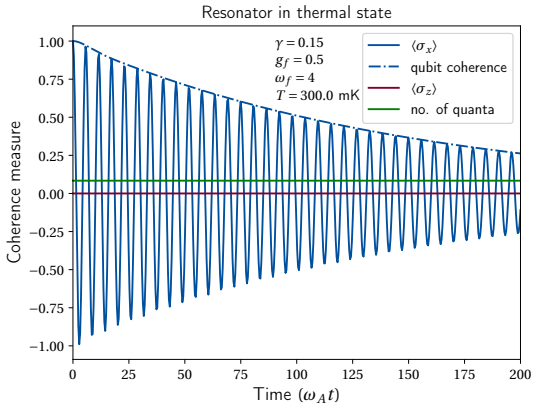

(a) Qubit coherence decays steadily when the resonator starts out in a thermal state. Resonator has a constant number of quanta.

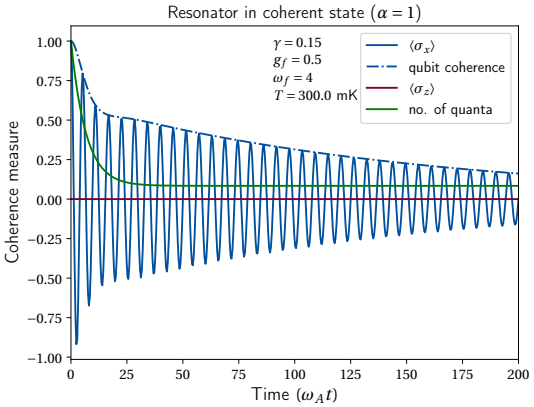

(b) Qubit experiences different decoherence when the resonator is initialized into a coherent state.

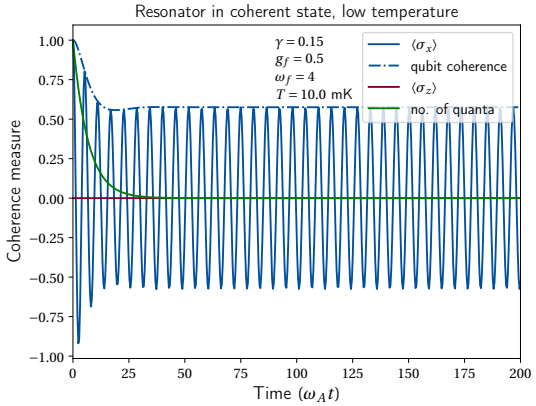

(c) At very low temperatures the qubit decoherence stops after a while, when the resonator reaches its steady state.

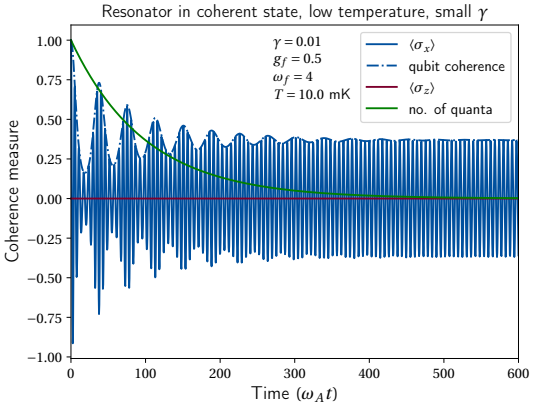

(d) At very low temperatures and for low γ the qubit and resonator have time to exchange coherences in a reversible fashion.

Figure 5.7: Allowing the different parameters to vary, we can explore regions where different kinds of dynamics are present. In 5.7a the initial state of the resonator is the thermal state. We see steady decoherence on the qubit and a constant number of quanta in the resonator. In 5.7b the resonator is initialized into a coherent state with $\alpha = 1$. We can notice fast decay of qubit decoherence in the beginning, which slows down as the resonator reaches the steady state. In figure 5.7c the resistor temperature has been lowered such that the steady state of the resonator becomes approximately the ground state $|0\rangle\langle 0|$. When that is reached, the qubit stops decohering. In 5.7d we decrease γ, which describes the interaction strength between the resonator and the resistor, essentially being the dissipation rate of the resonator. We can see that for small γ the resonator and qubit have time to exchange coherences in a reversible fashion before the resonator reaches its ground state and the decoherence stops.

Figure 5.7c shows what happens if we drop the temperature of the resistor significantly. In this case the steady state of the resonator is very close to the ground state $|0\rangle\langle 0|$ (see Eq. (5.53): since $\bar{n} \approx 0$ all elements except one become zero). Remembering our results from section 5.2.1, we notice that this corresponds to the case of computing the coherence evolution when the resonator was in a Fock state $|n\rangle\langle n|$. There we noticed that the coherences do not decay (see Eq. (5.12)). Therefore, once the resonator reaches its steady state, this time the coherence decay stops.[13]

An interesting behaviour can be seen in figure 5.7d, where we decrease the value γ for the resonator-resistor interaction strength. This makes the resonator move slowly towards its steady state, giving thus time for the qubit and resonator to exhange coherences reversibly. This is seen as the oscillatory behaviour of the coherence measure.

The oscillations in the qubit coherence resemble well the oscillations we saw when we computed the unitary dynamics in the case where the resonator was at a coherent state (see Eq. (5.21) and figure 5.3). It is also notable that this time the qubit coherence stabilizes at a lower value than in the case of higher γ in the previous figure. Similarly to the previous figure, also this time when the resonator reaches its steady state the decoherence stops.

One last aspect we will discuss is how does the decoherence time T_2 depend on the temperature of the resistor? As discussed in section 5.2.3 and shown in equation (5.52), we pick the coherence decay rate from the eigenvalues of the Liouvillian block $\mathscr{L}_1$. What we do in practice is that we compute the eigenvalues for the Liouvillian block for a specific temperature using a proper Hilbert space truncation for that temperature, determined by the method discussed in section 5.3.1, and apply equation (5.52) to those eigenvalues. This gives an estimate on how the decay behaves with respect to temperature.

In figure 5.8 we plot the T_2 times for the system whose parameters were given in table 5.1. In figure 5.8a we see diverging T_2 values for low temperatures. This is because near absolute zero the resonator's steady state approaches the ground state and thus the absolute value of the real part of the eigenvalues get smaller, indicating a situation where coherence decays very slowly. Physically the decoherence times get longer because expected number of thermal photons that populate the readout resonator is supressed.

The low temperature behaviour in figure 5.8a assumes perfect thermalization of the resistor and that its temperature can be brought to these arbitrarily low values. However, we know that experimentally this is very difficult. In reality the T_2 times find a constant value when the temperature of the mixing chamber is decreased [76]. This is explained by the existence of excess thermal photons that leak to the readout resonator from the attenuators [76, 77]. The excess thermal photons can be modelled by introducing a background decay rate Γ_B, which corresponds to the lower bound of noise temperature. The effects of this background decay rate are shown in figure 5.8b.

To implement the backgrond decay, we modify equation (5.52) to be

$$\Gamma_2 = \min_i \left(\left| \mathrm{Re}\left[\lambda_i^{(1)} \right] \right| \right) + \Gamma_\mathrm{B}\,, \tag{5.58}$$

[13] In reality the time scale associated to the coherence decay becomes so large that it seems like the qubit stops decohering.

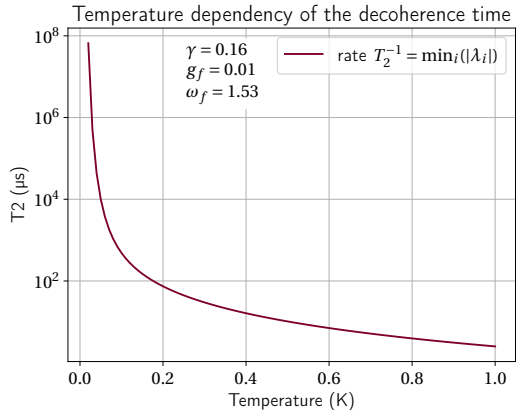

(a) Temperature dependency of T_2 with no background decay rate.

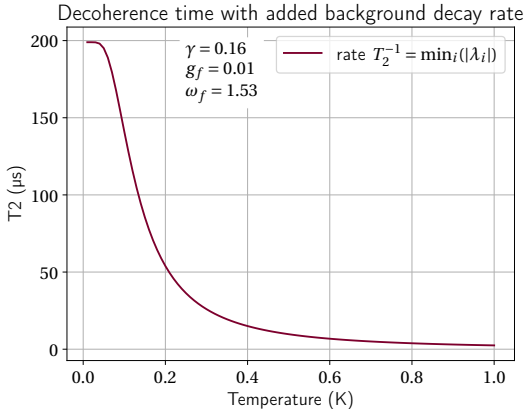

(b) Temperature dependency of T_2 with added background decay rate of $\Gamma_B = 2 \cdot 10^{-7}$.

Figure 5.8: Plots of the temperature dependency of the decoherence time scale. The figure 5.8a shows the pure effect of the noise coming from the resistor at temperature T. As temperature is lowered the relevant time scales for the decoherence grow arbitrarily large. This behaviour is inhibited via the introduction of a phenomenological background decay rate Γ_B. This is shown in figure 5.8b. The background decay rate stops the T_2 times from growing above a certain threshold, which is what is seen experimentally [76, 77].

where Γ_B is the background decay rate. To obtain the behaviour in figure 5.8b we set $\Gamma_B = 2 \cdot 10^{-7}$ (in the units of ω_A), which corresponds to the decay time of around 200 μs.

The choice of Γ_B is quite arbitrary and its exact value is dependent on for example the manufacturing details of the qubit chip [77]. However, if this background decay rate could be controlled and made smaller and if the attenuator thermalization is taken care of, then longer qubit decoherence times could be achievable.

One last point worth discussing is how does our model compare to the ones that are frequently used when the qubit coherence times are approximated. One simple way of deducing the temperature dependency of the thermalization time used in experimental papers is to assume that the thermalization is driven purely by thermal photons in the resonator [76]. This approximation can be written as

$$\Gamma_2 = \gamma \bar{n}, \tag{5.59}$$

where γ is the same dissipation rate of the resonator used in earlier calculations and $\bar{n}$ is the expected number of quanta. This approximation (5.59) is valid when $\bar{n}$ is small and when the coupling rates γ and g_f are small compared to the resonance frequency of resonator ω_f [76], which is usually the case experimentally. Another requirement for (5.59) to hold is that the ratio γ / g_f is small [78].

We can plot this approximation (5.59) and compare it to the T_2 dependency we get from equation (5.52). This is done in figure 5.9. We can see that when we use the values from table 5.1, the approximation (5.59) gives very low relaxation times. This is due to the

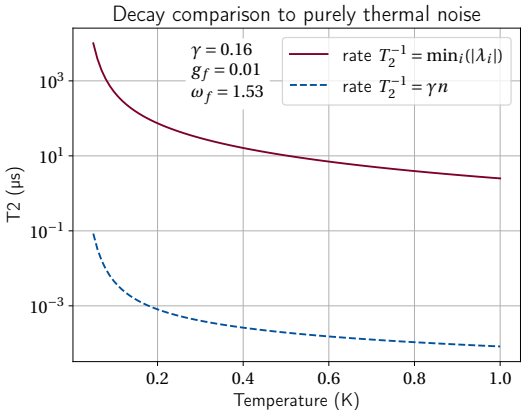

(a) Comparison of decay rates obtained from equation (5.52) (in red) and (5.59) (in blue).

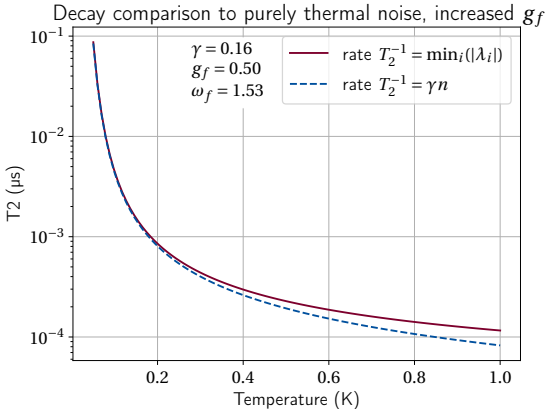

(b) Comparison of decay rates from the two approaches with increased qubit-resonator coupling.

Figure 5.9: Comparison between the decay times obtained by using the block diagonalization method of the Liouvillian (equation (5.52), in red) with the approximation of the relaxation being caused purely by thermal photons in the resonator (equation (5.59), in blue). On the left we see that for low qubit-resonator couplings the relaxation times obtained from the full Liouvillian analysis are much longer than what could be predicted by simply using $\Gamma_2 = \gamma\bar{n}$ due to small qubit-resonator coupling. Increasing g_f shows how our model includes the approximation as a limiting case shown in the right-side figure, where we can see how the two approaches match well for low temperatures.

qubit-resonator coupling g_f being too small for (5.59) to represent the situation accurately ($\gamma/g_f \approx 16$). Then, when we increase the inner coupling, we see in figure 5.9b how the two approaches agree with each other well for low enough temperatures ($\gamma/g_f \approx 0.32$).

We can thus conclude that our model expands the approximation of relaxation being linearly dependent on the number of thermal photons in the resonator. For weak qubit-resonator couplings we predict longer coherence times than the $\Gamma_2 = \gamma\bar{n}$ model. We recover the approximation (5.59) in the range $\gamma/g_f \ll 1$, which agrees with the results derived in reference [78].

◆ ◆ ◆

This chapter began with the discussion of dissipation and decoherence on a qubit and where do these two phenomena come from. We derived a way to quantify the coherence of qubits using the coherence measure, which depends on the expectation values of the Pauli σ_x and σ_y operators. We also argued that in our case the qubit should not experience any dissipation due to the driving Hamiltonian having no transverse coupling to the qubit.

Setting aside the open quantum system dynamics for a moment, we analyzed the unitary dynamics of the qubit-resonator system and how they exchange coherences. This analysis, and the derivation of the system's steady state, was useful later when we solved numerically

the open system dynamics and saw no coherence decay at low temperature and also some oscillations in the qubit coherences. Finally we presented the results for the behaviour of the T_2 time with respect to temperature, noticing how it drops quickly when temperature is raised. We ended the discussion by considering how our model compares to a frequently used approximation of coherence decay and showed that it is included in our model as a limiting case.

6 Conclusions and Discussion

The time evolution of the quantum state of the qubit is largely affected by the noise coming from its environment. In this thesis we have characterized the contribution of the noise coming from the system's feedline, which is used for qubit control and readout. The main question we set out to answer is if we can build a theoretical model for the superconducting circuit of the qubit and other circuit elements, and use that model to predict qubit behaviour in the presence of noise coming from a 50 Ω resistor installed in the qubit drive line. We have shown that indeed such a model can be constructed. We are able to precisely characterize the time evolution of the qubit in terms of the exact values for the circuit elements used to build the quantum circuit.

Starting from the microscope image of the quantum circuit, we were able to build the corresponding lumped element model describing the circuit with discrete elements. From the drawn circuit diagram it was possible to identify the energies involved with each of the circuit elements. Then, using the Caldeira-Leggett model for the resistor quantization, we were able to write down first the Lagrangian, and then the Hamiltonian describing the associated energies. As we quantized the circuit Hamiltonian, we obtained a fully quantum description of the superconducting circuit.

The Hamiltonian that we obtained for the circuit was essentially a Jaynes-Cummings Hamiltonian describing the qubit-resonator system with an added coupling between the resonator and the resistor. Assuming sufficiently large detuning between the resonance frequencies of the qubit and the resonator allowed us to move to the dispersive regime. This transformed the Hamiltonian of the circuit into a form that we could use in the open quantum systems formalism to derive a master equation describing the dynamics of the quantum system.

The resulting master equation turned out to be relatively simple, describing a system where the readout resonator absorbs or emits quanta. The rate of these processes is determined by the temperature of the resistor and the coupling strength between the resonator and the resistor. The coupling strength in turn is determined by the actual values of the circuit parameters used to construct the superconducting circuit. Thus we were able to derive a master equation, where the effect of the chosen circuit parameter values is visible in the expressions of the coupling parameters.

Having derived the master equation the next step was to solve it. Since the complete solution to the master equation was out of reach using analytical methods, we resorted to numerical simulations done in Python. The numerical results show how the qubit coherence evolves in time, showing clear decay which is quickened by the raising of temperature. Finally we were able to obtain predictions for the behaviour of the decoherence times with respect to the temperature of the resistor in the drive line.

The behaviour of the T_2 time with respect to temperature shows that in the ideal case the thermal noise emanating from the resistor decreases such that arbitrarily large coherence times could be, in theory, achieved. However, this assumes perfect thermalization of the qubit drive line attenuator and that it could be brought down to arbitrarily low temperatures. Experimentally this is very difficult to achieve. Thus in reality an excess of thermal photons is present inside the resonator, which are driving the decoherence in the background. Using our model we introduce the background decay rate Γ_B by adding it as an extra term to the model.

As a final step we considered how our model pairs against a fequently used approximation that the decoherence rate of the qubit is linearly dependent on the amount of thermal photons in the resonator. We managed to show that this approximation is indeed included within our model as a limiting case which is reached when $\gamma/g_f \ll 1$. However, our model is not restriced to this range of values but can accomodate also other regimes. Most notably, we see that our model predicts longer coherence times compared to the often used approximation, when the qubit-resonator coupling g_f is decreased. Thus we can conclude that if the thermalization of the attenuators is taken care of, the background noise from other sources minimized and the coupling between qubit and resonator made weak, longer coherence times could be reached.

The results shown and discussed in this thesis should be experimentally proven. Experimental data would allow us to predict the background decay rate accurately. It would also show if the model works and in which limits. If the theoretical model held when compared against experimental evidence, that would be an indication that we could expand the model by adding more circuit elements and analyzing their effect. Examples could be different signal filters in the feedline before the readout resonator. Another aspect worth researching would be for example going from the dispersive regime to the coherent regime, where the detuning between the qubit and resonator becomes small. This would allow us to study different dynamics altogether.

A Impedance calculation

Claim:
The impedance of an infinite chain of parallel LC-oscillators is given by equations (2.34) and (2.35):

$$\mathrm{Re}[Z_\infty(\omega)] = \mathrm{Re}[Z(\omega)] \tag{A.1}$$

$$\mathrm{Im}[Z_\infty(\omega)] = \frac{1}{\pi}\left[\mathrm{P.V.}\int_0^\infty \mathrm{d}\omega_j \frac{\mathrm{Re}[Z(\omega_j)]}{\omega+\omega_j} + \mathrm{P.V.}\int_0^\infty \mathrm{d}\omega_j \frac{\mathrm{Re}[Z(\omega_j)]}{\omega-\omega_j}\right] \tag{A.2}$$

for some impedance of interest $Z(\omega)$. The impedance given in equation (2.36)

$$Z_R(\omega) = R\frac{\omega_C^2}{\omega_C^2+\omega^2} + \mathrm{i}R\frac{\omega\omega_C}{\omega_C^2+\omega^2} \tag{A.3}$$

fulfills the above equations.

Proof:
The real part of the impedance $Z_\infty(\omega)$ is trivial to get as seen from equation (A.1). Essentially what needs to be shown is that the imaginary part in equation (A.3) arises from (A.2). Let's consider (A.2):

$$\begin{aligned}\mathrm{Im}[Z_\infty(\omega)] &= \frac{1}{\pi}\left[\mathrm{P.V.}\int_0^\infty \mathrm{d}\omega_j \frac{\mathrm{Re}[Z(\omega_j)]}{\omega+\omega_j} + \mathrm{P.V.}\int_0^\infty \mathrm{d}\omega_j \frac{\mathrm{Re}[Z(\omega_j)]}{\omega-\omega_j}\right] \\ &= \frac{R\omega_c^2}{\pi}\left[\mathrm{P.V.}\int_0^\infty \mathrm{d}\omega_j \frac{1}{(\omega+\omega_j)(\omega_c^2+\omega_j^2)} + \mathrm{P.V.}\int_0^\infty \mathrm{d}\omega_j \frac{1}{(\omega-\omega_j)(\omega_c^2+\omega_j^2)}\right].\end{aligned} \tag{A.4}$$

Let's compute the second integral above. It's Cauchy principal value so we must be mindful about the pole at $\omega_j = \omega$. Let's therefore split the integral into two parts with a small parameter $\epsilon > 0$ and then take the limit $\epsilon \to 0$.

$$\begin{aligned}I_2 &= \mathrm{P.V.}\int_0^\infty \mathrm{d}\omega_j \frac{1}{(\omega-\omega_j)(\omega_c^2+\omega_j^2)} \\ &= \int_0^{\omega-\epsilon} \mathrm{d}\omega_j \frac{1}{(\omega-\omega_j)(\omega_c^2+\omega_j^2)} + \int_{\omega+\epsilon}^\infty \mathrm{d}\omega_j \frac{1}{(\omega-\omega_j)(\omega_c^2+\omega_j^2)}.\end{aligned} \tag{A.5}$$

We compute the indefinite integral using Mathematica or similar software to get

$$I_2 = \int_0^{\omega-\epsilon} \frac{-2\omega_C \ln(|\omega_j-\omega|)+\omega_c\ln(\omega_j^2+\omega_c^2)+2\omega\arctan\left(\frac{\omega_j}{\omega_c}\right)}{2\omega_c(\omega_c^2+\omega^2)} + \int_{\omega+\epsilon}^{\infty} \frac{-2\omega_C \ln(|\omega_j-\omega|)+\omega_c\ln(\omega_j^2+\omega_c^2)+2\omega\arctan\left(\frac{\omega_j}{\omega_c}\right)}{2\omega_c(\omega_c^2+\omega^2)}.$$

Let's analyze the terms with the natural logarithm as $\omega_j \to \infty$:

$$\underbrace{-2\omega_c\ln(|\omega_j-\omega|)+\omega_c\ln(\omega_j^2+\omega_c^2)}_{\omega_j \text{ is large, at least } \omega_j>\omega} = -2\omega_c\ln(\omega_j-\omega)+\omega_c\ln(\omega_j^2+\omega_c^2)$$

$$= -2\omega_c\ln\left[\omega_j\left(1-\frac{\omega}{\omega_j}\right)\right]+\omega_c\ln\left[\omega_j^2\left(1+\frac{\omega_c^2}{\omega_j^2}\right)\right]$$

$$= -2\omega_c\ln\omega_j - 2\omega_c\ln\left(1-\frac{\omega}{\omega_j}\right)+\omega_c\ln\omega_j^2+\omega_c\ln\left(1+\frac{\omega_c^2}{\omega_j^2}\right)$$

$$= -2\omega_c\ln\left(1-\frac{\omega}{\omega_j}\right)+\omega_c\ln\left(1+\frac{\omega_c^2}{\omega_j^2}\right).$$

Both terms become $\ln 1 = 0$ as $\omega_j \to \infty$. Now we can substitute the limits of the integral. Using the above result for the infinity term and doing a bit of algebra gives us

$$I_2 = \frac{2\omega_c\ln\omega - 2\omega_c\ln\omega_c+\pi\omega}{2\omega_c(\omega_c^2+\omega_2)}, \tag{A.6}$$

where the limit $\epsilon \to 0$ was taken. Similarly, we compute the first integral from equation (A.4) to get

$$I_1 = \text{P.V.}\int_0^{\infty} \mathrm{d}\omega_j \frac{1}{(\omega+\omega_j)(\omega_c^2+\omega_j^2)} = \frac{2\omega_c\ln\omega_c - 2\omega_c\ln\omega+\pi\omega}{2\omega_c(\omega_c^2+\omega_2)}. \tag{A.7}$$

The sum of equations (A.6) and (A.7) gives

$$I_1 + I_2 = \frac{\pi\omega}{\omega_c(\omega_c^2+\omega^2)} \tag{A.8}$$

Therefore according to equation (A.4) the imaginary part of the impedance is given as

$$\text{Im}[Z_\infty(\omega)] = \frac{R\omega_c^2}{\pi}[I_1+I_2] = R\frac{\omega\omega_c}{\omega_c^2+\omega^2}. \tag{A.9}$$

So in conclusion, we have shown that the impedance given in equation (A.3) satisfies equations (A.1) and (A.2) such that

$$Z_\infty(\omega) = R\frac{\omega_C^2}{\omega_C^2+\omega^2} + \mathrm{i}R\frac{\omega\omega_C}{\omega_C^2+\omega^2}. \tag{A.10}$$

For frequencies $\omega \ll \omega_c$ the above gives that the impedance of the infinite series of LC-oscillators is approximately R. So for low frequencies the Caldeira-Leggett model gives the resistance of the resistor, which is a result we were looking for.

B Derivation of the thermal state

Claim:
The thermal state density matrix for an environment at some single mode frequency ω is given by

$$\rho_{\text{Th}}(\omega) = \frac{1}{1+\bar{n}(\omega)} \sum_{n=0}^{\infty} \left(\frac{\bar{n}(\omega)}{1+\bar{n}(\omega)} \right)^n |n\rangle \langle n| ,$$

where $\bar{n}(\omega)$ is the expected number of quanta of frequency ω given by the Bose-Einstein distribution.

Proof:
It is a well known result of quantum statistical mechanics that the state in a thermal equilibrium is given by the *Gibbs state* [79]

$$\rho_{\text{Th}} = \frac{1}{Z} e^{-\beta H} , \tag{B.1}$$

where the *partition function* $Z = \text{Tr}(e^{-\beta H})$ and H is the Hamiltonian. Let's now assume that the Hamiltonian describes the environment, which can be thought of as an infinite bath of harmonic oscillators [31]

$$H = \sum_{i=1}^{\infty} \hbar \omega_i a_i^\dagger a_i , \tag{B.2}$$

where $a_i^\dagger$ and a_i are respectively the creation and annihillation operators of the bath modes i. Let's now consider only one mode for simplicity. Then we get the Gibbs state as

$$\rho_{\text{Th}}(\omega) = \frac{1}{Z} e^{-\beta \hbar \omega a^\dagger a} . \tag{B.3}$$

This can be diagonalized in the Fock-basis $\{|n\rangle\}$ to yield

$$\rho_{\text{Th}}(\omega) = \frac{1}{Z} \sum_{n=0}^{\infty} e^{-\beta \hbar \omega n} |n\rangle \langle n| . \tag{B.4}$$

The exponential in the above equation can be written in terms of the Bose-Einstein distribution $\bar{n}(\omega) = 1/(e^{\beta \hbar \omega} - 1)$ as

$$\frac{\bar{n}(\omega)}{1+\bar{n}(\omega)} = \frac{\frac{1}{e^{\beta \hbar \omega} - 1}}{1 + \frac{1}{e^{\beta \hbar \omega} - 1}} = e^{-\beta \hbar \omega} . \tag{B.5}$$

Using equation (B.5) in (B.4) gives us

$$\rho_{\mathrm{Th}}(\omega) = \frac{1}{Z}\sum_{n=0}^{\infty}\left(\frac{\bar{n}(\omega)}{1+\bar{n}(\omega)}\right)^n |n\rangle\langle n| \,. \tag{B.6}$$

Last thing to figure out is the partition function Z. Density matrices have the requirement of unit trace. Let's therefore compute the trace of (B.6):

$$\begin{aligned}\mathrm{Tr}(\rho_{\mathrm{Th}}(\omega)) &= \frac{1}{Z}\sum_{m=0}^{\infty}\sum_{n=0}^{\infty}\left(\frac{\bar{n}(\omega)}{1+\bar{n}(\omega)}\right)^n \langle m|n\rangle\langle n|m\rangle = \frac{1}{Z}\sum_{n=0}^{\infty}\left(\frac{\bar{n}(\omega)}{1+\bar{n}(\omega)}\right)^n \\ &= \frac{1}{Z}\sum_{n=0}^{\infty}\left(\mathrm{e}^{-\beta\hbar\omega}\right)^n = \frac{1}{Z}\frac{1}{1-\mathrm{e}^{-\beta\hbar\omega}}\,.\end{aligned}$$

Setting the trace equal to one yields

$$\frac{1}{Z} = 1-\mathrm{e}^{-\beta\hbar\omega}. \tag{B.7}$$

Writing this in terms of the Bose-Einstein distributions gives

$$\frac{1}{1+\bar{n}(\omega)} = \frac{1}{1+\frac{1}{\mathrm{e}^{\beta\hbar\omega}-1}} = \mathrm{e}^{-\beta\hbar\omega}(\mathrm{e}^{\beta\hbar\omega}-1) = 1-\mathrm{e}^{-\beta\hbar\omega} = \frac{1}{Z}\,. \tag{B.8}$$

Using the above equation in (B.6) yields the thermal state we've been looking for

$$\rho_{\mathrm{Th}}(\omega) = \frac{1}{1+\bar{n}(\omega)}\sum_{n=0}^{\infty}\left(\frac{\bar{n}(\omega)}{1+\bar{n}(\omega)}\right)^n |n\rangle\langle n| \,. \tag{B.9}$$

If our environment is a collection of harmonic oscillators like equation (B.2) (which is the case when we consider a resistor as an environment to our qubit, see Eq. (2.38)), then the state of the environment is a tensor product between the different thermal states corresponding to different modes ω_i [10]

$$\rho_B = \bigotimes_{i=1}^{\infty}\rho_{\mathrm{Th}}(\omega_i)\,. \tag{B.10}$$

C Superket triple product identity

Claim:
Let A, B and C be operators that act on Hilbert space $\mathscr{H}_d$. Thus their product is also an operator on $\mathscr{H}_d$. Applying the bra-flipper operator $\mho$ to the product ABC gives us the corresponding superket in the Liouville space $\mathscr{L}_d$, for which the superket triple product identity holds:

$$|ABC\rangle\rangle = \left(A \otimes C^{\top}\right)|C\rangle\rangle\,.$$

Proof:
The proof follows reference [54]. Let $\mathscr{H}_d$ have an orthonormal basis $\{|i\rangle\}$. Let us consider two operators A and B acting on $\mathscr{H}_d$. The product of their matrix elements satisfies the following:

$$A_{ij}B_{kl} = \langle i|A|j\rangle\,\langle k|B|l\rangle = \langle\langle i,l|A \otimes B^{\top}|j,k\rangle\rangle\,. \tag{C.1}$$

This can be shown to hold as follows:

$$\begin{aligned}\langle\langle i,l|A \otimes B^{\top}|j,k\rangle\rangle &= \left(\langle i| \otimes \langle l|^*\right)\left(A \otimes B^{\top}\right)\left(|j\rangle \otimes |k\rangle^*\right) = \left(\langle i|A|j\rangle\right)\left(\langle l|^* B^{\top}|k\rangle^*\right)\\ &= \langle i|A|j\rangle\,\langle k|B|l\rangle = A_{ij}B_{kl}\,,\end{aligned}$$

where we used the superket definition (3.75), the mixed product property of the Kronecker product and when going to the second line the following result

$$\langle l|^* B^{\top}|k\rangle^* = l_\alpha B^{\top}_{\alpha\beta}k^*_\beta = l_\alpha B_{\beta\alpha}k^*_\beta = k^*_\beta B_{\beta\alpha}l_\alpha = \langle k|B|l\rangle\,, \tag{C.2}$$

where we implicitly sum over the matrix indices α, β.

Let's now consider the product ABC.

$$ABC = \sum_{i,j}^{d}(ABC)_{ij}\,|i\rangle\,\langle j| \quad \Rightarrow \quad \mho[ABC] = |ABC\rangle\rangle = \sum_{i,j}^{d}(ABC)_{ij}|i,j\rangle\rangle \tag{C.3}$$

The coefficient $(ABC)_{ij}$ is given by

$$(ABC)_{ij} = \langle i|A\mathbb{1}_d B\mathbb{1}_d C|j\rangle = \sum_{k,l}^{d}\langle i|A|k\rangle\,\langle k|B|l\rangle\,\langle l|C|j\rangle\,, \tag{C.4}$$

where we wrote the identity as $\mathbb{1}_d = \sum_k^d |k\rangle\langle k|$.

Next we show that a matrix element of an operator can be expressed as an inner product between suitable superkets:

$$\langle\langle \alpha,\beta|A\rangle\rangle = \sum_{\mu,\nu}^{d} A_{\mu\nu}\langle\langle \alpha,\beta|\mu,\nu\rangle\rangle = \sum_{\mu,\nu}^{d} A_{\mu\nu}\delta_{\alpha\mu}\delta_{\beta\nu} = A_{\alpha\beta} = \langle\alpha|A|\beta\rangle \tag{C.5}$$

Let's now work with (C.4).

$$\begin{aligned}(ABC)_{ij} &= \sum_{k,l}^{d} \langle i|A|k\rangle\langle k|B|l\rangle\langle l|C|j\rangle = \sum_{k,l}^{d} \langle i|A|k\rangle\langle l|C|j\rangle \underbrace{\langle k|B|l\rangle}_{(C.5)} \\ &= \sum_{k,l}^{d} \underbrace{A_{ik}C_{lj}}_{(C.1)}\langle\langle k,l|B\rangle\rangle = \sum_{k,l}^{d}\langle\langle i,j|A\otimes C^{\top}|k,l\rangle\rangle\langle\langle k,l|B\rangle\rangle \\ &= \langle\langle i,j|A\otimes C^{\top}|B\rangle\rangle\,. \end{aligned} \tag{C.6}$$

And then using (C.6) in (C.3) gives the superket triple product identity

$$|ABC\rangle\rangle = \sum_{i,j}^{d} |i,j\rangle\rangle\langle\langle i,j|A\otimes C^{\top}|B\rangle\rangle = \left(A\otimes C^{\top}\right)|B\rangle\rangle\,,$$

which we wanted to prove.

D Studying the Lamb-shift

The starting point in the discussion about the Lamb-shift in the qubit-resonator system discussed in chapter 4 is equation (4.104) for the bath correlation function and equation (3.58) for the coefficient $\Gamma(\omega)$ of the master equation. Equation (3.66) shows how the Lamb-shift Hamiltonian is constructed from the imaginary parts of $\Gamma(\omega)$ according to the decomposition (3.62). Thus our goal is to find the coefficients $S(\omega)$.

As we have found the form of the bath correlation function, we can write $\Gamma(\omega_\mathrm{f})$ as its one-sided Fourier transform like in (3.58):

$$\begin{aligned}\Gamma(\omega_\mathrm{f}) &= \hbar^2 \int_0^\infty \mathrm{d}\tau \int_0^\infty \mathrm{d}\omega_k J(\omega_k)\left[\left(1+\bar{n}(\omega_k)\right)\mathrm{e}^{-\mathrm{i}\omega_k\tau} + \bar{n}(\omega_k)\mathrm{e}^{\mathrm{i}\omega_k\tau}\right]\mathrm{e}^{\mathrm{i}\omega_\mathrm{f}\tau} \\ &= \hbar^2 \int_0^\infty \mathrm{d}\omega_k J(\omega_k)\left[\left(1+\bar{n}(\omega_k)\right)\int_0^\infty \mathrm{e}^{\mathrm{i}(\omega_\mathrm{f}-\omega_k)\tau}\mathrm{d}\tau + \bar{n}(\omega_k)\int_0^\infty \mathrm{e}^{\mathrm{i}(\omega_\mathrm{f}+\omega_k)\tau}\mathrm{d}\tau\right]. \end{aligned} \tag{D.1}$$

Here we don't get straight away the delta functions like in equation (4.105). To evaluate the above equation we use the formula

$$\int_0^\infty \mathrm{d}\tau \mathrm{e}^{\mathrm{i}a\tau} = \pi\delta(a) + \mathrm{P.V.}\frac{\mathrm{i}}{a}. \tag{D.2}$$

Here P.V. means Cauchy principal value. Using the above in (D.1) gives

$$\begin{aligned}\Gamma(\omega_\mathrm{f}) = \hbar^2\pi \int_0^\infty \mathrm{d}\omega_k J(\omega_k)\left[\left(1+\bar{n}(\omega_k)\right)\delta(\omega_\mathrm{f}-\omega_k) + \bar{n}(\omega_k)\delta(\omega_\mathrm{f}+\omega_k)\right] \\ + \mathrm{i}\hbar^2\mathrm{P.V.}\int_0^\infty \mathrm{d}\omega_k J(\omega_k)\left[\frac{1+\bar{n}(\omega_k)}{\omega_\mathrm{f}-\omega_k} + \frac{\bar{n}(\omega_k)}{\omega_\mathrm{f}+\omega_k}\right].\end{aligned} \tag{D.3}$$

The real part of the above gives the coefficient $\gamma(\omega_\mathrm{f})$ we already derived in chapter 4. The imaginary part $S(\omega_\mathrm{f})$ is what we need for the calcualtion of the Lamb-shift:

$$S(\omega_\mathrm{f}) = \hbar^2\mathrm{P.V.}\int_0^\infty \mathrm{d}\omega_k J(\omega_k)\left[\frac{1+\bar{n}(\omega_k)}{\omega_\mathrm{f}-\omega_k} + \frac{\bar{n}(\omega_k)}{\omega_\mathrm{f}+\omega_k}\right]. \tag{D.4}$$

Equation (3.66) shows how the Lamb-shift Hamiltonian is constructed from the jump operators and coefficients $S(\omega)$. In deriving the equation the full secular approximation

was already done but as discussed in chapter 4 we cannot perform it in our case. Taking into account the different frequencies for the jump operators gives us the the Lamb shift Hamiltonian as

$$H_{\mathrm{LS}} = \frac{\alpha^2}{\hbar} \sum_{\omega,\omega' \in \{\omega_{gg},\omega_{ee}\}} S(\omega) A^\dagger(\omega) A(\omega') + \frac{\alpha^2}{\hbar} \sum_{\omega,\omega' \in \{-\omega_{gg},-\omega_{ee}\}} S(\omega) A^\dagger(\omega) A(\omega') \tag{D.5}$$

Opening this up explicitly and using the definitions for the jump operators (4.75) to (4.80) gives us the Lamb-shift Hamiltonian as

$$H_{\mathrm{LS}} = \frac{\alpha^2}{\hbar} \big[S(\omega_{\mathrm{f}}) + S(-\omega_{\mathrm{f}}) \big] a_{\mathrm{f}}^\dagger a_{\mathrm{f}}. \tag{D.6}$$

Since the system Hamiltonian was written as

$$H_{\mathrm{Sys}} = \frac{1}{2}\hbar(\omega_{\mathrm{A}} + 2g_{\mathrm{f}}\lambda)\sigma_z + \hbar(\omega_{\mathrm{f}} + g_{\mathrm{f}}\lambda\sigma_z) a_{\mathrm{f}}^\dagger a_{\mathrm{f}} + \hbar g_{\mathrm{f}} \lambda \sigma_- \sigma_+ , \tag{D.7}$$

we can notice that the Lamb-shift renormalizes the resonator oscillation frequency $\omega_{\mathrm{f}} \to \omega_{\mathrm{f}} + \omega_{\mathrm{LS}}$, where the Lamb-shift frequency is given by

$$\omega_{\mathrm{LS}} = \frac{\alpha^2}{\hbar^2} \big[S(\omega_{\mathrm{f}}) + S(-\omega_{\mathrm{f}}) \big] . \tag{D.8}$$

Using equation (D.4) in the above leads into an integral

$$\omega_{\mathrm{LS}} = \alpha^2 \mathrm{P.V.} \int_0^\infty \mathrm{d}\omega_k J(\omega_k) \left(\frac{1}{\omega_{\mathrm{f}} - \omega_k} - \frac{1}{\omega_{\mathrm{f}} + \omega_k} \right). \tag{D.9}$$

Using the spectral density from equation (4.47) gives us the integral as

$$\omega_{\mathrm{LS}} = \alpha^2 \mathrm{P.V.} \int_0^\infty \mathrm{d}\omega_k \frac{R\mu^2}{\hbar L_R^2} \frac{\omega_c^2}{\pi \omega_k (\omega_c^2 + \omega_k^2)} \left(\frac{1}{\omega_{\mathrm{f}} - \omega_k} - \frac{1}{\omega_{\mathrm{f}} + \omega_k} \right). \tag{D.10}$$

Rearranging, defining $\xi = \omega_c / \omega_{\mathrm{f}}$ and performing a change of variables $x = \omega_k / \omega_{\mathrm{f}}$ leads into the following form:

$$\frac{\omega_{\mathrm{LS}}}{\omega_{\mathrm{f}}} = \frac{\alpha^2 R \mu^2}{\pi L_{\mathrm{R}}^2 \hbar \omega_{\mathrm{f}}^2} \mathrm{P.V.} \int_0^\infty \mathrm{d}x \frac{1}{x(1 + \xi^{-2} x^2)} \left(\frac{1}{1+x} - \frac{1}{1-x} \right). \tag{D.11}$$

The integral and the whole equation is now in a dimenionless form. The integral itself can be evaluated using for example Mathematica. The final result for the Lamb shift frequency will be

$$\frac{\omega_{\mathrm{LS}}}{\omega_{\mathrm{f}}} = \frac{\alpha^2 R \mu^2}{\pi L_{\mathrm{R}}^2 \hbar \omega_{\mathrm{f}}^2} \frac{\xi \pi}{1 + \xi^2} . \tag{D.12}$$

Bibliography

[1] A. G. J. MacFarlane, Jonathan P. Dowling, and Gerard J. Milburn. Quantum technology: the second quantum revolution. *Philos. T. Roy. Soc. A*, 361(1809):1655–1674, 2003.

[2] Jiajun Chen. Review on quantum communication and quantum computation. *J. Phys. Conf. Ser.*, 1865(2):022008, apr 2021.

[3] Anil Shaji and Carlton M. Caves. Qubit metrology and decoherence. *Phys. Rev. A*, 76:032111, Sep 2007.

[4] I. M. Georgescu, S. Ashhab, and Franco Nori. Quantum simulation. *Rev. Mod. Phys.*, 86:153–185, Mar 2014.

[5] M.A. Nielsen and I.L. Chuang. *Quantum Computation and Quantum Information: 10th Anniversary Edition*. Cambridge University Press, 2010.

[6] Maximilian Schlosshauer. Quantum decoherence. *Phys. Rep.*, 831:1–57, Oct 2019.

[7] Alexandre Blais, Arne L. Grimsmo, S. M. Girvin, and Andreas Wallraff. Circuit quantum electrodynamics. *Rev. Mod. Phys.*, 93:025005, May 2021.

[8] P. Krantz, M. Kjaergaard, F. Yan, T. P. Orlando, S. Gustavsson, and W. D. Oliver. A quantum engineer's guide to superconducting qubits. *Appl. Phys. Rev.*, 6(2):021318, 2019.

[9] Eliot Kapit. The upside of noise: engineered dissipation as a resource in superconducting circuits. *Quantum Sci. Technol.*, 2(3):033002, aug 2017.

[10] Marco Cattaneo and Gheorghe Sorin Paraoanu. Engineering dissipation with resistive elements in circuit quantum electrodynamics. *Adv. Quantum Technol.*, 4(11):2100054, 2021.

[11] Slawomir Simbierowicz, Visa Vesterinen, Joshua Milem, Aleksi Lintunen, Mika Oksanen, Leif Roschier, Leif Grönberg, Juha Hassel, David Gunnarsson, and Russell E. Lake. Characterizing cryogenic amplifiers with a matched temperature-variable noise source. *Rev. Sci. Instrum.*, 92(3):034708, 2021.

[12] Iulia Buluta, Sahel Ashhab, and Franco Nori. Natural and artificial atoms for quantum computation. *Rep Prog. Phys.*, 74(10):104401, sep 2011.

[13] Alexandre Blais, Ren-Shou Huang, Andreas Wallraff, S. M. Girvin, and R. J. Schoelkopf. Cavity quantum electrodynamics for superconducting electrical circuits: An architecture for quantum computation. *Phys. Rev. A*, 69:062320, Jun 2004.

[14] Steven M Girvin. *Circuit QED: superconducting qubits coupled to microwave photons*, volume 96, pages 113–256. Oxford University Press, 2014.

[15] Uri Vool and Michel Devoret. Introduction to quantum electromagnetic circuits. *Int. J. Circ. Theor. App.*, 45(7):897–934, 2017.

[16] A. O. Caldeira. *An Introduction to Macroscopic Quantum Phenomena and Quantum Dissipation*. Cambridge University Press, 2014.

[17] A. J. Leggett. Macroscopic Quantum Systems and the Quantum Theory of Measurement. *Prog. Theor. Phys. Supp.*, 69:80–100, 03 1980.

[18] Yasunobu Nakamura, Yu A Pashkin, and JS Tsai. Coherent control of macroscopic quantum states in a single-cooper-pair box. *Nature*, 398(6730):786–788, 1999.

[19] Yu. A. Pashkin, T. Yamamoto, O. Astafiev, Y. Nakamura, D. V. Averin, and J. S. Tsai. Quantum oscillations in two coupled charge qubits. *Nature*, 421(6925):823–826, Feb 2003.

[20] S.E. Rasmussen, K.S. Christensen, S.P. Pedersen, L.B. Kristensen, T. Bækkegaard, N.J.S. Loft, and N.T. Zinner. Superconducting circuit companion—an introduction with worked examples. *PRX Quantum*, 2:040204, Dec 2021.

[21] David J Griffiths. *Introduction to electrodynamics; 4th ed.* Pearson, Boston, MA, 2013. Re-published by Cambridge University Press in 2017.

[22] David J. Griffiths and Darrell F. Schroeter. *Introduction to Quantum Mechanics*. Cambridge University Press, 3rd edition, 2018.

[23] A.O Caldeira and A.J Leggett. Quantum tunnelling in a dissipative system. *Ann. Phys-New York*, 149(2):374–456, 1983.

[24] Ronald M. Foster. A reactance theorem. *Bell Syst. Tech. J.*, 3(2):259–267, 1924.

[25] Luis Barreira. Poincaré recurrence: old and new. In *XIVth International Congress on Mathematical Physics*, pages 415–422. World Scientific, 2006.

[26] P. Bocchieri and A. Loinger. Quantum recurrence theorem. *Phys. Rev.*, 107:337–338, Jul 1957.

[27] Michael E Peskin and Daniel V Schroeder. *An introduction to quantum field theory*. Westview, Boulder, CO, 1995.

[28] Leonard Mandel and Emil Wolf. *Optical Coherence and Quantum Optics*. Cambridge University Press, 1995.

[29] Antonio Acín, Immanuel Bloch, Harry Buhrman, Tommaso Calarco, Christopher Eichler, Jens Eisert, Daniel Esteve, Nicolas Gisin, Steffen J Glaser, Fedor Jelezko, Stefan Kuhr, Maciej Lewenstein, Max F Riedel, Piet O Schmidt, Rob Thew, Andreas Wallraff,

Ian Walmsley, and Frank K Wilhelm. The quantum technologies roadmap: a european community view. *New J. Phys.*, 20(8):080201, aug 2018.

[30] J.E Baggott. *The Quantum Story: A History in 40 Moments*. EBSCO ebook academic collection. OUP Oxford, 2011.

[31] H.P. Breuer, F. Petruccione, and S.P.A.P.F. Petruccione. *The Theory of Open Quantum Systems*. Oxford University Press, 2002.

[32] James B Carrell. Fundamentals of linear algebra. *The University of British Columbia*, 2005.

[33] Thomas E Roth, Ruichao Ma, and Weng C Chew. An introduction to the transmon qubit for electromagnetic engineers. *arXiv preprint arXiv:2106.11352*, 2021.

[34] Daniel Loss and David P. DiVincenzo. Quantum computation with quantum dots. *Phys. Rev. A*, 57:120–126, Jan 1998.

[35] Yoon-Ho Kim. Single-photon two-qubit entangled states: Preparation and measurement. *Phys. Rev. A*, 67:040301, Apr 2003.

[36] Jens Koch, Terri M. Yu, Jay Gambetta, A. A. Houck, D. I. Schuster, J. Majer, Alexandre Blais, M. H. Devoret, S. M. Girvin, and R. J. Schoelkopf. Charge-insensitive qubit design derived from the cooper pair box. *Phys. Rev. A*, 76:042319, Oct 2007.

[37] B.D. Josephson. Possible new effects in superconductive tunnelling. *Phys. Lett.*, 1(7):251 – 253, 1962.

[38] Daniel Manzano. A short introduction to the lindblad master equation. *AIP Adv.*, 10(2):025106, 2020.

[39] Daniel A. Lidar. Lecture notes on the theory of open quantum systems. *arXiv preprint arXiv:1902.00967*, 2019.

[40] V. V. Sargsyan, Z. Kanokov, G. G. Adamian, and N. V. Antonenko. Application of the theory of open quantum systems to nuclear physics problems. *Phys. Part. Nuclei*, 47(2):157–205, Mar 2016.

[41] Alán Aspuru-Guzik and Philip Walther. Photonic quantum simulators. *Nat. Phys.*, 8(4):285–291, Apr 2012.

[42] Neill Lambert, Yueh-Nan Chen, Yuan-Chung Cheng, Che-Ming Li, Guang-Yin Chen, and Franco Nori. Quantum biology. *Nat. Phys.*, 9(1):10–18, Jan 2013.

[43] I. Rotter and J. P. Bird. A review of progress in the physics of open quantum systems: theory and experiment. *Rep. Prog. Phys.*, 78(11):114001, oct 2015.

[44] J. F. Haase, A. Smirne, S. F. Huelga, J. Kołodynski, and R. Demkowicz-Dobrzanski. Precision limits in quantum metrology with open quantum systems. *QMTR*, 5(1):13–39, Aug 2016.

[45] M. Naghiloo, A. N. Jordan, and K. W. Murch. Achieving optimal quantum acceleration of frequency estimation using adaptive coherent control. *Phys. Rev. Lett.*, 119:180801, Nov 2017.

[46] Markus J. Storcz and Frank K. Wilhelm. Decoherence and gate performance of coupled solid-state qubits. *Phys. Rev. A*, 67:042319, Apr 2003.

[47] Jukka P. Pekola and Bayan Karimi. Ultrasensitive calorimetric detection of single photons from qubit decay. *Phys. Rev. X*, 12:011026, Feb 2022.

[48] Jun John Sakurai and Jim Napolitano. *Modern quantum mechanics; 2nd ed.* Addison-Wesley, San Francisco, CA, 2011.

[49] Marco Cattaneo, Gian Luca Giorgi, Sabrina Maniscalco, and Roberta Zambrini. Local versus global master equation with common and separate baths: superiority of the global approach in partial secular approximation. *New J. Phys.*, 21(11):113045, nov 2019.

[50] Willi-Hans Steeb and Yorick Hardy. *Matrix calculus and Kronecker product: a practical approach to linear and multilinear algebra*. World Scientific Publishing Company, 2011.

[51] Willis E. Lamb and Robert C. Retherford. Fine structure of the hydrogen atom by a microwave method. *Phys. Rev.*, 72:241–243, Aug 1947.

[52] Vittorio Gorini, Andrzej Kossakowski, and E. C. G. Sudarshan. Completely positive dynamical semigroups of n-level systems. *J. Math. Phys.*, 17(5):821–825, 1976.

[53] G. Lindblad. On the generators of quantum dynamical semigroups. *Commun. Math. Phys.*, 48(2):119–130, Jun 1976.

[54] Jerryman A Gyamfi. Fundamentals of quantum mechanics in liouville space. *Eur. J. Phys.*, 41(6):063002, oct 2020.

[55] Jonathan J. Burnett, Andreas Bengtsson, Marco Scigliuzzo, David Niepce, Marina Kudra, Per Delsing, and Jonas Bylander. Decoherence benchmarking of superconducting qubits. *Npj Quantum Inf.*, 5(1):54, Jun 2019.

[56] R. Barends, J. Kelly, A. Megrant, D. Sank, E. Jeffrey, Y. Chen, Y. Yin, B. Chiaro, J. Mutus, C. Neill, P. O'Malley, P. Roushan, J. Wenner, T. C. White, A. N. Cleland, and John M. Martinis. Coherent josephson qubit suitable for scalable quantum integrated circuits. *Phys. Rev. Lett.*, 111:080502, Aug 2013.

[57] D.M. Pozar. *Microwave Engineering, 4th Edition*. Wiley, 2011.

[58] M. Göppl, A. Fragner, M. Baur, R. Bianchetti, S. Filipp, J. M. Fink, P. J. Leek, G. Puebla, L. Steffen, and A. Wallraff. Coplanar waveguide resonators for circuit quantum electrodynamics. *J. Appl. Phys.*, 104(11):113904, 2008.

[59] R.K. Nagle, E.B. Saff, and A.D. Snider. *Fundamentals of Differential Equations*. Pearson Education, 2012.

[60] A Parra-Rodriguez, E Rico, E Solano, and I L Egusquiza. Quantum networks in divergence-free circuit QED. *Quantum Sci. Technol.*, 3(2):024012, apr 2018.

[61] Christopher Gerry and Peter Knight. *Introductory Quantum Optics*. Cambridge University Press, 2004.

[62] David Zueco, Georg M. Reuther, Sigmund Kohler, and Peter Hänggi. Qubit-oscillator dynamics in the dispersive regime: Analytical theory beyond the rotating-wave approximation. *Phys. Rev. A*, 80:033846, Sep 2009.

[63] É A. Tur. Jaynes–cummings model: Solutions without rotating-wave approximation. *Opt. Spectrosc.*, 89(4):574–588, Oct 2000.

[64] Shu He, Chen Wang, Qing-Hu Chen, Xue-Zao Ren, Tao Liu, and Ke-Lin Wang. First-order corrections to the rotating-wave approximation in the jaynes-cummings model. *Phys. Rev. A*, 86:033837, Sep 2012.

[65] E.T. Jaynes and F.W. Cummings. Comparison of quantum and semiclassical radiation theories with application to the beam maser. *P. IEEE*, 51(1):89–109, 1963.

[66] A. Wallraff, D. I. Schuster, A. Blais, L. Frunzio, J. Majer, M. H. Devoret, S. M. Girvin, and R. J. Schoelkopf. Approaching unit visibility for control of a superconducting qubit with dispersive readout. *Phys. Rev. Lett.*, 95:060501, Aug 2005.

[67] M. Scala, B. Militello, A. Messina, J. Piilo, and S. Maniscalco. Microscopic derivation of the jaynes-cummings model with cavity losses. *Phys. Rev. A*, 75:013811, Jan 2007.

[68] J. G. Peixoto de Faria and M. C. Nemes. Dissipative dynamics of the jaynes-cummings model in the dispersive approximation: Analytical results. *Phys. Rev. A*, 59:3918–3925, May 1999.

[69] A.-S.F. Obada, H.A. Hessian, and A.-B.A. Mohamed. The effects of thermal photons on entanglement dynamics for a dispersive jaynes-cummings model. *Phys. Lett. A*, 372(20):3699–3706, 2008.

[70] T. Baumgratz, M. Cramer, and M. B. Plenio. Quantifying coherence. *Phys. Rev. Lett.*, 113:140401, Sep 2014.

[71] Victor V. Albert and Liang Jiang. Symmetries and conserved quantities in lindblad master equations. *Phys. Rev. A*, 89:022118, Feb 2014.

[72] Marco Cattaneo, Gian Luca Giorgi, Sabrina Maniscalco, and Roberta Zambrini. Symmetry and block structure of the liouvillian superoperator in partial secular approximation. *Phys. Rev. A*, 101:042108, 2020.

[73] B. Bellomo, G. L. Giorgi, G. M. Palma, and R. Zambrini. Quantum synchronization as a local signature of super- and subradiance. *Phys. Rev. A*, 95:043807, Apr 2017.

[74] Marco Cattaneo, Gian Luca Giorgi, Sabrina Maniscalco, Gheorghe Sorin Paraoanu, and Roberta Zambrini. Bath-induced collective phenomena on superconducting qubits: Synchronization, subradiance, and entanglement generation. *Ann. Phys.-Berlin*, 533(5):2100038, 2021.

[75] J.R. Johansson, P.D. Nation, and Franco Nori. Qutip 2: A python framework for the dynamics of open quantum systems. *Comput. Phys. Commun.*, 184(4):1234–1240, Apr 2013.

[76] Jen-Hao Yeh, Jay LeFebvre, Shavindra Premaratne, F. C. Wellstood, and B. S. Palmer. Microwave attenuators for use with quantum devices below 100 mk. *J. Appl. Phys.*, 121(22):224501, 2017.

[77] Z. Wang, S. Shankar, Z.K. Minev, P. Campagne-Ibarcq, A. Narla, and M.H. Devoret. Cavity attenuators for superconducting qubits. *Phys. Rev. Applied*, 11:014031, Jan 2019.

[78] A. A. Clerk and D. Wahyu Utami. Using a qubit to measure photon-number statistics of a driven thermal oscillator. *Phys. Rev. A*, 75:042302, Apr 2007.

[79] Alain Joye. Introduction to quantum statistical mechanics. In *Open Quantum Systems I*, pages 41–67. Springer, 2006.